Titre: Title:	Development of a Hybrid Deterministic-Stochastic Method for Full Core Neutronics
Auteur: Author:	Seyed Rida Housseiny Milany
Date:	2017
Type:	Mémoire ou thèse / Dissertation or Thesis
Référence: Citation:	Housseiny Milany, S. R. (2017). Development of a Hybrid Deterministic-Stochastic Method for Full Core Neutronics [Ph.D. thesis, École Polytechnique de Montréal]. PolyPublie. https://publications.polymtl.ca/2499/

UNIVERSITÉ DE MONTRÉAL

DEVELOPMENT OF A HYBRID DETERMINISTIC - STOCHASTIC METHOD FOR FULL CORE NEUTRONICS

SEYED RIDA HOUSSEINY MILANY
DÉPARTEMENT DE GÉNIE PHYSIQUE
ÉCOLE POLYTECHNIQUE DE MONTRÉAL

THÈSE PRÉSENTÉE EN VUE DE L'OBTENTION
DU DIPLÔME DE PHILOSOPHIÆ DOCTOR
(GÉNIE NUCLÉAIRE)
FÉVRIER 2017

UNIVERSITÉ DE MONTRÉAL

ÉCOLE POLYTECHNIQUE DE MONTRÉAL

Cette thèse intitulée:

DEVELOPMENT OF A HYBRID DETERMINISTIC - STOCHASTIC METHOD FOR FULL CORE NEUTRONICS

présentée par: HOUSSEINY MILANY Seyed Rida
en vue de l'obtention du diplôme de: Philosophiæ Doctor
a été dûment acceptée par le jury d'examen constitué de:

M. TEYSSEDOU Alberto, Ph. D., président
M. MARLEAU Guy, Ph. D., membre et directeur de recherche
M. KOCLAS Jean, Ph. D., membre
M. NICHITA Eleodor, Ph. D., membre externe

DEDICATION

To the one who leads me through the routes of life
and to my father ...

ACKNOWLEDGEMENTS

The work presented in this thesis has been partly funded through a research grant from the Natural Sciences and Engineering Research Council of Canada. The financial support I received through the duration of the project is acknowledged.

This research project has been carried under close supervision by professor Guy Marleau. His feedback, comments and input has helped greatly shape the work since the initiation point up to accomplishment. Professor Marleau is acknowledged for granting me the opportunity to complete my PhD research under his supervision and for his close mentorship and support.

As this thesis marks the end of my academic journey, I would like to express my gratitude and thankfulness to every tutor and teacher that taught me a single word throughout my education. Professor Malcolm Joyce from Lancaster University is especially acknowledged for encouraging me to pursue a research path towards a PhD and for securing me a research grant to complete my Master degree that was a key point in my education.

Professor Seyed Fadhel Milany is always acknowledged for his continuous support and encouragement during my higher education.

Finally, my family are always thanked and acknowledged for their limitless care and love. Achieving this work would'nt have been possible without their encouragement and love.

RÉSUMÉ

La conception, l'analyse et le fonctionnement des réacteurs de fission nucléaire dépendent de la compréhension des vitesses des différentes réactions neutroniques dans le cœur du réacteur. C'est pour cela que la distribution du flux neutronique dans le cœur doit être estimée avec une bonne précision. Depuis la découverte de la fission nucléaire et l'introduction des réacteurs nucléaires, différentes approches déterministes et stochastiques ont été développées ayant pour but la modélisation des cœurs du réacteur ainsi que l'étude de la distribution du flux des neutrons. Les méthodes neutroniques actuelles utilisées pour simuler des réacteurs complets souffrent d'une précision relativement faible ou nécessitent des ressources en mémoire et en temps de calcul extrêmes. La conception de nouvaux réacteurs nucléaires demande de nouvelles méthodes qui soient à la fois précises et pratiques dans les applications de production pour la simulation et l'étude de la neutronique.

Dans ce travail, une revue de la méthode Monte Carlo (MC) et de ses défis est incluse. La méthode MC est basée sur le suivi statistique des neutrons basés sur des distributions de probabilité physique qui le rend très proche d'un réacteur virtuel. La solution qu'elle fournit est largement acceptée comme une estimation précise de la distribution du flux neutronique bien que les coûts de calculs soient importants. Dans les études MC de cœur complet, un grand nombre de paramètres physiques sont enregistrés et la taille de l'échantillon statistique doit être très grande pour obtenir une solution avec une confiance élevée. L'extrême charge de calcul des simulations de cœur complet basées sur MC son utilisation pour des calculs de production peu pratiques et la méthode a été limitée pour l'étalonnage et la validation. La convergence lente de la source de fission, la difficulté de la coupler aux solveurs de rétroaction multiphysique et l'estimation de la variance vraie sont d'autres défis pour les études MC de cœur.

L'utilisation des méthodes déterministes s'avère donc inévitables. Ces dernières sont basées sur la discrétisation de l'équation du transport dans l'espace de phase. Ces méthodes sont également fondées sur l'obtention d'une solution approximative à l'aide des méthodes numériques. Ici, un résumé de l'étude de l'équation de transport et de l'approximation des probabilités de collision est présenté. En plus de la solution du mode fondamental décrivant la répartition asymptotique du flux neutronique, l'équation de transport suppose un grand nombre de solutions qui peuvent être très utiles dans les études de la perturbation, la cartographie et la synthèse des flux neutroniques. Les méthodes de calcul impliquant des solutions bien ordonnées de l'équation de transport telles que la déflation et la décomposition QZ ont été ex-

aminées. Celles-ci sont appliquées à un certain nombre de problèmes, dans le but d'effectuer une comparaison entre eux. On observe que la déflation souffre d'une convergence médiocre et de long temps de calcul, alors que la méthode QZ assure la convergence des solutions pour les modes d'ordre élevé durant un temps raisonnable. L'application des modes dominants de l'équation de transport à la cartographie du flux a été décrite. Ainsi, la reconstruction d'une solution de transport sur un maillage spatial fin, telle que la solution de la diffusion homogène a été présentée.

Afin de remédier aux dépenses extrêmes des simulations MC, nous proposons ici une approche hybride basée sur la combinaison des solveurs conventionnels MC et de la cartographie du flux déterministe. Premièrement, nous avons réalisé une simulation stochastique pour produire des flux de neutrons dans quelques régions, ou sur un réseau grossier, ainsi qu'en utilisant des sections efficaces neutroniques homogénéisées et condensées. Les sections efficaces sont utilisées pour un calcul de réseau déterministe afin d'obtenir les modes dominants de l'équation de transport. Une fois les modes dominants calculés, et dans le but d'estimer les amplitudes des modes et effectuer la synthèse du flux pour obtenir une distribution de flux complète, ces modes seront combinés aux solution du solveur MC. Deux approches sont envisagées pour réduire la charge de calcul des simulations MC. La première approche consiste à compter quelques régions du réacteur et reconstruire de façon précise une distribution plus détaillée du flux neutronique en utilisant les modes dominants de l'équation de transport et de la cartographie des flux. Alternativement, les solutions MC sont évaluée sur un maillage grossier et la reconstruction du flux est obtenue en utilisant des modes dominants calculés sur un maillage fin. Ce dernier est plus efficace car une réduction du nombre d'enregistrements et d'histoires de neutrons est réalisable.

Nous avons également évalué la précision de la reconstruction d'une solution MC en utilisant des modes dominants de l'équation de transport et du flux neutronique. La possibilité de reconstruire une distribution du flux neutronique basée sur l'évaluation du flux dans quelques régions a été étudiée et montre la faisabilité de cette méthode. En se basant sur les résultats obtenus, l'étude confirme que l'approche hybride est capable de reconstituer une distribution de flux MC à partir de données de flux dans quelques régions. Par conséquent, une réduction considérable de la dépense de calcul est réalisable.

Pour une meilleure performance, la méthode hybride est développée pour reconstruire une solution à mailles fines à partir d'une solution MC à mailles grossières en utilisant les modes dominants de l'équation de transport. La méthode est appliquée à un certain nombre de problèmes 2D et 3D et la précision et la performance de calcul sont évaluées. Les résultats confirment que dans une simulation de cœur complet, l'approche hybride pourrait être jusqu'à

90% plus rapide que le methode conventionnelle tout en maintenant une précision comparable. Les solutions produites par la méthode hybride pour les exemples étudiés sont comparées à une référence MC. Dans la plupart des cas, la différence relative entre la solution hybride et la référence est inférieure à 2%, tandis que des erreurs jusqu'à 5% sont observées dans quelques cas. Enfin, les effets du le l'évolution du combustible sont évalués et il est conclu que la méthode peut être utilisée pour des simulations dynamiques à condition que les modes dominants soient recalculés à la fin de chaque étape de combustion.

Le travail présenté dans ce projet de recherche sert de preuve du concept essentiel de la méthode hybride. Néanmoins, cette nouvelle méthode présente quelques limitations et quelques points faibles. Ces limitations devraient être étudiées dans le futur.

Durant ce travail, pour tous les exemples étudiés, la méthode hybride a été appliquée pour l'étude du flux de neutron à deux groupes d'énergie. Le temps de calcul pour obtenir les modes dominants de l'équation de transport dans un maillage spatial fin constitue 16% du temps de calcul de la méthode hybride. Ce temps devrait augmenter significativement avec l'augmentation des nombres des groupes d'énergie. De plus, la demande de mémoire pour le calcul des modes dominants sera relativement importante lorsqu'une structure de groupe plus détaillée ou un maillage spatial plus fin sont utilisés. L'augmentation du temps de calcul et de l'espace mémoire demandé, pourraient contrebalancer les économies réalisées en utilisant cette méthode. Par conséquent, nous pouvons déduire que la méthode hybride est limitée aux problèmes à quelques groupes d'énergie.

Les effets de plusieurs facteurs tels que le nombre de modes dominants utilisés dans l'expansion modale, les effets des conditions aux limites et l'estimation des erreurs sont aussi étudiés. Dans les exemples considérés, différents nombres de modes ont été utilisés pour la cartographie du flux. Une comparaison entre les résultats montre que la précision de la solution reconstruite est légèrement sensible au nombre de modes utilisés dans le modèle d'expansion modale. Il semble que l'augmentation du nombre de modes ne garantit pas une meilleure solution par rapport aux cas où peu de modes sont utilisés. Une stratégie pour sélectionner le nombre de modes dans la synthèse de flux n'est pas décidée dans ce travail et doit être développée. Ces critères pourraient être l'utilisation de modes ayant des valeurs propres non nulles ou de valeurs propres supérieures à un seuil prédéterminé.

L'introduction de conditions aux frontières entraîne des erreurs relativement importantes, près des frontières ou des interfaces. Les résultats confirment que les conditions aux frontières utilisées dans le calcul des modes dominants ont une influence importante sur la précision de la solution. La prise en compte des effets interfaciaux dans le solveur déterministe améliore la précision de la solution. L'utilisation d'une approche par essais et erreurs pour définir

les conditions aux limites d'albédo confirme que l'inclusion des effets d'interface dans le solveur déterministe améliore la précision de la solution près des interfaces. Cependant, une approche par essais et erreurs n'est pas pratique. Alors, pour déterminer les conditions limites optimales dans le calcul des modes dominants, une autre méthode doit être développée. Une approche possiblement utile est de définir les conditions aux limites d'albedo en utilisant les courants aux les interfaces comptées par le solveur stochastique. Dans les problèmes 3D présentant des conditions aux limites des fuites dans la direction axiale, la précision de la reconstruction de flux avec des modes 2D est moins précise dans les plans proches des frontières. Ceci met en évidence les effets des fuites axiales et la nécessité de les comptabiliser dans le calcul des modes et pour la cartographie des flux.

Une tentative d'estimation de l'erreur de reconstruction des flux est proposée. La méthode semble être utile pour éliminer ou réduire la sensibilité de l'approche hybride au nombre de modes dominants. Néanmoins, la méthode d'estimation d'erreur ne réussit pas à estimer ou à réduire ces erreurs de reconstruction. Par conséquent, une meilleure approche pour l'évaluation des erreurs de cartographie est nécessaire. A partir des problèmes présentés dans le cas des combustibles homogénéisés, on déduit que cette erreur est liée à l'absorption des neutrons. Il serait intéressant de developer une approche similaire pour affronter des problèmes hétérogènes de maille fine.

Enfin, la méthode hybride décrite dans ce travail utilise la méthode de décomposition QZ avec l'approximation de probabilité de collision isotrope pour calculer les modes dominants de l'équation de transport. L'approche QZ peut être très exigeante sur le plan informatique. Toutefois, afin de résoudre des problèmes de valeurs propres, d'autres méthodes numériques doivent être étudiées. Le calcul des modes dominants de l'équation de transport à partir de modèles alternatifs tels que des ordonnées discrètes ou des caractéristiques doit être considéré.

ABSTRACT

Research efforts in reactor physics focus on the improvement of current analysis methods for neutronics or development of advanced ones. Recently, there is a renewed interest in stochastic simulations due to their superior accuracy and the advances in computing platforms. In particular, there is an interest in the development of hybrid stochastic deterministic methods for accelerating the inactive cycles of Monte Carlo. However, such hybrid approaches are not very efficient as the inactive cycle constitute a very small portion of the simulation. In this work, a novel hybrid method is developed and discussed. The approach combines conventional Monte Carlo with deterministic flux mapping to reduce computational costs of full core simulations. The main contributors to the computational expenses of Monte Carlo is the number of tallies scored and the number of neutron histories tracked. In the proposed hybrid method, the Monte Carlo simulation is performed with a small number of neutron histories while maintaining good confidence and scoring flux tallies on a coarse mesh. Then, the dominant modes of the transport equation and flux mapping are employed to reconstruct the neutron flux and reaction rates on a finer mesh. Application to a number of example problems show that the studied hybrid method can achieve up to 90% reduction in the computational time compared to conventional Monte Carlo while maintaining comparable accuracy.

TABLE OF CONTENTS

LIST OF TABLES

LISTE OF FIGURES

CHAPTER 1 INTRODUCTION

The design, analysis and operation of nuclear fission reactors depend on understanding the rates of different neutron reactions within the reactor core. For this purpose, the neutron flux distribution over the core needs to be estimated with good confidence. Since the discovery of nuclear fission and the introduction of nuclear reactors, different deterministic and stochastic approaches have been developed for modelling reactor cores and studying the neutron flux distribution.

Deterministic methods are mathematical approaches developed to find an approximate solution for the Boltzmann neutron transport equation which states the law of conservation of neutrons. Given the complexity of reactor configurations, it is almost impossible to find an analytical solution of the transport equation and numerical methods based on direct discretisation of the independent variables demand extreme computing resources. Hence, several simplifications in the elements defining the problem (geometry, neutron energy, etc.) are applied. Current practice in deterministic methods is based on a two steps process comprising a lattice calculation for a single unit cell followed by a diffusion calculation for a simplified reactor geometry. In the lattice calculation, the reactor is represented by a single unit cell that defines the characteristics of the reactor and extends in an infinite lattice. The transport equation is numerically solved on a detailed spatial mesh and a relatively large number of neutron energy groups. The lattice solution is then condensed, both in space and energy, to compose a reactor database that can be utilised in the next step. The second step is a low order approximation, such as diffusion, where the reactor is represented by a finite domain of homogenised unit cells and an approximate integral solution is calculated. The lattice solution is then imposed on the low order one using form functions and form factors and fuel optimisation and reactor safety analysis are performed. Due to the number of simplifications involved in deterministic methods, the accuracy of the solution is jeopardised and large safety margins are applied in design and optimisation of reactor cores. [1]

On the other hand, stochastic methods are statistical approaches used to simulate the physical behaviour of neutrons within the reactor core. Unlike deterministic methods, stochastic approaches such as Monte Carlo require few simplifications in defining the problem; this method can handle very complex geometries and can treat neutron properties in the continuous domain. Typically, a Monte Carlo simulation follows the history of a number of neutrons along their path from the point of birth to the point of consumption or removal. Along this path, different reactions or interactions are sampled based on provided probability distributions.

A statistical estimate of the neutron population is then obtained from the average behaviour of the neutron histories. Due to the stochastic nature of the simulation and the limited number of simplifications applied, the Monte Carlo method presents a superior approach to deterministic methods in terms of accuracy and confidence in the solution. However, despite the advancement of computing platforms, the computational burden encountered in full core Monte Carlo simulations renders it impractical for production calculations and the method has been limited in reactor physics to benchmarking. [2]

1.1 Problem Formulation

With the introduction of new nuclear fuels, advanced fuel cycles and novel reactor designs, there is a growing need for advanced and accurate methods in reactor physics. Current trend within the research community shows a renewed interest in the Monte Carlo method and efforts focus on improving its performance through reducing the computational costs. Recently, it has been recognised that some improvement in the performance of Monte Carlo can be achieved through coupling the stochastic method with deterministic approaches. In particular, such hybrid approaches are utilised for accelerating the inactive portion of the Monte Carlo simulation which is used to converge the fission source of which neutrons are sampled [3]. Nevertheless, the inactive portion of the Monte Carlo simulation comprises less than 2% of the total run; any acceleration of the inactive cycle remains insignificant.

In this work, a new hybrid method based on coupling a stochastic solver to a deterministic flux mapping algorithm for reducing the computing time for full core calculations is developed.

1.2 Research Definition and Aims

Unlike current hybrid methods, the described approach does not aim to accelerate the stochastic solver. Rather, the approach combines a continuous energy continuous space domain stochastic solver with a deterministic multi-energy groups flux mapping algorithm to study full core neutronics within reasonable computational time and expense, while maintaining good accuracy compared to the Monte Carlo method.

In the proposed approach, the Monte Carlo solver is used to estimate the neutron flux in a limited number of regions over the reactor core and to produce a set of few energy groups neutron cross sections. A deterministic solver uses the generated data from the Monte Carlo run to solve the transport equation or one of its approximations in a lattice calculation and obtain the high order modes over a single unit cell. Then, flux mapping using the high order dominant modes and the Monte Carlo tallies are utilised to construct the neutron flux

distribution over the complete spatial domain. By reducing the number of regions tallied by the stochastic solver, reduction in both the computing time and memory demand can be achieved.

Development of the hybrid method is undertaken with the aim of completing a full core neutronics simulation with a running time that should be at least 50% faster than conventional Monte Carlo. The target accuracy of the solution is 5% or better on the fission rate when compared to a reference Monte Carlo solution.

In order to achieve the aims stated above, the following methodology is applied:

- Investigate the feasibility of the proposed hybrid method.
- Evaluate different mathematical approaches for performing neutron flux mapping.
- Implement a dominant modes solver in the lattice code DRAGONv5.
- Implement the hybrid method and perform sample reactor physics studies.
- Identify strengths and weaknesses of the hybrid method and recommend improvements.

1.3 Thesis Structure

This thesis proceeds by a literature review of the Monte Carlo (MC) method, challenges for full core MC and a brief description of few MC codes. Chapter 3 deals with the transport equation and its solutions. A brief literature review on the transport equation is provided. Mathematical methods for obtaining the high order modes are described with some sample calculations. The chapter concludes with an introduction to the concept of flux mapping and its application for finding a solution for the transport equation. In chapter 4, the feasibility of the hybrid method is investigated through reconstructing a MC solution in a single PWR fuel assembly using the dominant modes and flux mapping. Practical implementation and application of the method to 2D and 3D problems are presented in chapter 5. The performance of the method is compared against the conventional Monte Carlo method. The work concludes by a summary of the results, identification of the deficiencies of the proposed hybrid method and suggestions for future developments.

CHAPTER 2 LITERATURE REVIEW

In this chapter, a literature review of the Monte Carlo method is presented. A brief description of the theory of MC is included. Then, challenges for full core MC neutronic simulations are described with different approaches for tackling these challenges. Recent hybrid methods used for accelerating the inactive portion of the simulation are reviewed. Finally, a presentation of some of the MC codes developed or under development for full core reactor physics is included.

2.1 The Monte Carlo Method

Unlike deterministic methods, the Monte Carlo approach does not solve an integral or differential equation. Rather, the method attempts to follow the behaviour of neutrons as they transport across the reactor core. In this sense, the method can be viewed as a virtual reactor on a computer.

From the point of their introduction to the point of removal, neutrons can undergo different types of interactions with nuclei in the medium. Such interactions are governed by probability distributions related to the neutron cross sections and properties of the medium, energy of neutrons and their direction of travel. The Monte Carlo method tracks a large number of neutrons, one by one, and determines the most probable interactions they would undergo through their history. The neutron flux distribution is then estimated by observing the average behaviour of tracked neutrons.

Between points of interactions, neutrons travel in straight paths. For a neutron of a given energy E, the probability of it surviving an interaction in the medium after travelling a distance l and then colliding in dl is given by [4]:

$$P(l)dl = \Sigma_t(E)e^{-\Sigma_t(E)l}dl \tag{2.1}$$

where $P(l)$ is the collision probability in dl, Σ_t is the total macroscopic neutron cross section. The history of a neutron proceeds by sampling from a set of sources distributed across the core. At an initial point of known coordinates, pseudo-random numbers are generated and statistical tests are performed to determine the initial neutron energy and its direction of travel. Another pseudo-random number is generated and compared to the cumulative probability distribution function corresponding to the probability distribution function of equation eq. (2.1) to sample a neutron path length. If the neutron does not cross an interface

along its path, it is moved to the point of interaction, otherwise the track length is reduced to the distance to the interface. At the point of interaction or interface, a pseudo-random number is generated and statistical tests are performed to determine the type of interaction. If the interaction is a scattering reaction, the energy and direction of travel are updated. If absorption is sampled, a statistical test is performed to determine the type of absorption. When fission or neutron emitting reaction occurs, neutron sources to be used in the next cycle are updated. Tracking of a neutron continues until it leaks outside the reactor domain or until removed by absorption. The process is repeated for a large number of neutron histories and simulation cycles. [2, 5]

The neutron flux distribution is estimated using one of two estimators. The track length estimator calculates the flux distribution in a given volume from the total length travelled by neutrons within the volume:

$$\phi(\vec{\Omega}, E) = \frac{1}{nNV} \sum_{j=1}^{N} \sum_{i=1}^{n} w_i^j \; l_i^j(\vec{\Omega}, E) \tag{2.2}$$

where $\phi(\vec{\Omega}, E)$ is the flux within a tally cell of volume V, n is the number of neutron histories per cycle, N is the number of cycles, w_i^j is the statistical weight of the i^{th} particle in the j^{th} cycle and $l_i^j(\vec{\Omega}, E)$ is the track length of the i^{th} particle of the j^{th} cycle along direction Ω with energy E within the tally cell. Alternatively, the collision estimator calculates the neutron flux distribution by recording the number of collisions scored within a given tally cell:

$$\phi(E) = \frac{1}{nNV} \sum_{j=1}^{N} \sum_{i=1}^{n} \frac{w_i^j}{\Sigma_t(E)} \tag{2.3}$$

Accuracy of the solution is influenced by different factors such as the effort used in defining the problem, accuracy of nuclear data and the number of neutron histories tracked. The confidence in the estimate is typically determined in terms of the standard deviation σ which is calculated according to [2]:

$$\sigma^2 = \frac{1}{N-1} \sum_{i}^{N} [\phi_i - \overline{\phi}]^2 \tag{2.4}$$

where N is the number of samples, ϕ_i is the estimate of the flux by the $i - th$ sample and $\overline{\phi}$ is the mean flux.

2.2 Challenges for Full Core Monte Carlo

Challenges for full core MC simulations can be described in two general categories, those inherent to the MC method and those arising from the physical nature of the problem. The second category becomes particularly important when multiphysics feedback is studied. Inherent challenges include the long computational time for acceptable results, large demand for computing memory, slow convergence of the source distribution as well as variance estimation. The origins of these as well as methods available to address them are reviewed in the subsequent sections.

2.2.1 Accounting for Multiphysics Feedback

Coupling MC simulations to multiphysics feedback such as fuel burnup and thermal-hydraulics poses a challenge for the development of MC as a mainstream reactor analysis tool as opposed to its traditional benchmarking role. The origin of this challenge lays in three issues: the inherent fluctuations of the MC solution, the discontinuous nature of the MC solution and the calculation of temperature dependant neutron cross section data [3]. In addition, taking into account the dynamic evolution of the reactor due to isotopic depletion or accumulation has its impact. The MC solution comprises a number of stochastic simulations of the physical behaviour of neutrons. The random nature of the simulation introduces significant fluctuations over different cycles. These fluctuations could introduce convergence issues for mutliphysics solvers which represents an outstanding issue that need to be addressed in developing new MC codes [3]. Furthermore, the MC solution is typically given in the form of a discontinuous tally histogram while multiphysics solvers rely on continuous physical models and data. Hence, there is a requirement for developing methods for calculating continuous tally data. Two methods are currently available to produce continuous MC tallies. These are the Functional Expansion Technique [6] and the Kernel Density Estimator [7]. Finally, an efficient approach for calculating the temperature dependent neutron cross section data is required to account for the different temperatures observed across the reactor. Temperature dependent cross section data can be calculated a priory on a fine or a coarse temperature mesh and an interpolation can be done to retrieve the cross section data at the required temperature [3]. A better approach is the on-the-fly Doppler broadening where only data at a reference temperature are stored and these are broadened to produce the data at the required temperatures when needed [8]. When fuel burnup is considered, it is necessary to obtain detailed flux distribution within fuel pins which means tallying on a very fine mesh. Furthermore, accurate flux distribution and reaction rates are required for burnup studies which necessitates increasing the number of histories to improve the simulation statistics.

The consequences are longer run times as well as an increase in the memory demand. Further illustrations on the relation between the computation costs and the number of histories or tallies can be found in subsequent sections.

2.2.2 Computational Time

MC estimate of the neutron flux is a statistical average of a number of tracked neutrons across the reactor geometry. The accuracy of the estimate is improved by increasing the number of neutron histories simulated according to the law of large numbers. The total time required by a MC run to obtain the flux distribution is proportional to the number of tracked neutrons and the time required per neutron history [3]. Smith [9] considered a LWR (Light Water Reactor) core with 70000 pins and estimated that 100 billion neutron histories are required to obtain a standard deviation of 1% on the neutron flux. This implies that the computational time would be prohibitively high on simple computer architectures such as PCs. Smith has estimated the time required to perform a full core calculation with fuel burnup to be about 5000 hours on a 2GHz PC [10]. Since the number of neutron histories required is also dictated by the size and configuration of the reactor, efficient reduction of the total time required by MC simulations can be only achieved by reducing the time required per neutron history. This depends on several factors such as the number of spatial points (meshes) where the flux is to be estimated, the number of tallies and availability of computer memory [3].

2.2.3 Memory Demand

The memory requirement of a MC simulation of a reactor core is imposed by three factors [3]: the simulated physical quantities (tallies), the cross section data and the geometry of the reactor. Typically, the neutron flux distribution on a fine mesh of the phase space is the main tally of a MC simulation. In addition, when the dynamic behaviour of the reactor is considered, additional tallies to account for fuel burnup and depletion/accumulation of isotopes are required. The total memory requirement for tallying is proportional to the number of regions tallied, the number of physical quantities recorded per region and the required accuracy of the estimates. Smith [9] evaluated the memory demand for a typical LWR core with 70000 pins. For the required 1% statistics on the neutron flux, he estimated that 10 radial and 100 axial meshes per fuel pin will be required; thus, a total of 70 millions tally regions. He also considered that 300 isotopes are to be tracked (which drives the number of tallies up) and allowed additional memory requirements for variance estimation. Assuming 8 bytes per tally, a rough estimate of the memory demand for a MC simulation of an LWR is

1 TB. The memory requirements are much larger if other phenomena such as the rim effect [11] and multiphysics feedback or advanced fuel designs are considered [3].
The geometry of the reactor also has an impact on the memory demand. This depends on the size of the reactor and the degree of details required from the simulation. On the other hand, memory demand by cross sections and isotopic data depends on the number of isotopes tracked [3]. When dynamic studies are considered, a large number of isotopes are tracked and the nuclear data for these must be stored. Given the wide temperature range within the reactor core, cross sections data are required at different temperatures to account for the Doppler broadening effect. Thus, significant memory is required for storing the cross sections. However, on flight calculation [8] of the temperature dependent cross sections from the stored 0 K data can be utilised to reduce the memory demand by cross sections.

2.2.4 Convergence of the Fission Source

MC simulations rely on sampling neutrons and their spatial position, energy and direction of travel from a sample that effectively represents the general population of neutrons. In criticality MC studies, neutrons are sampled in consecutive cycles from the set of neutrons born from fission reactions in previous cycles. Thus, MC simulations are performed in two stages, a number of inactive cycles where no tallies are recorded followed by active cycles to estimate the required tallies. The first stage is used to converge the fission source spatial distribution that is to be used in neutron sampling. Conventional MC simulations suffer from very slow convergence of the fission source [3]. Hence, some acceleration schemes are required to increase the efficiency of MC runs. Acceleration methods include the fission matrix approach, importance sampling and hybrid deterministic-stochastic methods.

Fission Matrix Approach

The fission matrix approach [12] was initially applied to accelerate the convergence of fission source spatial distribution in criticality safety calculations and was later extended to full core studies. The method builds on the fact that the fission source distribution is an eigenvector that satisfies the following relation:

$$HS = \frac{1}{k}S \tag{2.5}$$

where S is the energy integrated fission source spatial distribution vector, k is the multiplication factor and H is the fission matrix. The elements of the fission matrix H_{ij} represent the number of fission neutrons created in a region i of the reactor domain due to the fission caused by a neutron born in region j of the domain. The elements of the fission matrix can

be determined by tallying the neutron transfer and fission rates during the MC run. Once the fission matrix is determined, the smallest eigenvalue (i.e. the largest k) and the corresponding eigenvector are determined by solving eq. (2.5). Hence, the accuracy of the fission source distribution relies on accurate estimation of the fission matrix. However, only a rough estimate of the matrix H is required to accelerate the convergence of the source distribution. The process is repeated in subsequent cycles until a converged fission source is obtained to start the active cycles. The main advantage of this method is the significant reduction in the number of inactive cycles as compared to the conventional iterative solution applied in conventional MC. [12]

Importance Sampling

Importance sampling is an approach borrowed from variance reduction techniques to accelerate the convergence of the fission source term [3]. The convergence of the fission source distribution is particularly slow when the simulated core is relatively large, characterised by a high dominance ratio [3]. This occurs when the distribution of fission neutrons converges in some regions while a reliable distribution is not obtained yet in many different regions. Thus, a large number of inactive cycles is required to ensure a reliable distribution is obtained everywhere in the reactor core. In the importance sampling approach, neutron sampling is biased such that regions that would require longer time to converge are sampled more frequently and a converged source is obtained in fewer cycles. One approach to importance sampling in criticality problems is the Forward Weighted Consistent Adjoint Importance Sampling (FW-CADIS) developed at ORNL [13]. In this approach, a deterministic adjoint calculation is performed to obtain the biasing weights for the MC run. This method is based on the fact that the physical significance of the adjoint flux is to quantify the contribution or importance of a particle to the overall flux or particular reaction rate. A deterministic calculation, typically S_N, is first performed to obtain an approximate solution of the flux $\Psi(\vec{r}, E, \vec{\Omega})$. This is then used to calculate an adjoint source [13]:

$$q^{+}(\vec{r}, E) = \frac{\nu\Sigma_f(\vec{r}, E)}{\int\int \Psi(\vec{r}, E, \vec{\Omega})\nu\Sigma_f(\vec{r}, E)dEd^2\Omega} \tag{2.6}$$

where q^{+} is the adjoint source and $\nu\Sigma_f(\vec{r}, E)$ is the neutron production cross section with ν being the average number of neutrons produced per fission reaction. Next, an adjoint calculation is performed to calculate the adjoint flux distribution $\Psi^{+}(\vec{r}, E, \vec{\Omega})$. Finally, the

space-energy-angle dependent neutron weights are evaluated:

$$w(\vec{r}, E, \vec{\Omega}) = \frac{\int\int \Psi(\vec{r}, E, \vec{\Omega})\nu\Sigma_f(\vec{r}, E)dEd^2\Omega}{\Psi^+(\vec{r}, E, \vec{\Omega})} \tag{2.7}$$

It has been reported that the FW-CADIS method was successfully employed to speed up the convergence of the fission source in a full core MC calculation up to seven times [13].

Hybrid Methods

Hybrid deterministic-stochastic methods are developed based on the fact that the calculation of the fission source distribution is the same in both approaches. Several hybrid methods were developed; of which the most popular is the Coarse Mesh Finite Difference (CMFD) [14]. In the CMFD method, the fission source distribution is obtained by solving a multigroup neutron conservation equation over a coarse discretisation of the reactor domain. The neutron conservation equation is obtained by integrating the steady state Boltzmann transport equation over the solid angle:

$$\nabla J_g(\vec{r}) + \Sigma_{tg}(\vec{r})\phi_g(\vec{r}) - \sum_{g'=1}^{G} \Sigma_{g'\to g}\phi'_g(\vec{r}) = \frac{\chi_g}{k}\sum_{g'=1}^{G}\nu\Sigma_{fg'}(\vec{r})\phi_{g'}(\vec{r}) \tag{2.8}$$

where $J_g(\vec{r})$ is the neutron current in energy group g, ϕ_g is the group neutron flux, and k is the eigenvalue (multiplication factor). Note that only one fissile isotope is considered for the simplicity of notation. If the spatial domain is discretised, a similar equation can be written to state the conservation of neutrons within the mesh cells. For a cell of index m:

$$\sum_{s=1}^{N_m^s}\frac{A_s^m}{V_m}\overline{J}_g^s + \overline{\Sigma}_{tg}^m\overline{\phi}_g^m - \sum_{g'=1}^{G}\overline{\Sigma}_{g'\to g}^m\overline{\phi}_g'^m = \frac{\chi_g}{k}\sum_{g'=1}^{G}\nu\overline{\Sigma}_{fg'}^m\overline{\phi}_{g'}^m \tag{2.9}$$

where N_m^s is the number of surfaces bounding the mesh cell, $\overline{J}^s$ is the average net neutron current passing across surface s of cross section A_s^m, $\overline{\phi}$ is the average neutron flux inside the mesh cell and the macroscopic cross sections are taken as the average inside the cell. To solve the above equation, a relation between the neutron current passing the surfaces of the mesh cell and the neutron flux inside it is required. A convenient approach is obtained by defining a current to flux conversion factor ($\tilde{D}$) using Fick's law ($J = -D\nabla\phi$). Finite discretisation results in [15]:

$$\overline{J_g}^s = -\tilde{D}_g^s(\phi_g^{m-1} - \phi_g^m) \tag{2.10}$$

where $\tilde{D}_g^s = \frac{2D_g^{m-1}D_g^m}{h^{m-1}D_g^{m-1}+h^m D_g^m}$ results from the finite discretisation of the diffusion equation and is a function of the diffusion coefficients and the mesh size h^m, ϕ^{m-1} is the average flux in the mesh cell to the left of the surface s and ϕ^m is the average flux in the right side cell. The validity of the above relation is challenged unless the mesh size is sufficiently small and the medium is highly scattering with weak neutron absorption. For a coarse mesh, a modified relation replaces the above equation by:

$$\overline{J_g}^s = -\tilde{D}_g^s(\phi_g^{m-1} - \phi_g^m) + \hat{D}_g^s(\phi_g^{m-1} + \phi_g^m) \tag{2.11}$$

where $\hat{D}_g^s$ is a correction factor obtained from a reference high-order or fine mesh calculation of the current and the flux in the neighbouring cells:

$$\hat{D}_g^s = \frac{J_g^{*s} + \tilde{D}_g^{*s}(\phi_g^{*m-1} - \phi_g^{*m})}{(\phi_g^{*m-1} + \phi_g^{*m})} \tag{2.12}$$

The asterisk denotes a value obtained from a reference calculation. Once the relation between the current and the flux is known, a system of coupled equations is obtained that can be solved to calculate the flux in each mesh. The resulting flux is employed for calculating the fission source density to be used in the criticality calculation. The coupled CMFD-MC utilised to estimate the fission source density is an iterative method where MC is used to obtain the reference flux (ϕ^*), the reference current (J^*) and cross sections for calculating $\hat{D}_g^s$. This approach proceeds by running the MC solution for a number of inactive cycles in order to obtain a semi-converged fission source distribution. The semi-converged solution is employed to calculate the coefficients $\tilde{D}_g^s$, $\hat{D}_g^s$, $\overline{\Sigma}_{tg}$, $\overline{\Sigma}_{g'\to g}$ and $\nu\overline{\Sigma}_{fg}$ of the coarse mesh system given by eq. (2.9) and eq. (2.11). Once the deterministic system is solved over all the mesh cells, the fission source distribution is calculated and is used in the next cycle of the MC calculation:

$$S^m = \frac{\chi_g}{k}\sum_{g'=1}^{G}\nu\overline{\Sigma}_{fg'}^m\overline{\phi}_{g'}^m$$

where S^m is the energy group fission neutron source within the cell m. The process is repeated until a converged fission source distribution is obtained [15]. The CMFD-MC method was successfully employed to reduce the number of the inactive cycles by a factor of 26 in an exemplar 3D problem as reported in [15].

Other hybrid methods were developed such as the Function Monte Carlo Method (FMC) [16]. Currently, the FMC method is limited to 1D geometries and thus is not of great interest in the context of this document. Finally, although hybrid methods described in literature achieve some acceleration, any improvement brought by these methods are marginal. All current

hybrid methods concentrate on the acceleration of the inactive cycles of the MC simulation; these constitute less than 2% of the complete simulation.

2.2.5 Variance Estimation

The error estimator based on the central limit theorem, eq. (2.4) would be correct if the simulation cycles were independent, one of each other. However, since neutrons in successive cycles are sampled from those estimated in the previous one, a bias is introduced into the final result due to an intercycle correlation [17]. This introduces a discrepancy between the estimated standard deviation obtained by the CLT (denoted "apparent variance") and the actual value (denoted "true variance") [18]. It has been reported that the ratio between the true to apparent variances is between 2-5 [19, 14]. Design and safety analysis of the reactor core require high confidence in the estimated flux which means that the discrepancy between the true and apparent variance cannot be ignored. Hence, new approaches are required to reduce the underestimation in the standard deviation of a MC simulation.
Four approaches are proposed for reducing the discrepancy between the apparent and the true variance. The Gelbard's batch approach [20] estimates the tallies from a batch of cycles rather than separate cycles. The standard deviation is calculated for the batch averages. The advantage of this approach is reducing the inter-cycle correlation by using the averages of a number of cycles rather than single cycles. The Ueki's [17] approach attempts to estimate the inter-cycle correlation by using the autocovariance of the successive cycles which can be calculated from the cycle averages. By estimating the bias, a correction can be made to the apparent variance and a better estimation of the uncertainty is obtained. Another approach based on the stochastic error propagation model [21] is utilised to estimate the inter-cycle correlation and provide an estimate of the true variance. Finally, the history-based batch method [22] attempts to better estimate the variance by eliminating the inter-generational dependence of the fission source distribution. This is achieved by treating a MC simulation of N cycles and M histories as a number of independent runs N_B each with N cycles and $\frac{M}{N_B}$ histories per run. That is, the number of neutron histories simulated are split over the number of repeated runs, called history batches, which are independent of each other.

2.3 Global Acceleration Techniques

Global acceleration of MC full core simulations can be achieved by reducing the time required per history as well as by reducing the total number of histories required for given statistics. Apart from using faster computers, a reduction in the time required per neutron history became feasible with modified tracking techniques. Reduction in the number of histories

while maintaining the same confidence in the results can be achieved by employing variance reduction techniques.

In analogue MC simulations, all neutrons are characterised by the same statistical weight. Neutron histories that are unlikely to contribute to the final tally are tracked from origin point until capture or leakage; such an approach is wasteful. Variance reduction techniques act as a filter to distinguish between neutrons contributing to the result and those having low or no contribution. Several approaches are available including splitting and roulette, implicit capture and interaction forcing. The splitting roulette approach is widely used in several MC codes. The basic idea is to split particles with expected high contribution to the result into a number of particles with same characteristics of the original particle. The split particles are tracked independently and share the same statistical weight. On the other hand, particles with unlikely contribution are subject to a statistical test. A random number is sampled and if this number falls below a predetermined threshold, the history is terminated, otherwise, tracking continues and the weight of the particle is increased. In the implicit capture method, no absorption reactions are allowed. When an absorption reaction is sampled from the cross section data, the neutron history is not terminated. Instead, the weight of the neutron is reduced by the probability of absorption. This approach is combined with Russian Roulette to terminate the histories of those neutrons whose weights become less than a user defined threshold. The implicit capture approach ensures that particles with low weight will have some contribution to the tallies. Finally, interaction forcing approach is used to ensure regions of high importance but small dimensions in the order of a mean free path are sampled more frequently. Sampling of the next collision site near such regions is modified to force some interactions within the region while adjusting the weight of the history. [23]

At the heart of the MC simulation is tracking of neutrons while they travel through the geometry from the point of origin to removal is followed. Tracking is a strong function of the geometry and becomes more lengthy as the complexity of the geometry increases. In the conventional form, the straight line distance travelled by a single neutron before undergoing an interaction is decided by sampling a mean free path using the total macroscopic cross section. If the neutron is to cross an interface between different material regions before making a collision, the travel distance need to be adjusted and sampling a new mean free path is required. The distance between the point of origin to the nearest interface is determined recursively from the sampled point of interaction. The process becomes very lengthy when the geometry comprises different heterogeneities. [23]

An alternative approach which reduces the dependence on the geometry is the delta tracking method; full details are given in [24]. In this approach, the concept of a virtual collision during which the neutron neither changes its energy or direction of travel is introduced. The

purpose of this virtual collision is to modify the total cross sections in all regions such that the whole system is characterised by a uniform interaction probability. Mathematically, the virtual cross section is given by:

$$\Sigma_0(\vec{r}, E) = \Sigma_m(E) - \Sigma_t(\vec{r}, E) \tag{2.13}$$

where $\Sigma_0(\vec{r}, E)$ is the local virtual collision macroscopic cross section, $\Sigma_m(E)$ is the maximum total cross section (majorant) among all materials in the system and $\Sigma_t(\vec{r}, E)$ is the local total cross section. Delta tracking is initiated by sampling a mean free path using the majorant cross section. After moving the neutron to the new location, the type of collision is determined whether virtual or physical. The probability of a virtual collision (P_v) is given by:

$$P_v = 1 - \frac{\Sigma_0(\vec{r}, E)}{\Sigma_m(E)} \tag{2.14}$$

If a physical interaction is sampled, the neutron characteristics are modified accordingly, otherwise a new mean free path is selected. Since the interaction probability is uniform over the system, tracking becomes independent of the geometry. This method is not error free. When the geometry contains localised strong neutron absorbers, the virtual collision cross section becomes dominated by the absorption cross section of the strong absorbers. Since these absorbers are present in small regions, the probability of neutrons interacting in such regions is relatively small. Hence, the rate of virtual collisions will be large and time is wasted by resampling. An extended version to overcome this limitation was developed by Leppänen [24]. In the modified version, a second majorant cross section is defined as the maximum total cross section of all materials excluding localised absorbers. If the difference between the two majorants is significantly large at a given energy, the mean free path is sampled using the second majorant. The distance to the nearest absorber is determined; if the neutron crosses the surface of an absorber along the sampled travel line, the mean free path is adjusted and a new mean free path is sampled using the first majorant [24]. This process is employed in the Serpent code and is the major contributor to its accelerated performance.

2.4 Full-Core MC Codes

In this section, a brief description of some of the MC codes being developed for full-core reactor physics analysis is presented. For brevity, emphasis is given on the distinctive features of these codes. The review includes the MC21, MCCARD, Serpent and OpenMC.

2.4.1 MC21

The MC21 code is being developed by Knoll's Atomic Power Laboratories and Bettis Atomic Power Laboratories as a part of a wider project to develop a MC based nuclear reactor design and analysis tool [25].
The code utilises continuous energy cross section data from common nuclear data libraries. The nuclear data are processed by a system of codes called Nuclear Data Extractor (NDEX) that read the data from ENDF, EPDL or ACE files stored in a Nuclear Data Repository (NDR) and produces data libraries for the specific MC21 run. The NDR contains data files for different elements in the form of several versions corresponding to different data libraries. Data processed by NJOY are stored in the NDR for use in MC21 simulations. When a job is executed, NDEX checks for the availability of required data in the NDR and copies these to a library file. Data not readily available in the NDR are processed by NJOY and stored in the NDR for future use. This reduces the computational expense for nuclear data processing as data at given conditions are processed only once and stored in the repository. [26]
The MC21 [25] code allows for modelling complex 3D geometries via a "flexible 3D combinational geometry coupled with dedicated geometry kernels for common shapes" [26]. The geometry definition is based on four elements: quadratic surfaces that define the boundaries/interfaces, components that define volumes bounded by intersection or union of surfaces, grids that allow the definition of geometrical details in a component and overlays that allows the definition of geometrical details inside a grid cell. In addition, MC21 allows the definition of movable geometries, a feature that is particularly useful for the representation of control rods. [25, 26]
Neutron flux tallying in MC21 is based on the standard track length estimator. Typically, a tally X is calculated by the integral:

$$X = \int dr \int d^2\Omega \int dR \; f(\vec{r}, \vec{\Omega}, E)\phi(\vec{r}, \vec{\Omega}, E) \tag{2.15}$$

where the user specifies the limits of the integration to define a mesh cell in the phase space as well as the function $f(\vec{r}, \vec{\Omega}, E)$ to determine the physical property to be tallied. For example, a reaction rate can be tallied by setting f to be the macroscopic cross section of the reaction of interest. The tallies of MC21 are written in the form of a census rather than integral tallies. Census tallies record the history of individual particles simulated including their detailed phase space coordinates and their statistical weight. The advantage of this approach is to enable the use of these histories in future simulations. Particle sources can be specified from predefined distributions or can be sampled from stored censuses obtained from previous results. The latter is particularly useful for accelerating the convergence of the fission source

distribution in criticality simulations. In addition, the efficiency of the tallying process is ensured through storing the tallies in hashed arrays which reduces the computational time for the tallying process.[25, 26]

The code is developed to perform full-core reactor calculations with the capability of coupling to multiphysics effects such as thermal-hydraulics, xenon feedback, heating and control device motion. An internal thermal feedback module calculates the thermal distribution across the geometry based on user defined heat transfer and coolant flow properties. The module tallies the power distribution in cells labelled heat sources and calculates the heat transferred to heat sinks. The steady state temperature distribution is then calculated using simplified energy and mass conservation and conductivity equations. In addition, the density and the temperature dependent nuclear data can be updated. Depletion calculations are performed using a burnup module that solves the system of ordinary differential equations for isotopic depletion. The code allows performing burnup calculation based on either a constant flux or constant power assumption. To account for xenon feedback, xenon equilibrium concentrations are also calculated in-line. The code also has the capability to perform criticality calculations when movable control rods are employed. The control rods can be manipulated by the code in search for a user specified multiplication factor. [26]

The variance estimation of the simulation in MC21 is based on the batches approach suggested by Gelbard [20]. In order to eliminate the inter-cycle correlation between successive generations, sets containing sufficient number of generation histories are arranged into batches and the variance is then calculated for the batches rather than for the generations. Variance reduction in fixed source calculations are based on the CADIS and FW-CADIS methods while for eigenvalue problems the Uniform Fission Site approach [27] is utilised [26]. In addition, the CMFD method has been implemented in MC21 for accelerating the fission source convergence [28].

The performance of the MC21 was measured for the Nuclear Energy Agency (NEA) benchmark problem [29] and the MIT PWR benchmark [30]. The NEA benchmark was simulated with 7.3 million mesh regions with the flux, absorption rate and power being tallied. The simulation consisted of 253 batches of 200 cycles (3 inactive batches) and took about 3.15 days on 750 parallel processors [31]. For the MIT PWR benchmark, 5.044 million mesh regions were tallied with a total number of 30520 generations (including inactive cycles) containing 4 million neutrons per generation. The simulation was run on 1000 parallel processors and was completed after 2.5 days [28].

2.4.2 McCARD

The McCARD MC code [32] is a reactor physics code under development at the Seoul National University Reactor Physics Laboratory. The code is developed as a reactor physics analysis tool and is capable of performing fuel burnup calculations. In addition to full core neutron studies, the code can be utilised for the generation of multigroup diffusion constants used in the diffusion approximation of neutron transport. The code can be utilised in both continuous energy simulations where neutron cross sections from data libraries such as ENDF/B can be used or it can be utilised to perform multigroup MC calculations where the cross sections are read from provided multigroup libraries. Tallies are obtained by the conventional track length and collision estimators. [32]
The code is capable of modelling complex geometries and is especially developed to be able to model the geometry of the Very High Temperature Reactor. The geometry definition in McCARD combines the conventional combinational hierarchical approach with Python scripts thus allowing the representation of very complex geometries while preserving simplicity. [32]
The major features of the McCARD code are automatic detection of the convergence of the fission source distribution, estimation of the real variance, generation of kinetic parameters, coupling to thermal-hydraulics and quantification of uncertainties propagated between the different modules of the code. [32]
The code allows the user to select automatic detection of the convergence of the fission source density during the inactive cycles. Once the code observes the convergence of the source distribution, the active cycles are switched on and the tallies are recorded. This approach reduces the computational costs wasted in the inactive cycles and ensures an appropriate source distribution is obtained before the active cycles are initiated. The code allows the user to choose between two approaches for the detection of the convergence of the source distributions. The first approach, denoted type-A, performs a set of statistical tests on the fluctuation of the source distributions for the inactive cycles. When a static source distribution is detected in a predefined fraction of the tally regions, the active cycles are initiated. The second approach, denoted type-B, performs a statistical test on the "square sum of the normalised relative difference" [32] between the source densities in all the tally regions. When the square sum satisfies a Chi square distribution related to the number of tally regions, convergence is detected and the active cycles are turned on. [32]
Burnup calculations in McCARD are performed by a built-in burnup module rather than coupling to an external burnup code. The module uses the matrix exponential method to estimate the depletion/accumulation of isotopes during the burnup step. Burnup calculations have the option of a predictor-corrector approach to the estimation of the isotopic concentrations. The user can choose between a no corrector calculation, a semi-predictor-corrector

calculation or a full predictor-corrector calculation. [32]
The McCARD code is capable of providing a good estimation of the real variance of the tallies. The user can choose to estimate the variance using one of the four available methods: the Gelbard's batch method [20], Ueki's method [17], the fission source distribution inter-cycle correlation method [21] and the history based batch method [22]. Validation calculations show that the code can obtain a good estimate of the variance, in particular when the last two methods are utilised. [32]
Finally, the code is capable of performing coupled thermal-hydraulics/neutronics calculations through an iterative scheme. A simple heat transfer model is used to estimate the temperature of the tally regions. Then, the neutron cross section data are read to the nearest temperature from pre-defined temperature dependent cross section libraries and the density of materials are updated from user defined density tables. The iteration is repeated until the temperature of the tally cells satisfy a convergence criterion. [32]

2.4.3 Serpent

The Serpent code [24] is developed at the VTT Technical Research Centre of Finland. The code is developed as an alternative to deterministic lattice codes used in reactor physics. The main purpose of the code is the evaluation of mutligroup cross sections required for diffusion simulators. The code is a 3D continuous energy MC code and is capable of performing full core simulations as well as burnup calculations. [33]
The code utilises continuous energy cross section data from standard evaluated data libraries such as JEFF and ENDF/B. A major advantage of the code is the use of a Universal Energy Grid for storing processed cross sections. This is compared to the conventional general point wise data format where each isotope has its own energy grid. The use of a universal energy grid for all isotopes reduces the time required for sampling interaction cross sections as the use of a single energy grid reduces the amount of processing. However, this has the disadvantage of increased memory demand as the energy grid must be fine enough to preserve the accuracy of data for different isotopes. [34]
Another distinguishing feature of the Serpent code is the use of delta-tracking technique suggested by Woodcock [24]. Sampling of neutron interactions in this strategy is virtually independent of any interfaces in the geometry which reduces processing time per neutron history. The use of this strategy is the main contributor to the accelerated performance of the code when compared to other codes.
Geometry definition in Serpent is similar to the MCNP strategy [35]. Material cells bounded by a combination of bounding surfaces are used to define the geometry. Combinations of

bounding surfaces include intersection, union and complements of elementary surfaces. [24]
As stated above, the main purpose of the code is the generation of homogenised multigroup macroscopic cross sections and diffusion parameters for full core deterministic calculations. The code also calculates assembly discontinuity factors as well as kinetic parameters. Burnup calculations in Serpent are performed by an internal algorithm without any coupling to external calculators. The number of burnup zones in the code are not limited and only restricted by the availability of computer memory. [24]
The performance of the code for full core calculations was measured for the NEA Benchmark. The simulation was performed using 40000 active cycles each of 2.5millions histories. Seven 3 GHz CPUs were used and the total run time was around 21 hours with 90% of the results having less than 2% standard deviation. [36]
Current development efforts focus on extending the capabilities of the code to account for multiphysics feedback. Development of the code around multigroup cross sections generation and advanced homogenisation techniques is also underway.

2.4.4 OpenMC

The OpenMC code [37] is an open source code currently under development at the Massachusetts Institute of Technology. The code is developed for full core calculations and is particularly optimised for high performance calculations on parallel computer architectures. [37]
Continuous energy cross section data are read from ACE formatted files. In order to improve the efficiency and reduce the time and memory requirements for cross section processing and interpolation, an indexed unionised energy grid is used. Like the unionised energy grid approach [34], a universal grid is constructed from the energy points for all the nuclides contained in the problem. However, the universal grid is stored only once and a list of indexing pointers is defined for each nuclide. The list of pointers is then utilised to link the universal grid indexes to those of the specific grid of the nuclide for interest. [38]
The definition of the geometry of the problem in OpenMC is based on a constructive solid geometry approach. The geometry is defined as a union, intersection and/or difference of a set of half-spaces defined by bounding surfaces. The code currently supports plane and quadratic surfaces. The input file in the OpenMC code is developed to be more user-friendly compared to other codes. The input takes the form of a set of XML files, each of which define a certain aspect of the problem such as the geometry, tallies, settings etc. [37]
The tallying procedure in OpenMC is very similar to that utilised in the MC21 code. The user specifies the phase space mesh over which the tallies are recorded and a response function to specifies the tally to be recorded. To improve the efficiency of the tallying procedure,

a mapping approach is developed. A list that identifies what tallies are scored for each tally region is utilised. Instead of performing a binary search, the tally-mesh combination are read from this list to significantly accelerate the process. Tallies in the OpenMC are obtained by three estimators, the analogue, the track-length and the collision density estimators. [37, 38] The variance estimation in the OpenMC code is based on the Central Limit Theorem[38]. Variance reduction techniques are not employed extensively in this code; only the survival biasing method is available. Finally, the OpenMC code employs the CMFD method for accelerating the convergence of the fission source distribution [37].

CHAPTER 3 THE TRANSPORT EQUATION AND ITS SOLUTIONS

Deterministic methods in reactor modelling include a number of approximations and simplifications of the Boltzmann neutron transport equation. In this chapter, the steady state transport equation is introduced along with its integral form. Then, the collision probability approximation is derived and methods for obtaining the high order solutions are described. Example problems are studied and sample results are presented. The chapter concludes by a presentation of neutron flux mapping using the high order modes for flux reconstruction.

3.1 The Transport Equation

The law of conservation of neutrons states that the rate of change in their population is equal to the difference between the rates of removal and generation. Neutrons at a particular energy are introduced into the system mainly by fission, scattering from different energies, streaming and external sources. Removal occurs by absorption, scattering into different energies and leakage out of the system. In reactor cores at steady state, the rate of generation balances out the rate of removal and no external sources are present. In this case, neutron conservation is mathematically stated by the steady state Boltzmann transport equation [4]:

$$\vec{\Omega}.\vec{\nabla}\phi(\vec{r},E,\vec{\Omega})+\Sigma_t(\vec{r},E)\phi(\vec{r},E,\vec{\Omega})=Q_s(\vec{r},E,\vec{\Omega})+\frac{1}{k}Q_f(\vec{r},E,\vec{\Omega}) \tag{3.1}$$

where $\phi(\vec{r},E,\vec{\Omega})$ is the density of neutrons at location $\vec{r}$ having energy E and travelling in the direction $\vec{\Omega}$, Σ_t is the neutron total macroscopic cross section, Q_s is the scattering source given by:

$$Q_s(\vec{r},E,\vec{\Omega})=\int dE'\int d^2\Omega'\Sigma_s(\vec{r},E'\rightarrow E,\vec{\Omega}'\rightarrow\vec{\Omega})\phi(\vec{r},E',\vec{\Omega}') \tag{3.2}$$

and Q_f is the fission source:

$$Q_f(\vec{r},E,\vec{\Omega})=\chi(E)\int dE'\int d^2\Omega'\nu\Sigma_f(\vec{r},E')\phi(\vec{r},E',\vec{\Omega}') \tag{3.3}$$

Since the energy of neutrons spans a wide interval from few meVs up to several MeVs, a multigroup descritisation of the energy variable is performed [1]. In the multigroup approximation, the energy interval is split into G small subintervals over which neutron cross sections are

assumed to be constant. The multigroup form of the transport equation is then given by:

$$\vec{\Omega}.\vec{\nabla}\phi^g(\vec{r},\vec{\Omega}) + \Sigma_t^g(\vec{r})\phi^g(\vec{r},\vec{\Omega}) = Q_s^g(\vec{r},\vec{\Omega}) + \frac{1}{k}Q_f^g(\vec{r},\vec{\Omega}) \tag{3.4}$$

where ϕ^g is the energy integrated neutron flux in the g^{th} interval, Σ_t^g is the multigroup total macroscopic cross section, Q_s^g and Q_f^g are the multigroup scattering and fission sources respectively given by:

$$Q_s^g = \sum_{h=1}^{G}\int d^2\Omega'\Sigma_s^{h\to g}(\vec{r},\vec{\Omega}'\to\vec{\Omega})\phi^h(\vec{r},\vec{\Omega}) \text{ and } Q_f^g = \chi^g\sum_{h=1}^{G}\nu\Sigma_f^h(\vec{r})\int d^2\Omega\phi^h(\vec{r},\vec{\Omega}) \tag{3.5}$$

with $\Sigma_s^{h\to g}$ is the multigroup scattering cross section from group h to group g and $\nu\Sigma_f^h$ is the average fission production cross section in energy group h.

In most deterministic codes, the integral form of the transport equation is utilised for obtaining an approximate solution of the neutron flux distribution. The transport equation is written in the integral form starting from the characteristic form [4]:

$$-\frac{d}{ds}\phi^g(\vec{r}-s\vec{\Omega},\vec{\Omega}) + \Sigma_t^g(\vec{r}-s\vec{\Omega})\phi^g(\vec{r}-s\vec{\Omega},\vec{\Omega}) = Q_s^g(\vec{r}-s\vec{\Omega},\vec{\Omega}) + Q_f^g(\vec{r}-s\vec{\Omega},\vec{\Omega}) \tag{3.6}$$

where s is the distance travelled by a neutron along its characteristic line of direction $\vec{\Omega}$ from an initial reference position $\vec{r}$. By introducing an integrating factor $e^{-\tau^g(s)}$ into eq. (3.6), where τ is the neutron optical path defined as:

$$\tau^g(s) = \int_0^s ds'\Sigma_t^g(\vec{r}-s'\vec{\Omega}) \tag{3.7}$$

and integrating over s, the integral form is obtained[4][39]:

$$\phi^g(\vec{r},\vec{\Omega}) = \int_0^\infty ds\ \ e^{-\tau^g(s)}\left[Q_s^g(\vec{r}-s\vec{\Omega},\vec{\Omega}) + Q_f^g(\vec{r}-s\vec{\Omega},\vec{\Omega})\right] \tag{3.8}$$

This is the integral form in an infinite reactor which is the subject of study in several lattice codes.

3.2 The Collision Probability Method

The collision probability method is a numerical approach for solving the integral transport equation [4, 39]. In this method, neutron scattering and fission sources are assumed to be isotropic in the laboratory system which simplifies the integration of eq. (3.8) over the

direction of travel $\vec{\Omega}$ and allows writing:

$$\phi^g(r) = \frac{1}{4\pi}\int_\infty d^3r' \frac{e^{-\tau(s)}}{s^2}\left[Q_s^g(r') + Q_f^g(r')\right] \tag{3.9}$$

where the change of variable $\vec{r}' = \vec{r} - s\vec{\Omega}$ is introduced with $s = |\vec{r} - \vec{r}'|$ and $d^3r' = s^2 d^2\Omega ds$. In order to derive the collision probability form, spatial discretisation is performed. The domain is decomposed into N regions each of volume V_i where the volumes are chosen such that neutron cross sections are uniform. Equation eq. (3.9) is multiplied by $\Sigma_t(\vec{r})$ and integrated over volume V_j to write:

$$V_j\Sigma_{t,j}^g\phi_j^g = \sum_{i=1}^{N}\sum_{h=1}^{G}\left[\Sigma_{s,i}^{h\to g} + \frac{1}{k}\chi_i^g\nu\Sigma_{f,i}^h\right]\phi_i^h V_i P_{ij}^g \tag{3.10}$$

where:

$$\phi_j^g = \frac{1}{V_j}\int_{V_j} d^3r\ \phi^g(\vec{r}) \tag{3.11}$$

is the average neutron flux in the j^{th} region,

$$\Sigma_{x,j}^g = \frac{1}{V_j\phi_j^g}\int_{V_j} d^3r\ \Sigma_x^g(\vec{r})\phi^g(\vec{r}) \tag{3.12}$$

is the neutron macroscopic cross section for reaction of type x in region j and

$$P_{ij} = \frac{1}{4\pi V_i}\int_{V_i} d^3r' \int_{V_j} d^3r\ \Sigma_t^g(\vec{r})\frac{e^{-\tau^g(s)}}{s^2} \tag{3.13}$$

is the probability for a neutron born in region i and energy group g to undergo its first collision in region j. Calculation of the collision probabilities involves geometry tracking to identify integration lines along a number of neutron trajectories. Using the integration lines and neutron total cross sections, neutron optical paths are calculated and integration of eq. (3.13) is performed numerically for each energy group. [40]

Equation eq. (3.10) is a system of linear equations that can be written in matrix notation as:

$$(I - PS_c)\Phi = \frac{1}{k}F\Phi \tag{3.14}$$

where:

- Φ is a column vector whose $N\times G$ elements are the values of the neutron flux distribution
- P is a block diagonal matrix of the order $N \times G$; each block is an $N \times N$ matrix containing energy dependent collision probabilities

- S_c is the matrix of scattering cross sections of the order $N \times G$; the $N \times N$ block diagonals contain within-group scattering cross sections while the other blocks contain out-of-group scattering cross sections
- F is the fission production matrix; the order of this matrix is $N \times G$ and its elements are the fission production cross sections weighted by the fission energy spectrum.
- k is the multiplication factor

Equation eq. (3.14) is a generalised eigenvalue problem of the form:

$$A\Phi = \lambda B\Phi \tag{3.15}$$

with $\lambda = \frac{1}{k}$.

Typically, deterministic codes aim to obtain the fundamental mode corresponding to the largest multiplication factor k. The main tool used for this purpose is the inverse power iterations method.

3.3 High Order Modes of the Transport Equation

For higher order modes, i.e. eigenpairs corresponding to smaller k eigenvalues, a number of numerical methods are available for obtaining the $N \times G$ eigenpairs of eq. (3.15). Here the inverse power iteration with deflation and QZ decomposition methods are discussed.

3.3.1 QZ Decomposition

QZ decomposition or the generalised Schur decomposition [41] is a robust and reliable approach for finding the eigenvalues and eigenvectors of eq. (3.15). The approach comprises a number of matrix decompositions and reductions to rewrite matrices A and B as:

$$A = QSZ^t \quad \text{and} \quad B = QTZ^t \tag{3.16}$$

where S and T are unitary matrices giving the Schur forms of matrices A and B and Q and Z are both upper triangular matrices. Once the Schur forms are established, the eigenvalues are obtained from the diagonal terms of S and T:

$$\lambda_i = \frac{1}{k_i} = \frac{S_{ii}}{T_{ii}} \tag{3.17}$$

The approach commences by a first factorisation to write:

$$A = Q_1 H Z_1^t \quad \text{and} \quad B = Q_1 K Z_1^t \tag{3.18}$$

with H being an upper Hessenberg matrix [42], Q_1 and Z_1 are two unitary matrices and K is an upper triangular matrix. To arrive at the forms given in eq. (3.16), a factorisation of H and K is performed:

$$H = Q_2 U Z_2^t \quad \text{and} \quad K = Q_2 V Z_2^t \tag{3.19}$$

where Q_2 and Z_2 are two unitary matrices and U and V are upper triangular matrices. By using equations eq. (3.16) through eq. (3.19), the eigenvalue problem can be written by orthogonal transformation as:

$$H\Phi_i' = \lambda_i K \Phi_i' \tag{3.20}$$

where Φ_i' is the i^{th} eigenvector in the transformation subspace. Equation eq. (3.20) is a linear system of equations that can be easily solved by backward substitution given that H and K are upper Hessenberg and upper triangular matrices respectively. Eigenvectors of the original problem can be retrieved by back transformation into the primary subspace:

$$\Phi_i = Z_1 Z_2 \Phi_i' \tag{3.21}$$

Since matrices A and B need to be established explicitly, the QZ approach could become memory demanding with increasing size of the problem; this is the major drawback of this approach for finding the high order modes of the transport equation.

Application and Validation: PWR Assembly

To examine the QZ decomposition method, the high order modes of the transport equation in the collision probability approximation are studied for a single reflected 17×17 PWR fuel assembly of typical PWR dimensions. The assembly, shown in figure 3.1, comprises 264 fuel pins of 3.25w% initial enrichment uranium burned to $22 MWd/t$ and 25 water filled guide tubes both clad in zircaloy.

The Monte Carlo code *Serpent* is used to produce pincell homogenised neutron cross sections in the thermal ($< 0.625eV$) and fast energy ($> 0.625eV$) groups; the standard deviation on the produced cross sections is below 0.1%. The lattice code *Dragon v5* [43] is used to track the geometry and calculate the collision probabilities. With 289 regions and 2 energy groups, 578 eigenpairs can be calculated in total. The QZ approach, based on the LAPACK open library, is implemented in *Dragon* [44] and used to calculate the first 20 most dominant

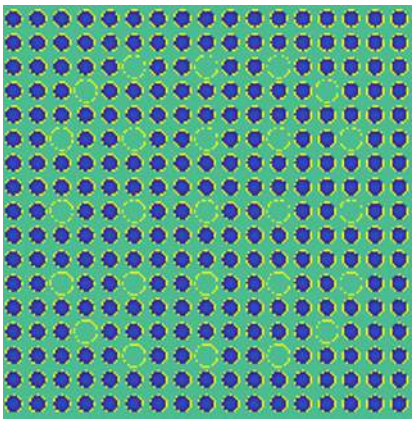

Figure 3.1 17×17 PWR fuel assembly

modes of the described PWR assembly. Sample results are shown in figures 3.2 and 3.3 where the eigenvectors are normalised such that the largest value of Φ is unity.
Convergence of the solution is verified by studying the residual vector of the i^{th} eigenpair:

$$R_i = A\Phi_i - \frac{1}{k_i} B\Phi_i \tag{3.22}$$

The euclidean norm of the residual and the eigenvalues for the first 20 most dominant modes are presented in table 3.1. The norms of the residual of all harmonics are in the order 10^{-14} or less which confirms the convergence of the solutions to the eigenvectors of the neutron flux. Furthermore, the solution of 578 eigenvectors is obtained in less than one minute on a 3.4 GHz CPU which confirms the efficiency of the QZ method.

Table 3.1 Verification of the flux harmonics obtained by QZ decomposition for a PWR assembly

Mode	k - eigenvalue	$\|\|R_i\|\|$	Mode	k - eigenvalue	$\|\|R_i\|\|$
1	9.90864E-01	2.36E-15	11	1.46589E-01	2.97E-16
2	6.48614E-01	6.54E-16	12	1.31448E-01	1.19E-14
3	6.48593E-01	7.24E-16	13	1.30408E-01	2.67E-16
4	4.73527E-01	6.53E-15	14	9.83014E-02	2.60E-15
5	3.01196E-01	5.03E-16	15	9.82952E-02	2.20E-15
6	3.01186E-01	4.78E-16	16	8.00912E-02	2.20E-16
7	2.50821E-01	4.10E-15	17	7.85528E-02	2.21E-16
8	2.50816E-01	1.91E-15	18	7.34528E-02	2.61E-16
9	1.62831E-01	3.15E-16	19	7.34516E-02	2.22E-16
10	1.46601E-01	3.06E-16	20	6.77598E-02	2.13E-16

The fundamental mode satisfies all the boundary conditions of the problem and is positive over the full domain as shown in figures 3.2 and 3.3. Hence, it represents the asymptotic behaviour of the neutron flux distribution at steady state. The higher order modes can be negative in some regions and positive in others as shown in the figures. They represent different perturbations around the fundamental mode. Typically, one or more of these modes would be excites if the configuration is perturbed, for example, by changes in the composition or the boundary conditions.

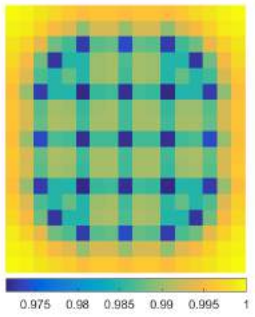

(a) Mode - 1

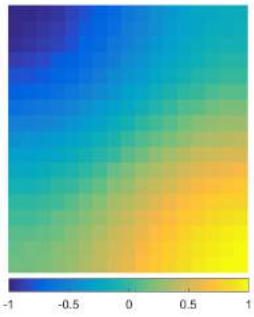

(b) Mode - 2

(c) Mode - 3

(d) Mode - 4

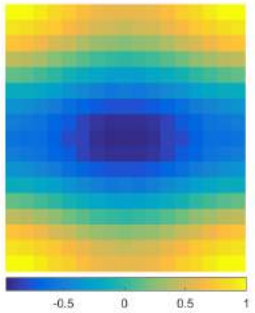

(e) Mode - 5

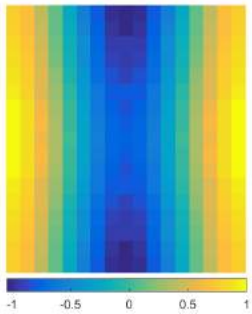

(f) Mode - 6

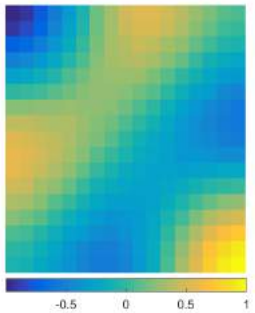

(g) Mode - 7

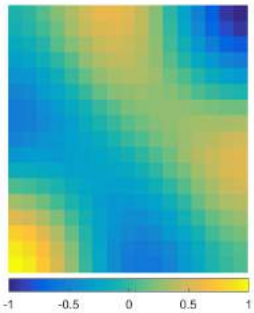

(h) Mode - 8

Figure 3.2 QZ modes 1-8 in the fast group for a PWR fuel assembly

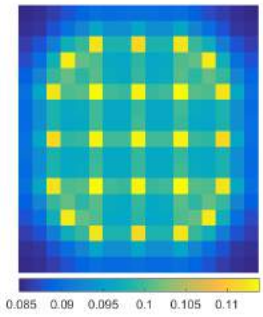

(a) Mode - 1

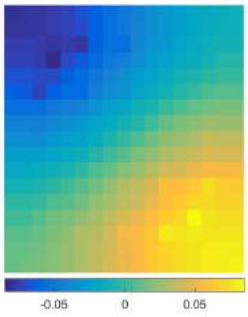

(b) Mode - 2

(c) Mode - 3

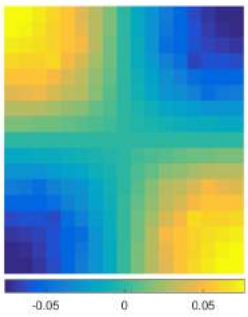

(d) Mode - 4

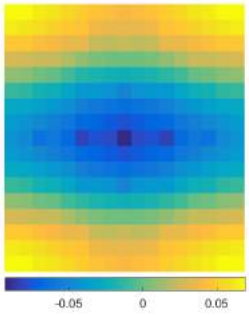

(e) Mode - 5

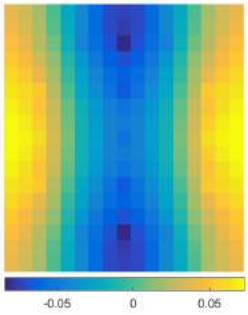

(f) Mode - 6

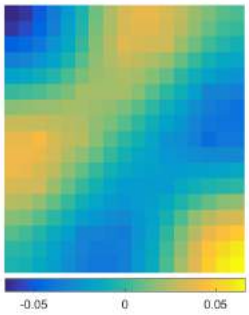

(g) Mode - 7

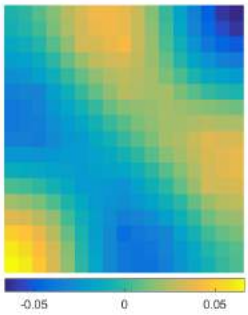

(h) Mode - 8

Figure 3.3 QZ modes 1-8 in the thermal group for a PWR fuel assembly

Application and Validation: CANDU-6 Supercell

The QZ approach is applied to study the high order harmonics of a CANDU-6 supercell [44]. The geometry comprises four unit cells each formed of a cluster of 37 fuel pins of natural enrichment uranium. Fuel pins clad in zircaloy and surrounded by heavy water coolant are arranged in a pressure tube made of zirconium-niobium alloy. The pressure tube is placed at the centre of zircaloy calandria tube with the outer region being heavy water moderator. The configuration is shown in figure 3.4.

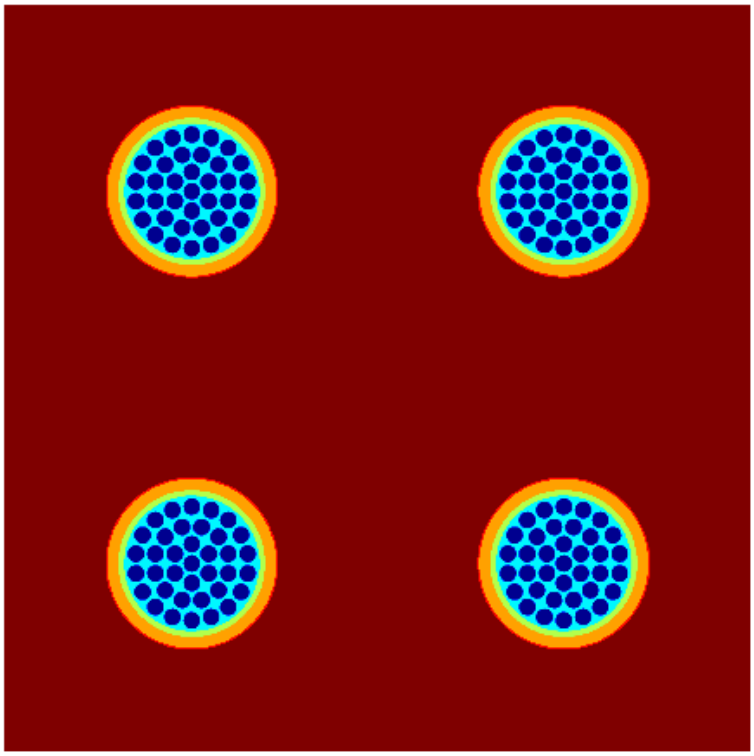

Figure 3.4 CANDU-6 supercell of 4×4 unit cells

For the calculation of the modes, each fuel pin is split into 10 regions in the radial direction. Coolant regions are split into 6 radial regions and each unit cell is split into 4 sub-cells in the x-direction and similar number of regions in the y-direction. Hence, a total of 264 mesh regions per unit cell is defined. The lattice code *Dragon* is utilised for tracking the geometry, solving the collision probability approximation and for calculating 2 groups cross sections. A total of 1968 eigenpairs can be calculated using the QZ decomposition method. Results for the first 6 modes are shown in figures 3.5 and 3.6.

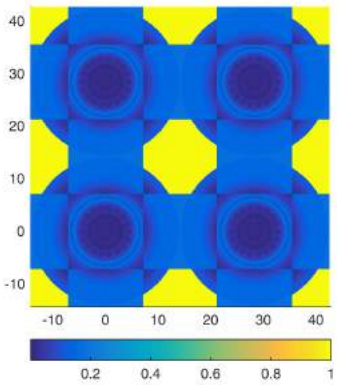

(a) Mode - 1

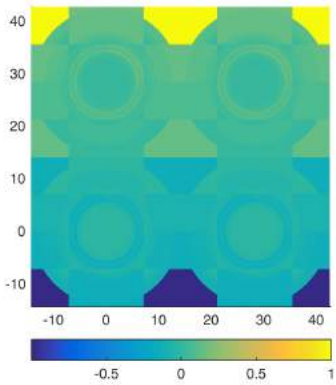

(b) Mode - 2

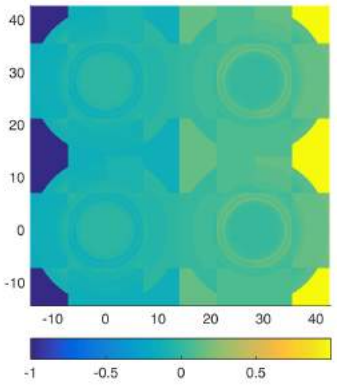

(c) Mode - 3

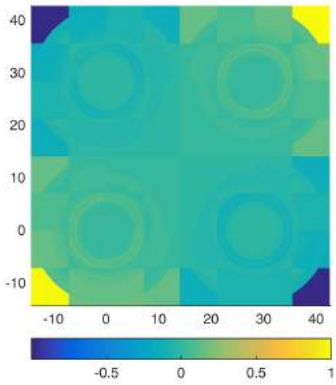

(d) Mode - 4

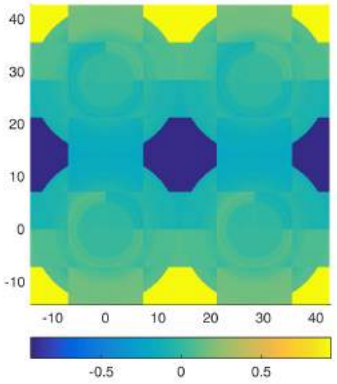

(e) Mode - 5

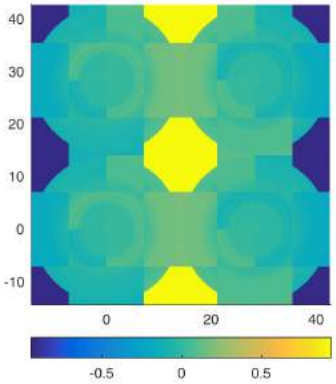

(f) Mode - 6

Figure 3.5 QZ modes 1-6 in the fast group for a CANDU-6 supercell

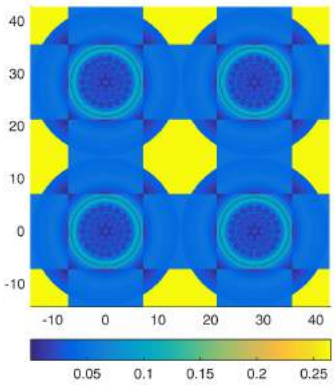

(a) Mode - 1

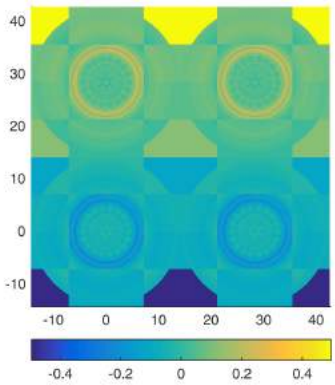

(b) Mode - 2

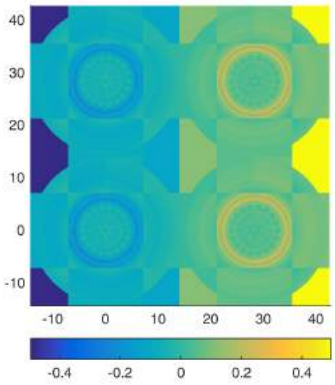

(c) Mode - 3

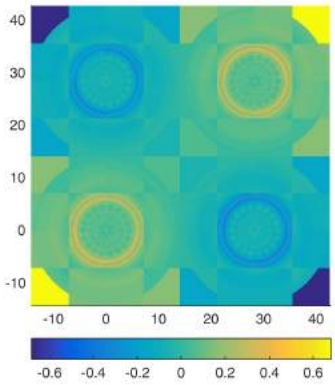

(d) Mode - 4

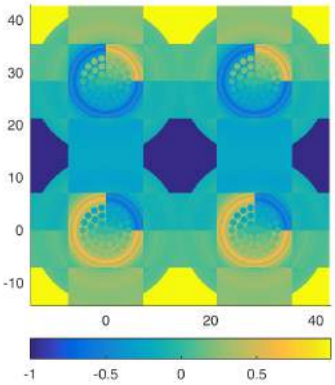

(e) Mode - 5

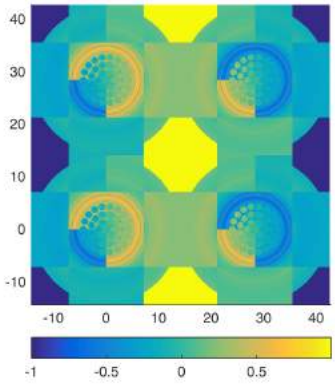

(f) Mode - 6

Figure 3.6 QZ modes 1-6 in the thermal group for a CANDU-6 supercell

As in the PWR case, only the fundamental mode provides a positive nonzero distribution as shown in figures 3.5 and 3.6 hence satisfying all the boundary conditions. Higher order modes signify different perturbations around the fundamental mode that can be excited by changes in the configuration. The euclidean norm of the residual vector and the eigenvalues of the first 20 most dominant modes are shown in table 3.2. Once again, the convergence of the QZ method is confirmed by the norm of the residual which is in the order 10^{-14}. The solution is obtained in about 3 minutes using a 3.4GHz CPU.

Table 3.2 Verification of the flux harmonics obtained by QZ decomposition for a CANDU-6 supercell

Mode	k - eigenvalue	$\|\|R_i\|\|$	Mode	k - eigenvalue	$\|\|R_i\|\|$
1	1.072500405	3.48E-14	11	0.095622322	2.70E-15
2	0.622102882	1.30E-14	12	0.088148822	2.54E-14
3	0.62210284	1.30E-14	13	0.070023411	3.34E-14
4	0.38112558	7.91E-15	14	0.057321677	1.81E-14
5	0.248490072	5.70E-15	15	0.057321677	1.17E-14
6	0.221692527	5.51E-15	16	0.050341328	1.79E-15
7	0.167497566	8.65E-14	17	0.049308753	2.79E-15
8	0.167497555	6.25E-14	18	0.044351072	2.07E-14
9	0.097088751	1.15E-14	19	0.04435107	9.95E-15
10	0.097088749	1.46E-14	20	0.040399802	1.14E-14

3.3.2 Inverse Power Iteration with Deflation

In the inverse power iteration method [45], the generalised eigenvalue problem of eq. (3.15) is re-written as:

$$A^{-1}B\Phi = k\Phi \tag{3.23}$$

The fundamental mode solution (Φ_1, k_1) is found through iteratively operating on an initial guess solution $(\Phi_1^{(0)}, k_1^{(0)})$ by the matrix $M = A^{-1}B$ and subsequently improving the guess in the next iteration until convergence is detected:

$$\Phi_1^{(i)} = \frac{1}{k_1^{(i-1)}} M\Phi_1^{(i-1)} \tag{3.24}$$

$$k_1^{(i)} = \frac{< B\Phi_1^{(i)}, B\Phi_1^{(i)} >}{< A\Phi_1^{(i)}, B\Phi_1^{(i)} >} \tag{3.25}$$

Convergence of the solution is determined against a convergence factor ϵ (i.e. 10^{-12}) according to the following criteria:

$$|k_1^{(i)} - k_1^{(i-1)} < \epsilon\, k_1^{(i)} \text{ and } \max|\Phi_1^{(i)} - \Phi_1^{(i-1)}| < \epsilon \max \Phi_1^{(i)} \tag{3.26}$$

When combined with spectral shift methods, power iterations can be used to compute eigenpairs corresponding to smaller k eigenvalues. Among spectral shift techniques is the Wielandt deflation method [46] where the iteration matrix M is modified such that only the largest eigenvalue is shifted in a desired direction. In order to compute the next eigenpair (Φ_2, k_2), matrix M is deflated:

$$M_{def} = M - \frac{1}{\sigma}\Phi_1 v^t \tag{3.27}$$

where σ is a scalar value chosen for convenience to be k_1 and v is a vector satisfying $\Phi_1^t v = 1$. Power iterations with the deflated system will converge to an eigenpair $(\hat{\Phi}_2, k_2)$ where the eigenvalue k_2 is identical to the second eigenvalue of the original system and the eigenvector $\hat{\Phi}_2$ is related to the second eigenvector of the original system Φ_2 by:

$$\hat{\Phi}_2 = \Phi_2 - \gamma\Phi_1 \tag{3.28}$$

It can be shown that the scalar γ is given by:

$$\gamma = \frac{\sigma v^t \hat{\Phi}_2}{\lambda_2 - \lambda_1} \tag{3.29}$$

where $\lambda_i = \frac{1}{k_i}$. In order to compute the next eigenpair, the deflated matrix is deflated and the procedure is repeated until the desired number of eigenpairs are calculated.

Application and Validation: PWR Assembly

The Wielandt deflation technique is used to calculate the first 20 harmonics for the PWR problem described in section 3.3.1.

The eigenvalues and the euclidean norm of the residual vector for the first 20 modes are shown in table 3.3. The eigenvalues are in good agreement with the values obtained by the QZ approach and shown in table 3.1. The euclidean norm of the residual for the first four eigenvectors can be assumed small enough to confirm the convergence of the eigenvectors. However, accumulation of errors render the convergence of the deflation procedure for higher harmonics very poor to assume reliable results even when a very small ϵ (10^{-12}) is used. Furthermore, the computational time for deflation is very high since the calculation of 30

modes for the PWR assembly takes more than one hour on a 3.4 GHz CPU.

Table 3.3 Verification of the flux harmonics obtained by deflation for a PWR assembly

Mode	k - eigenvalue	$\|k_{def} - k_{QZ}\|$	$\|\|R_i\|\|$	Mode	k - eigenvalue	$\|k_{def} - k_{QZ}\|$	$\|\|R_i\|\|$
1	9.90880E-01	1.60E-05	5.60E-11	11	1.46590E-01	1.00E-06	1.74E-04
2	6.48618E-01	4.00E-06	5.92E-15	12	1.31449E-01	1.00E-06	2.61E-06
3	6.48601E-01	8.00E-06	7.75E-08	13	1.30409E-01	1.00E-06	2.03E-04
4	4.73529E-01	2.00E-06	1.44E-07	14	9.83016E-02	2.00E-07	7.23E-05
5	3.01198E-01	2.00E-06	2.11E-04	15	9.82953E-02	1.00E-07	7.16E-05
6	3.01188E-01	2.00E-06	8.26E-05	16	8.00910E-02	2.00E-07	1.43E-04
7	2.50820E-01	1.00E-06	7.76E-05	17	7.85533E-02	5.00E-07	9.60E-04
8	2.50817E-01	1.00E-06	7.73E-05	18	7.34528E-02	0.00E+00	2.07E-04
9	1.62831E-01	0.00E+00	7.46E-05	19	7.34518E-02	2.00E-07	2.08E-04
10	1.46602E-01	1.00E-06	1.77E-04	20	6.77600E-02	2.00E-07	4.21E-05

3.4 Flux Mapping using the High Order Modes

The general solution of the transport equation in neutron multiplying media at steady state can be expressed as a summation over the eigenvectors of the eigenvalue problem eq. (3.9) [47]:

$$\phi^g(r) = \sum_i a_i \psi_i^g(r) \tag{3.30}$$

where ψ_i^g is the eigenvector corresponding to the i^{th} eigenvalue and a_i is its relative amplitude. Equation eq. (3.30) is the modal expansion model of the neutron flux distribution. In matrix notation, eq. (3.30) is written as:

$$\Phi^g = \Psi^g a \tag{3.31}$$

where Ψ is a matrix whose columns are the eigenvectors and a is a column vector containing the modal amplitudes.

Neutron flux mapping or synthesis is a mathematical approach that uses eq. (3.30) to reconstruct the neutron flux distribution on a fine mesh starting from known flux values at a limited number of regions or on a coarse mesh. Assuming that the high order modes of the transport equation are pre-calculated on a fine mesh and that the general solution is known to a good approximation on a coarse mesh, it is sufficient to estimate the modal amplitudes in order to obtain a detailed fine mesh neutron flux distribution. The concept of flux reconstruction is further illustrated in the following paragraphs with examples.

Neutron flux mapping is extensively used in on-line monitoring and control of nuclear reactors [48]. Typically, a number of in-core neutron flux detectors are installed or inserted at the centre of fuel assemblies or bundles to provide readings from different parts of the reactor. Full core neutron flux modes are pre-calculated using the diffusion approximation on a finer mesh. By combining the flux readings with the flux modes, the modal amplitudes can be estimated in order to reconstruct a more detailed neutron flux distribution over the full core. The modal expansion model of eq. (3.30) is truncated after a number of modes; typically the number of flux readings is larger than the number of modes used which necessitates calculating the modal amplitudes by approximate methods such as the least squares method:

$$a = (\Psi^{gt}\Psi^{g})^{-1}\Psi^{gt}\Phi^{g} \tag{3.32}$$

where Ψ^{gt} is the transpose matrix of Ψ.

A possible application of the most dominant modes of the transport equation and flux synthesis is the improvement of full core deterministic calculations based on diffusion. For example, neutron flux synthesis is applied to reconstruct a transport-like neutron flux distribution for detailed full core geometry starting with a homogeneous diffusion solution [49]. Eq. (3.30) is assumed to be valid at the level of each unit cell independently. Another assumption is that the homogeneous diffusion solution is an adequate approximation of the general solution of the transport equation on a simplified geometry (i.e. problem dependent). Finally, it is assumed that the flux harmonics calculated for a single unit cell in an infinite lattice are representative. Boundary effects at the interfaces between different assemblies are accounted for by changes in the excitation amplitudes of the modes between distinct assemblies.
As in the current deterministic approach, the simulation commences by a lattice calculation where the multigroup transport equation is solved on a detailed spatial mesh and relatively large number of energy groups. In addition to producing few energy group cross sections, the modes of the transport equation Ψ^{g*} on a detailed spatial mesh for few energy groups are calculated. Once the reactor database is produced, diffusion calculation is executed to estimate the neutron flux distribution Φ^{gd} over simplified geometry. To reconstruct a transport-like solution, flux mapping is applied for each fuel assembly in the core.

To illustrate, flux mapping in full core deterministic calculations is applied for a partial PWR core featuring a 3×3 supercell shown in figure 3.7 [49]. Fuel assemblies are of the typical 17×17 arrangement with 264 fuel pins and 25 water filled guide tubes. The centre assembly contain fresh 3.25% enriched uranium dioxide while the peripheral assemblies contain fuel at mid-burnup (22 MWd/t) from an initial enrichment of 3.25%. For the partial core, reflective boundary conditions are defined in the radial directions and the geometry is assumed infinite

in the z-direction.

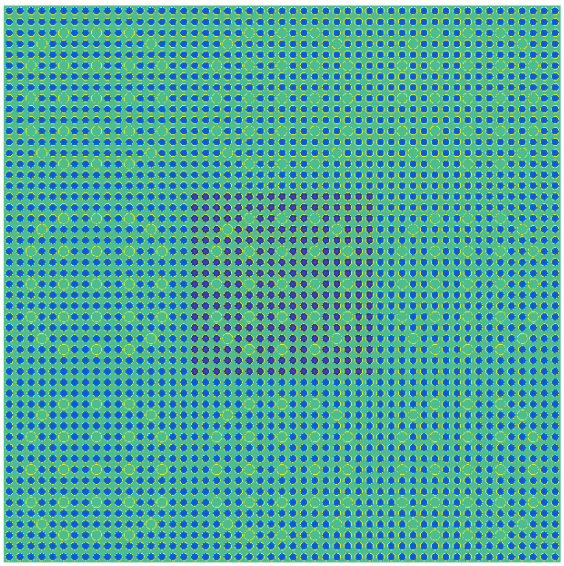

Figure 3.7 PWR 3×3 supercell

An independent lattice calculation using the collision probability approximation as implemented in the lattice code *Dragon* is performed for each of the two types of assemblies to produce 2 groups neutron cross sections. The transport equation is solved on a very fine spatial mesh; each fuel pellet is split radially into 10 regions in addition to the cladding and the coolant channel while guide tubes contain a total of 3 regions. For each of the two types of assemblies, the first 50 dominant modes in 2 energy groups are calculated with reflective boundary conditions for the described fine mesh.

Neutron cross sections are spatially homogenised on a pincell level and employed in a diffusion calculation using the code *Dragon* to estimate the integral neutron flux over homogenised pincells in the partial core. The diffusion solution (Φ^{gd}) in the two energy groups is benchmarked against a reference MC solution produced by the code *Serpent* and the relative error e^g is studied; the standard deviation for the reference MC solution is below 1%.

$$\boldsymbol{e^g} = \frac{\Phi^{gd} - \Phi^{MC}}{\Phi^{MC}} \tag{3.33}$$

The diffusion solution and the relative error with respect to the reference MC solution are shown in figures 3.8 and 3.9; the flux distribution is normalised such that the euclidean norm of Φ is unity.

Neutron flux mapping is applied for each of the 9 assemblies independently to calculate the

modal amplitudes as given by eq. (3.32). The fine mesh flux modes are homogenised to obtain the modes over pincells (Ψ) and allow solving for the amplitudes. The modal amplitudes are then obtained as:

$$a = (\Psi^{gt}\Psi^{g})^{-1}\Psi^{gt}\Phi^{gd} \tag{3.34}$$

Once the modal amplitudes are obtained, a neutron flux map over the homogenised geometry is obtained by combining the modal amplitudes with homogenised flux modes. The relative error between the MC reference and reconstructed homogeneous solution is shown in figure 3.10.

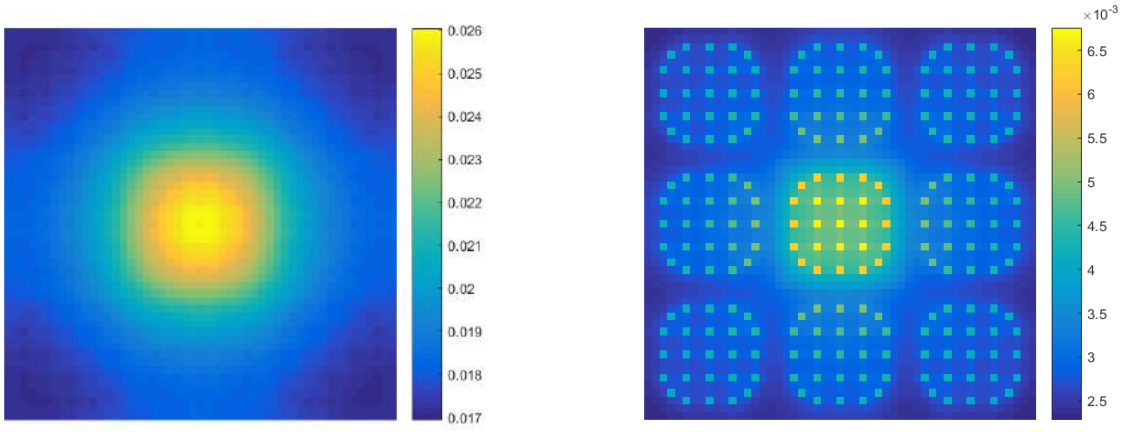

(a) Fast Group

(b) Thermal Group

Figure 3.8 Diffusion solution in the thermal and fast groups for a partial PWR core

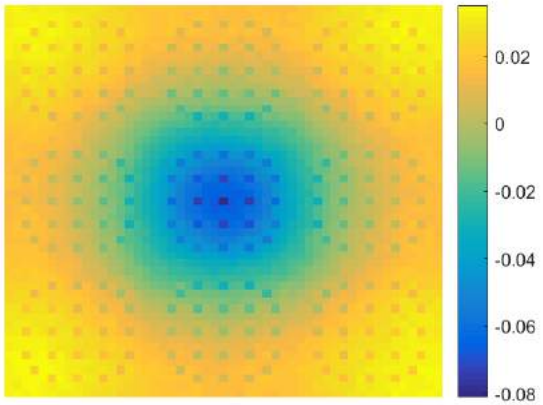

(a) Fast Group

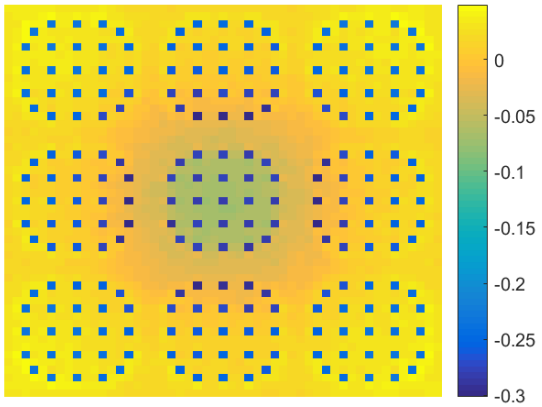

(b) Thermal Group

Figure 3.9 Relative error between diffusion solution and MC reference in the thermal and fast groups for a partial PWR core

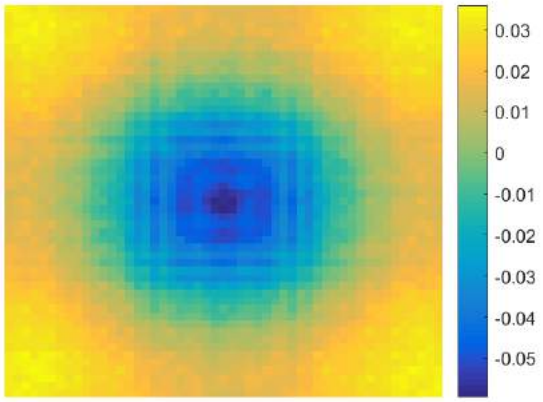

(a) Fast Group

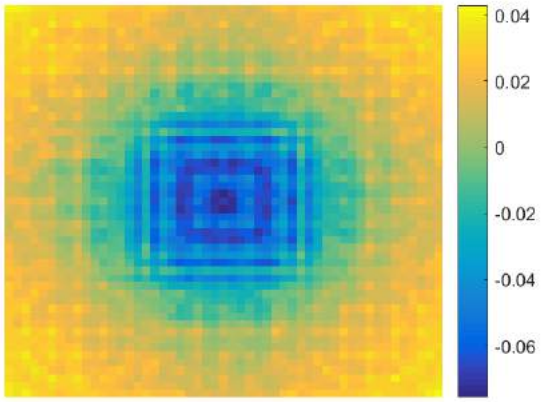

(b) Thermal Group

Figure 3.10 Relative error between reconstructed homogeneous solution and MC reference in the thermal and fast groups for a partial PWR core

Comparing figures 3.9 and 3.10, the homogeneous neutron flux distribution is improved by using the mapping approach; the largest relative error is reduced from 8% to 6% in the fast group and from 30% to 7% in the thermal group.

By combining the modal amplitudes a with the fine mesh flux harmonics Ψ^{g*}, a detailed

transport-like neutron flux map Φ^{g*} can be constructed:

$$\Phi^{g*} = \Psi^{g*} a \tag{3.35}$$

The detailed neutron flux distribution over 10 radial regions per fuel pellet is shown in figure 3.11. The constructed flux map is benchmarked against a MC reference and the relative error is presented in figure 3.12.

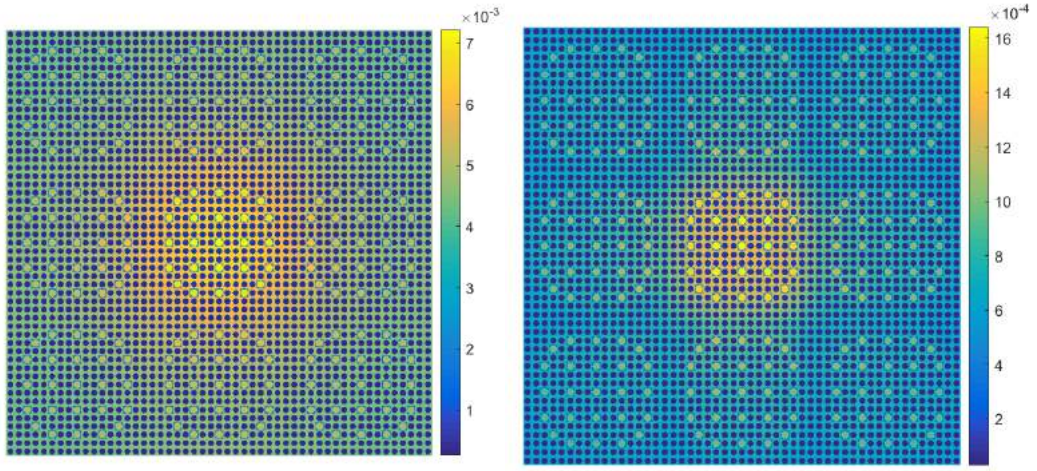

(a) Fast Group (b) Thermal Group

Figure 3.11 Constructed neutron flux map on a fine mesh in the thermal and fast groups for a partial PWR core

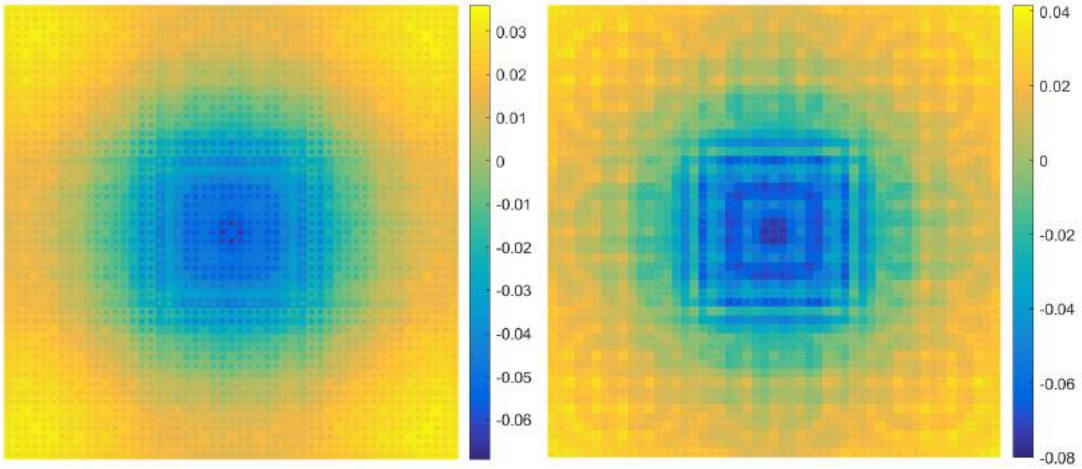

(a) Fast Group (b) Thermal Group

Figure 3.12 Relative error between constructed detailed flux map and MC reference in the thermal and fast groups for a partial PWR core

Results confirm that flux mapping using the high order modes of the transport equation performs very well for reconstructing pin-wise neutron flux distribution on a very fine spatial mesh; the largest error is better than 8% in both energy groups. Furthermore, the rate of fission reactions $r_{fission}$ is examined:

$$r_{fission} = \Sigma_f^g \phi^g \tag{3.36}$$

and the constructed pin-wise fission rate is benchmarked against a MC reference. Results shown in figure 3.13 show that the maximum error on the fission rate is around 6% which can be considered satisfactory given that.

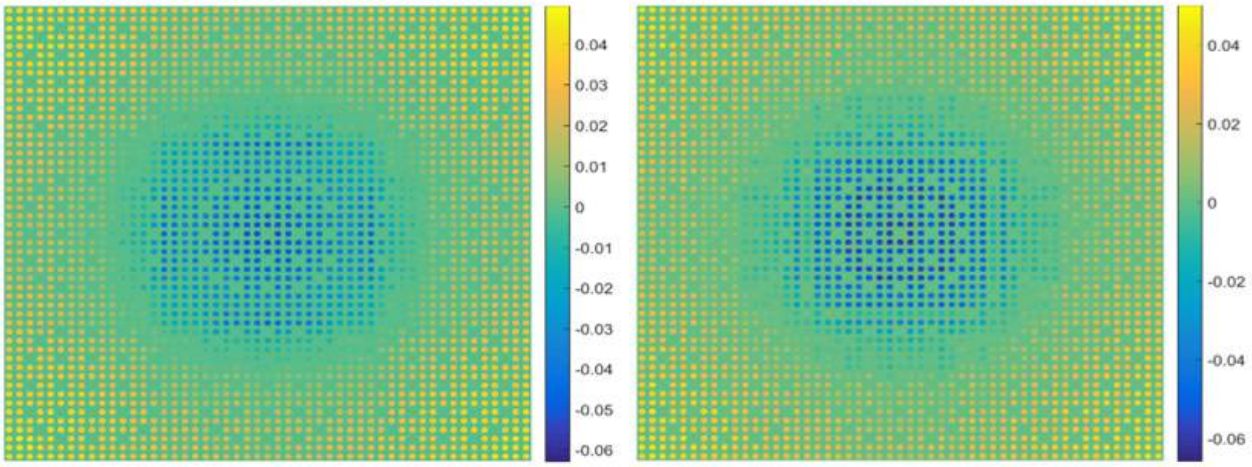

(a) Fast Group (b) Thermal Group

Figure 3.13 Relative error between constructed pin-wise fission rate and MC reference in the thermal and fast groups for a partial PWR core

3.5 Summary

Reactor design and analysis relies on finding the solution of the transport equation. In this chapter, the transport equation with the integral form are derived and the collision probability approximation is described. Two numerical methods for solving the transport equation and finding the high order harmonics are studied. QZ decomposition proved to be a reliable, robust and time efficient with the only drawback of slightly high memory demand when the size of the problem becomes large. Power iterations with deflation suffers from error accumulations which renders it unreliable. In addition, the computational time for power iterations is very long even for problems with little details.

Application of the modes of the transport equation for neutron flux mapping and flux reconstruction in full core calculations is evaluated. By combining a full core diffusion solution with the transport modes from lattice calculations, it is possible to reconstruct a transport-like flux distribution in full cores to a good accuracy. Such an approach could prove very useful in fuel management and performance, safety analysis and optimisation studies.

CHAPTER 4 FEASIBILITY STUDY

The development of deterministic methods in full core reactor physics based on diffusion is approaching a limit where any further advances would only bring marginal benefits. On the other hand, despite the advancement of computer platforms, Monte Carlo is still too expensive as a main stream reactor analysis tool. In this chapter, a novel hybrid approach for full core analysis is proposed. This method aims to enable full core neutronic studies with an accuracy that is comparable to the MC approach while keeping computation expenses comparable to deterministic methods. Then, a feasibility study is conducted in order to mathematically validate the approach.

4.1 The Hybrid Method

The calculation costs of MC simulations are determined mainly by the number of neutron histories tracked and the number of tallies scored. The number of tallies is dictated by the mes size of the phase space and the number of physical quantities to be evaluated. For each tally in any mesh of phase space, the integral of eq. (2.15) needs to be evaluated, which affects the computational time. Confidence in MC estimates of the neutron flux in a given mesh element is described by the statistical error which is inversely proportional to the number of neutron histories recorded. Hence, high confidence in the MC estimate demands for a large number of neutron histories. When fine mesh tallies are required, as in burnup studies, the number of physical quantities recorded becomes very large and the number of neutron histories tracked must be large enough to ensure adequate sampling in all regions of the phase space. In conclusion, for the same statistical error on the solution, a larger number of neutron histories is required for a solution obtained on a fine mesh compared to a solution on a coarse mesh.

To address the extreme expense of full core MC simulations, a hybrid approach based on combining conventional MC solvers with deterministic flux mapping is presented. Two approaches are considered for reducing the computational expense of MC simulations. First, one can choose to tally few regions of the reactor and deterministically reconstruct more detailed neutron flux distribution using the dominant modes of the transport equation and flux mapping. Alternatively, MC tallies are scored on a coarse mesh and flux reconstruction is achieved using the dominant modes calculated on a fine mesh. The latter is more efficient as both reductions in the number of tallies and neutron histories are achievable. In this chapter, the first approach is studied in order to evaluate the mathematical feasibility of the

hybrid method and to investigate its accuracy.

Here, full core MC simulations are performed with the minimum number of neutron histories and tallies while keeping high confidence in the solution obtained. As in conventional MC, the simulation proceeds with a number of inactive cycles in order to converge the fission source; the methods discussed in section 2.2.4 can be utilised to accelerate these inactive cycles. Once a reliable fission source distribution is obtained, active cycles are initiated where neutrons are tracked across the full core. The output of the MC solver is neutron tallies recorded in a limited number of regions and multigroup neutron cross sections required for solving the transport equation. Once the MC part of the simulation completes, generated neutron cross sections are employed in a lattice (unit cell) calculation, to obtain the dominant modes of the transport equation. If the reactor geometry contains different types of lattices, an independent deterministic calculation is performed for each type to obtain local dominant modes. Finally, the tallies scored in few regions are combined with the most dominant modes in order to estimate the modal amplitudes and to reconstruct the neutron flux distribution across the complete reactor geometry.

4.2 MC Solution Reconstruction Using Dominant Modes

Due to the stochastic nature of MC, the estimate it provides for the flux distribution is assumed to be an accurate approximation of the general solution of the transport equation. Hence, the MC solution should be well represented by the modal expansion model of eq. (3.30). To investigate the validity of these assumptions, the expansion of the MC solution in terms of the dominant modes in a PWR 17×17 fuel assembly in an infinite lattice is studied. Since the hybrid approach applies flux mapping on a unit cell or assembly level, testing the expansion model on a single assembly would be sufficient for investigating mathematical feasibility while retaining simplicity. Other effects such as boundary conditions are not included in this chapter but investigated in later chapters.

The geometry of the assembly is identical to the one shown in figure 3.1. The assembly contains 264 fuel pins of uranium dioxide at mid-burnup stage; isotropic concentrations are shown in table 4.1 [29].

Table 4.1 Fuel composition of a PWR assembly at mid-burnup

Isotope	Atomic Concentration (/barn-cm)	Isotope	Atomic Concentration (/barn-cm)
U234	4.6476E-6	Mb95	2.6497E-5
U235	4.8218E-4	Tc99	3.2772E-5
U236	9.0402E-5	Ru101	3.0742E-5
U238	2.1504E-2	Ru103	2.3505E-6
Np237	7.3733E-6	Ag109	2.0009E-6
Pu238	1.5148E-6	Xe135	1.0801E-8
Pu239	1.3955E-4	Cs133	3.4612E-5
Pu240	3.4405E-5	Nd143	2.6078E-5
Pu241	2.1439E-5	Nd145	1.9898E-5
Pu242	3.7422E-6	Sm147	1.6128E-6
Am241	4.5041E-7	Sm149	1.1627E-7
Am242	9.2301E-9	Sm150	7.1727E-6
Am243	4.7878E-7	Sm151	5.4947E-7
Cm242	1.0485E-7	Sm152	3.0221E-6
Cm243	1.4268E-9	Eu153	2.6209E-6
Cm244	8.8756E-8	Gd155	1.5369E-9
Cm245	3.5285E-9	O16	4.5737E-2

4.2.1 MC vs. Fundamental Mode

Deterministic methods for solving the steady state transport equation in multiplying media find the fundamental mode solution which describes the asymptotic behaviour of the flux distribution. In order to investigate the contribution of the higher modes, i.e. the perturbations around the asymptotic solution, the fundamental mode is compared to the MC estimate. The *Serpent* [33] MC code is used to simulate the PWR assembly lattice described above. Continuous energy neutron cross sections are used for sampling and neutron flux tallies are scored in homogenised pincells in the fast (>0.625eV) and thermal (<0.625eV) energy groups. The solution, normalised such that the euclidean norm of Φ is unity, is shown in figure 4.1. The standard deviation on the shown solution is below 0.5% in the thermal group and around 0.1% in the fast group.

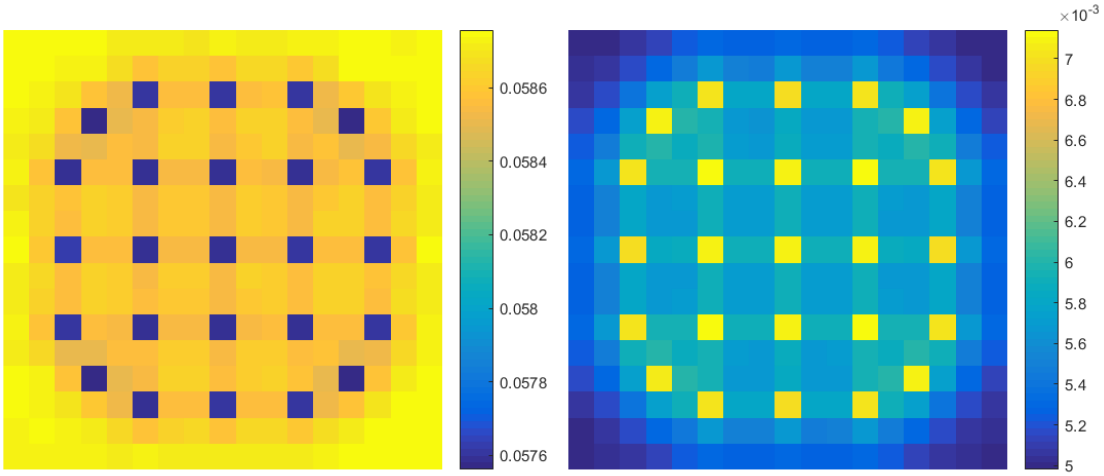

(a) Fast Group (b) Thermal Group

Figure 4.1 MC solution for the neutron flux in a PWR assembly

The lattice code *Dragon* [43] is used to calculate the fundamental mode solution in two energy groups in homogenised pincells. The geometry is tracked and 2 groups transport corrected macroscopic cross sections produced by *Serpent* are used for calculating the collision probabilities and constructing system matrices. Inverse power iterations are used for obtaining the fundamental mode solution. The effective multiplication factor estimated by *Dragon* is 0.990864 compared to 0.985238 as estimated by *Serpent*. The relative error as described by eq. (3.33) between the MC solution and the fundamental mode is evaluated and presented in figure 4.2. Results show that for a single assembly in an infinite lattice, the difference between the MC estimate and the fundamental mode solution in the thermal group could be up to 1% in fuel containing cells and 6% in water filled cells while it can be up to 1% in the fast group. The differences can be attributed to discretisation errors in space and energy as well as assumptions made on the physics of the problem such as isotropic scattering. These differences can be reduced, on the expense of increasing computational costs, by using a finer spatial mesh in the lattice solver and more energy groups. In full cores, the presence of interfaces and boundary conditions introduce more perturbations and it is expected that the difference between the fundamental mode solution and the MC solution will be larger.

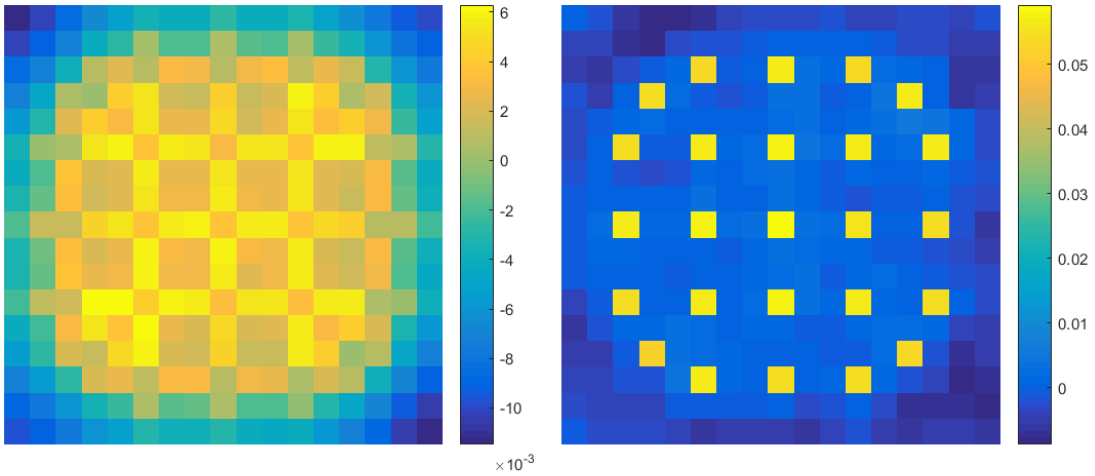

(a) Fast Group (b) Thermal Group

Figure 4.2 Relative differences between MC solution and fundamental mode solution of the flux in a PWR assembly

4.2.2 MC Flux Reconstruction Using the Most Dominant Modes

To investigate the validity of eq. (3.30) for representing the stochastic solution, attempts are made to reconstruct the MC estimate using the dominant modes of the transport equation. For the modes calculation, QZ decomposition as implemented in *Dragon* [44] and described in section 3.3.1 is utilised with the collision probability approximation. The dominant modes are calculated on a spatial mesh composed of 289 homogenised pincells. Flux tallies in all pincells are combined with the dominant modes to obtain an approximation of the modal amplitudes as given by eq. (3.32). The expansion model is truncated after a number of dominant modes and reconstructed flux map is compared to the MC solution. For the first attempt, modal expansion is truncated after 264 modes, that is the number of eigenvectors with non-zero eigenvalues corresponding to the number of pincells containing fissile materials. The expansion in the dominant modes with non-zero eigenvalues estimates the flux in most fuel containing pincells with zero error for both energy groups as presented in figure 4.3; however, errors up to 2.5% in the thermal group and 0.7% in the fast group are observed in water filled cells and fuel cells surrounding them. These large errors in water filled cells might be attributed to flux peaking, as shown in figure 4.1, due to dominating scattering interactions in these regions which is over estimated by deterministic solvers. In addition, discretisation errors and the multigroup approximation also contribute to the differences. Using more energy groups and finer spatial mesh in the calculation of the dominant modes

will improve the results of flux mapping by reducing discretisation errors, however, on the expense of longer time for the calculation of the dominant modes.

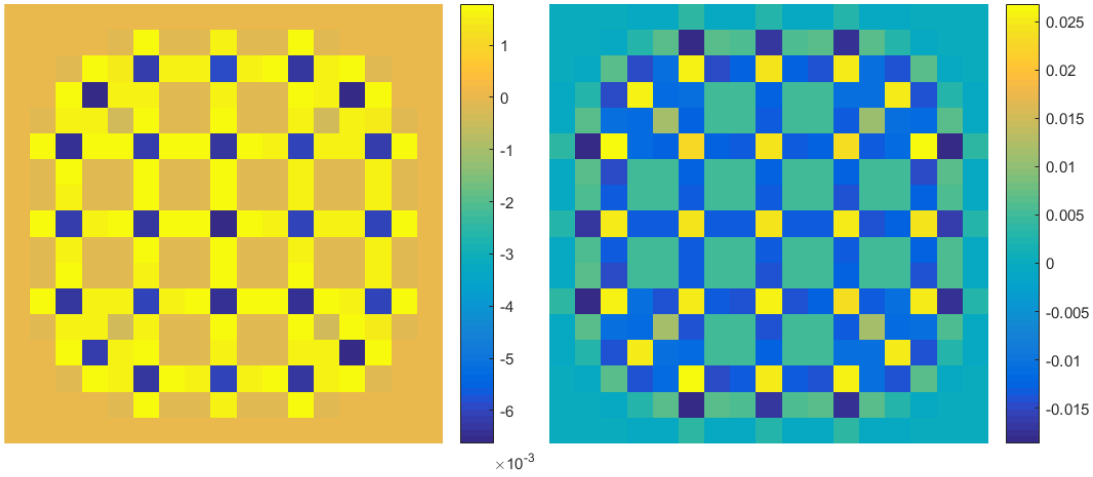

(a) Fast Group (b) Thermal Group

Figure 4.3 Relative difference between MC solution and neutron flux reconstructed using 264 dominant modes

In order to obtain the modal amplitudes using eq. (3.32), the number of tallies should be at least equal to the number of modes in order to have a defined or over-defined linear system of equations. Since the studied hybrid method aims to reduce the computational expenses by keeping a small number of tallies, flux reconstruction with a small number of modes is evaluated.

Reconstruction Using 20 Most Dominant Modes

Tallies of 289 pincells are combined with the most dominant modes corresponding to the largest 20 eigenvalues to reconstruct the MC estimate of the flux distribution. Results are presented in figure 4.4.

Compared to the fundamental mode solution, the error in fuel containing cells is generally reduced when effects of the higher order modes are included. In most fuelled cells, the error in the thermal group is close to 0% and some reductions are noticed in water containing cells where the maximum relative difference is about 5% compared to 6%; the observed maximum error in the fast group is reduced from 1% to about 0.7%. Comparing the case where 264 modes were used in modal expansion, larger differences are noticed especially in water filled

cells. This highlights the importance of truncation errors in the modal expansion series. Results suggest that the use of a larger number of dominant modes could account for errors due to discretisation and physical assumptions.

The amplitudes of the modes employed in flux mapping are shown in table 4.2. As expected, the fundamental mode, which describes the asymptotic flux, has the largest contribution to the general solution. The amplitudes of the higher order modes are very small compared to the fundamental mode which means that the perturbations around the asymptotic distribution are tiny. In a perturbed problem, it is expected that higher order modes would be excited and their amplitudes would be larger. Nevertheless, it is assumed these small excitations have some contribution to the general solution and can be used for reducing the differences between the fundamental mode and the MC reference.

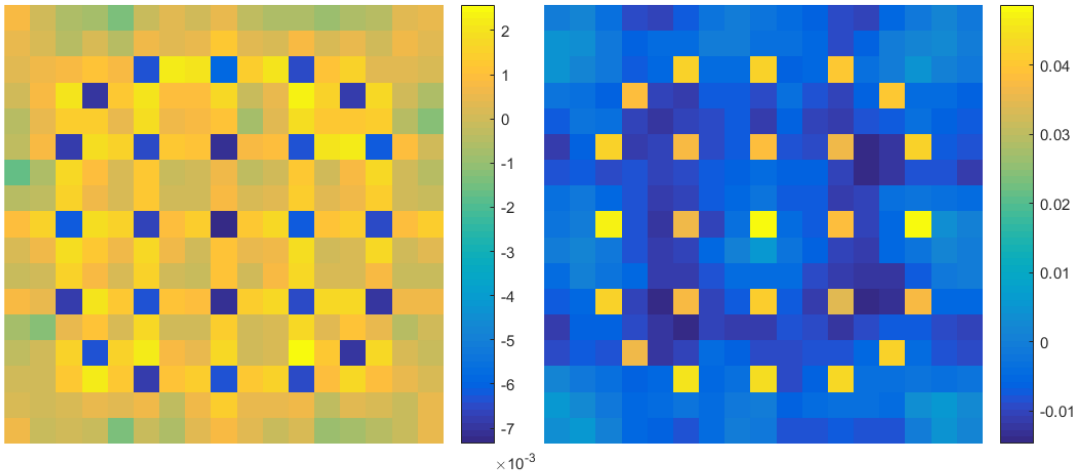

(a) Fast Group (b) Thermal Group

Figure 4.4 Relative difference between MC solution and neutron flux reconstructed using 20 dominant modes

Table 4.2 Absolute value of the amplitudes of the 20 most dominant modes

Mode	a_i^{Fast}	$a_i^{Thermal}$	Mode	a_i^{Fast}	$a_i^{Thermal}$
1	1.70E+01	2.67E+01	11	3.43E-04	4.25E-03
2	2.71E-03	8.87E-03	12	1.78E-03	2.41E-02
3	8.45E-03	2.71E-02	13	2.50E-03	1.07E-02
4	9.57E-03	3.70E-02	14	3.44E-03	1.27E-02
5	6.21E-03	1.28E-01	15	2.00E-03	2.65E-02
6	1.01E-02	3.20E-03	16	6.18E-04	1.16E-02
7	1.20E-02	5.17E-02	17	6.15E-03	8.12E-02
8	1.77E-04	1.51E-02	18	1.66E-03	1.13E-02
9	2.23E-03	1.47E-04	19	1.02E-03	3.01E-02
10	3.19E-03	3.72E-03	20	2.45E-03	7.07E-03

Reconstruction Using 50 Most Dominant Modes

When the number of dominant modes utilised in the modal expansion model is increased to 50, very slight changes are noticed; results are shown in 4.5. Flux reconstruction using 50 dominant modes produces very similar results in both energy groups compared to the case where 20 dominant modes where utilised.

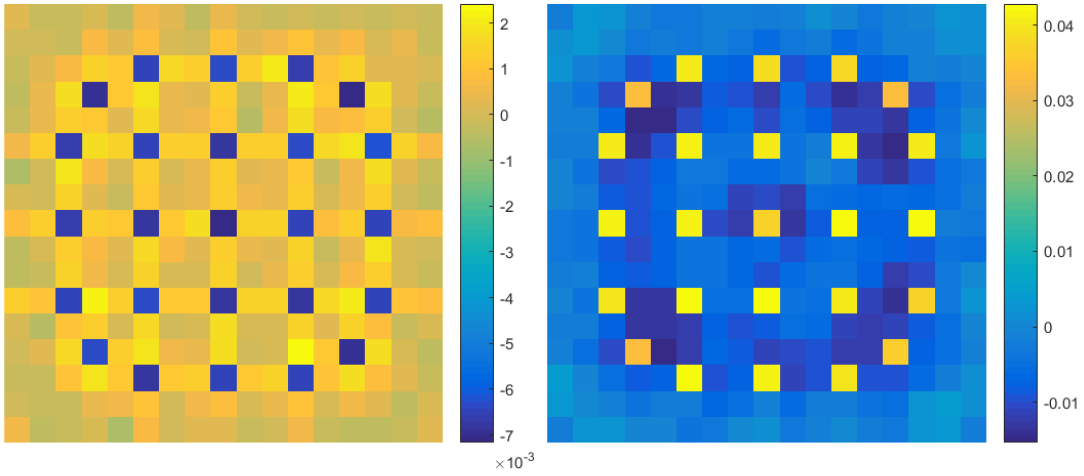

(a) Fast Group (b) Thermal Group

Figure 4.5 Relative difference between MC solution and neutron flux reconstructed using 50 dominant modes

Reconstruction Using 89 Most Dominant Modes

Here, the series expansion is truncated after 89 modes which corresponds to the eigenvectors with eigenvalues greater than or equal to 0.01; it is assumed that eigenvectors with smaller eigenvalues have less important contributions. Results are shown in figure 4.6. Very slight improvements are observed in the accuracy of the flux reconstruction model.

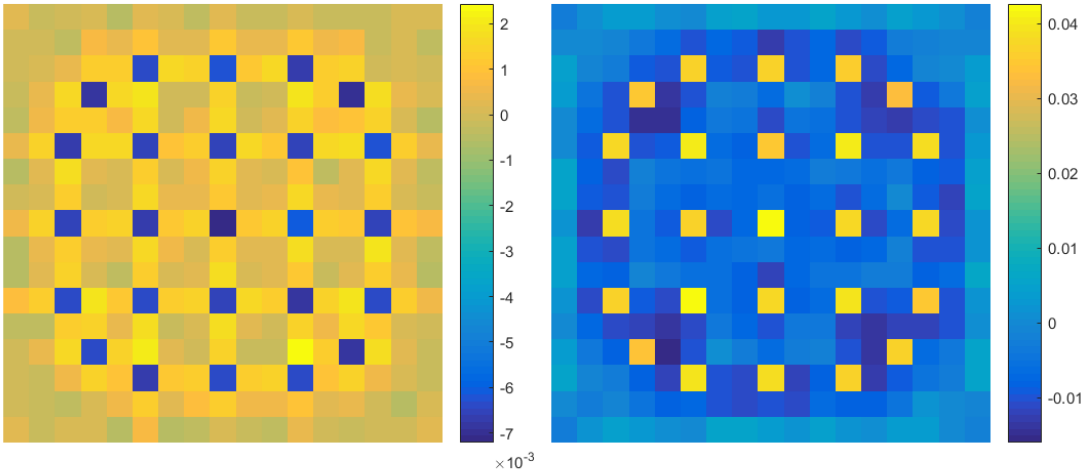

(a) Fast Group (b) Thermal Group

Figure 4.6 Relative difference between MC solution and neutron flux reconstructed using 89 dominant modes

4.2.3 Mapping Optimisation and Error Reduction

Results presented above confirm that a MC estimate of neutron flux distribution can be expressed and reconstructed in terms of the dominant modes of the transport equation. The accuracy of the reconstruction model is sensitive, to some extent, to the number of modes included. When all modes with non-zero eigenvalues are employed, satisfactory results are observed. The accuracy of the modal expansion model in representing a MC estimated flux degrades slightly when the series is truncated at a smaller number of modes. Small errors are observed on the reconstructed flux and these can be attributed to truncation in the series expansion, discretisation in space and any physical assumptions made in deterministic solvers. In general, errors are slightly reduced when the number of modes used is increased to include eigenvectors with non-zero eigenvalues. However, for practical purposes, using a small number of modes is desirable.

Since the aim of the hybrid method is to retain the highest possible accuracy compared to conventional MC, attempts are made to improve flux reconstruction by minimising the errors. For this purpose, the modal expansion model of eq. (3.30) is modified to account for systematic errors:

$$\phi^g(r) = \sum_i a_i \psi_i^g(r) + \epsilon^g(r) \tag{4.1}$$

where $\epsilon(r)$ is the mapping error; or in matrix form:

$$\Phi^g = \Psi^g a + E^g \tag{4.2}$$

where E is a column vector whose elements are the mapping errors.

Uniform Error

For the first attempts, it might be desirable to reconstruct the MC flux with uniform errors in all regions. This would be useful as it is sufficient to calculate this error in a single region to obtain a global estimate. Assuming that ϵ is a uniform function:

$$\epsilon^g(r) = a^* \tag{4.3}$$

where a^* is a constant to be determined, eq. (4.1) becomes:

$$\phi^g(r) = \sum_i a_i \psi_i^g(r) + a^* \tag{4.4}$$

or in matrix form:

$$\Phi^g = \Psi^{g*} a \tag{4.5}$$

where Ψ^{g*} is formed by adding a unity column to the matrix Ψ. Equation (4.5) can be solved using eq. (3.32) and used to reconstruct the MC flux estimate using 20, 89 and 264 dominant modes. Results are shown in figures 4.7, 4.8 and 4.9 respectively.

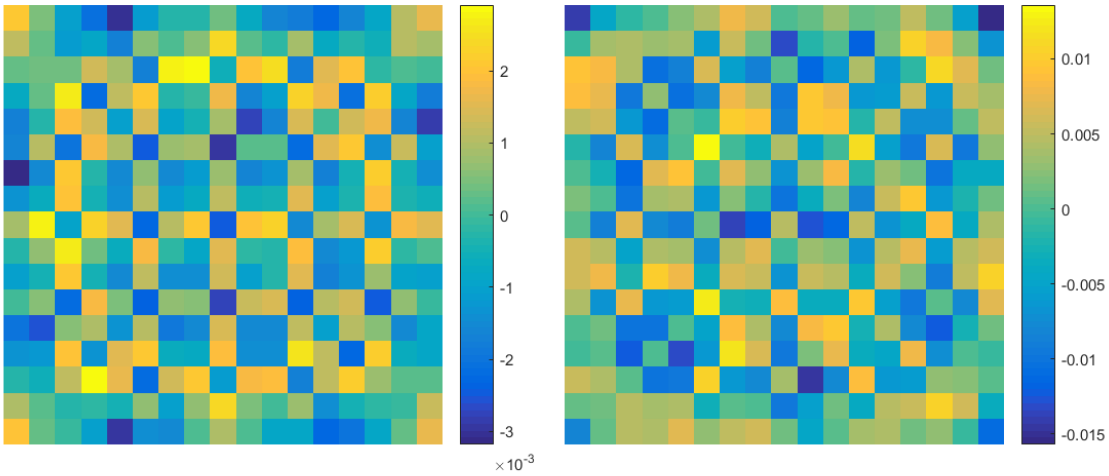

(a) Fast Group (b) Thermal Group

Figure 4.7 Relative difference between MC solution and neutron flux reconstructed using 20 dominant modes assuming uniform mapping error

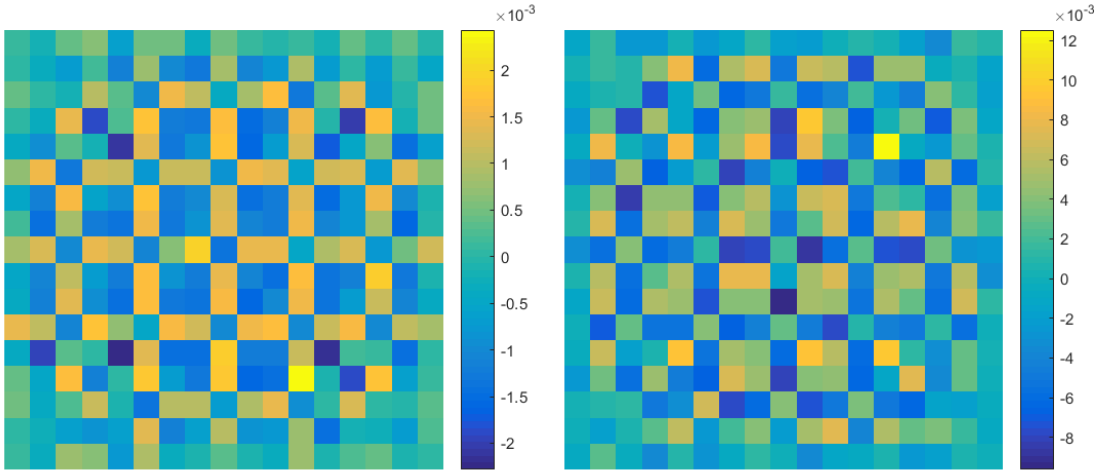

(a) Fast Group (b) Thermal Group

Figure 4.8 Relative difference between MC solution and neutron flux reconstructed using 89 dominant modes assuming uniform mapping error

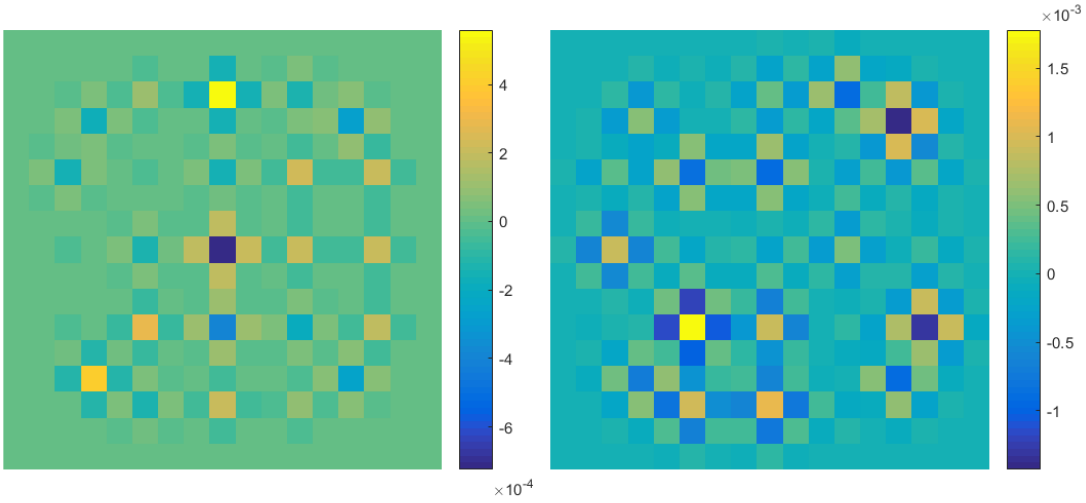

(a) Fast Group (b) Thermal Group

Figure 4.9 Relative difference between MC solution and neutron flux reconstructed using 264 dominant modes assuming uniform mapping error

With the modified model, the relative error on the mapped flux show no preference to the cell type and is more uniformly distributed around 0. In the case where 20 dominant modes are employed, the maximum error in the thermal group is around 1.5% while it is under 0.3% in the fast group. When modal expansion is truncated after 89 modes, the maximum error observed in the thermal group is around 1.2% while it is near 0.2% in the fast group. When all modes with non-zero eigenvalues are employed, the thermal flux is reconstructed with errors no more than 0.2% and the fast flux is reconstructed with errors no more than 0.06%. These are compared to errors that can be up to 4% when no correction is used as shown in figures 4.3 through 4.6.

Errors Related to Absorption

When no correction is applied on the modal expansion model, it is noticed that the largest errors are observed in regions containing no fissile materials, or in other words, regions where scattering interactions dominate over absorption. In such regions, neutron flux peaking occurs and the largest errors in the modal expansion models are scored. In order to improve the modal expansion model, an assumption is made that the error $\epsilon^g(r)$ is inversely proportional to the absorption macroscopic cross section Σ_a^g:

$$\epsilon^g(r) = \frac{a^*}{\Sigma_a^g} \tag{4.6}$$

where a^* is the proportionality constant. The matrix form is similar to eq. (4.5) with Ψ^{g*} formed by adding a column vector containing the inverse of the absorption cross sections to Ψ^g. This assumption is tested by reconstructing the MC estimate of the neutron flux distribution using 20, 89 and 264 dominant modes as shown in figures 4.10, 4.11 and 4.12 respectively.

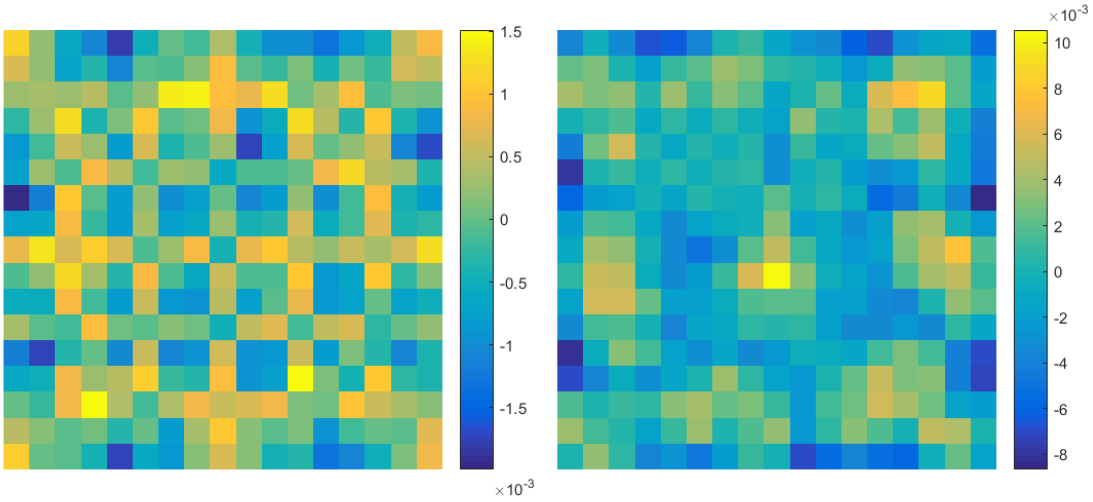

(a) Fast Group (b) Thermal Group

Figure 4.10 Relative difference between MC solution and neutron flux reconstructed using 20 dominant modes assuming absorption related mapping error

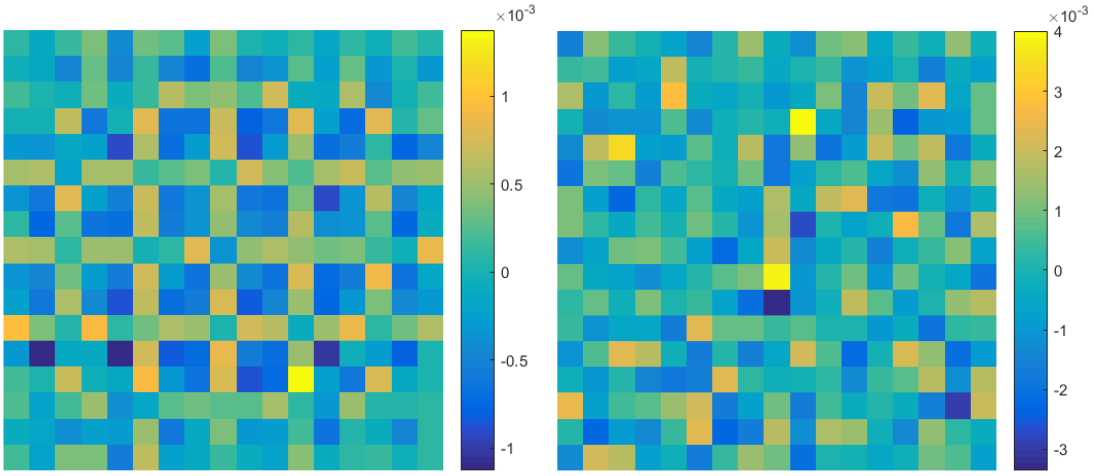

(a) Fast Group (b) Thermal Group

Figure 4.11 Relative difference between MC solution and neutron flux reconstructed using 89 dominant modes assuming absorption related mapping error

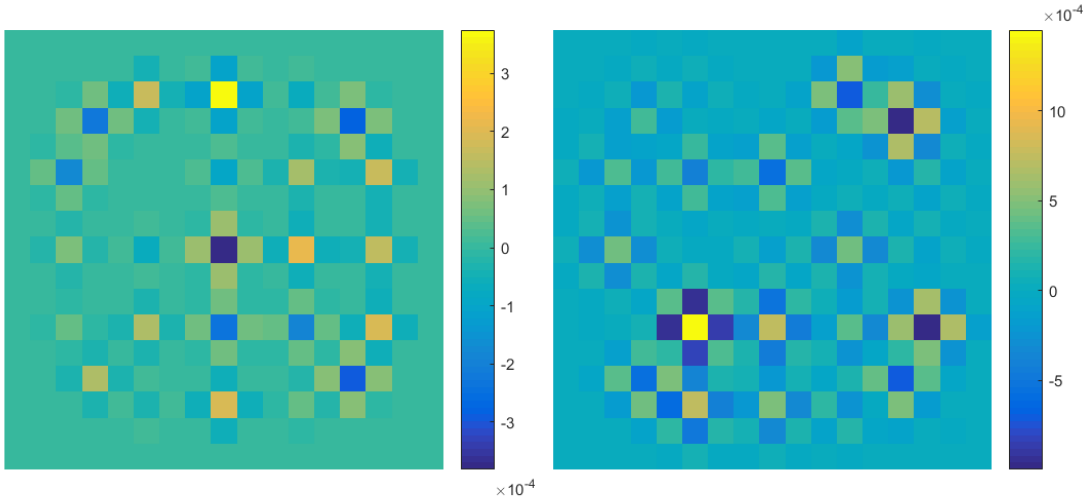

(a) Fast Group (b) Thermal Group

Figure 4.12 Relative difference between MC solution and neutron flux reconstructed using 264 dominant modes assuming absorption related mapping error

In this model for estimating the difference between modal expansion and the MC estimate, the relative error describing the discrepancy is reduced in the thermal group in all cases

compared to the previous results where uniform errors were assumed. The maximum relative difference in the thermal group is 1% when 20 modes are used, and 0.4% when 89 and 264 modes are used. For the fast group, the maximum relative difference is below 0.15% when 20 and 89 modes are used and below 0.04% when 264 modes are used.

All in all, application of the modal expansion model for reconstructing a MC estimate of the neutron flux appears to be mathematically valid; errors can be accounted for by increasing the number of modes in the series expansion and/or modifying the expansion model as discussed.

4.3 MC Flux Reconstruction Using Few Tallies

The aim of the hybrid method as presented in this chapter is to reduce the computation expense through tallying a small number of regions and reconstructing complete neutron flux distribution using dominant modes calculated deterministically. Attempts for reconstructing the neutron flux with few tallies using different number of modes are performed. In all cases, tallies of the neutron flux in 100 pincells, which correspond to about 65% reduction in the number of tallies, are randomly selected and combined with the dominant modes to calculate the modal amplitudes. Error reduction is based on the assumption that mapping errors are inversely proportional to the absorption cross section as described in section 4.2.3.

Reconstruction Using 20 Most Dominant Modes

One hundred pincells are randomly tallied by the MC solver for the neutron flux distribution in two energy groups. The results are combined with 20 dominant modes of the transport equation to calculate the modal amplitudes as given by eq. (3.32); results are shown in figure 4.13.

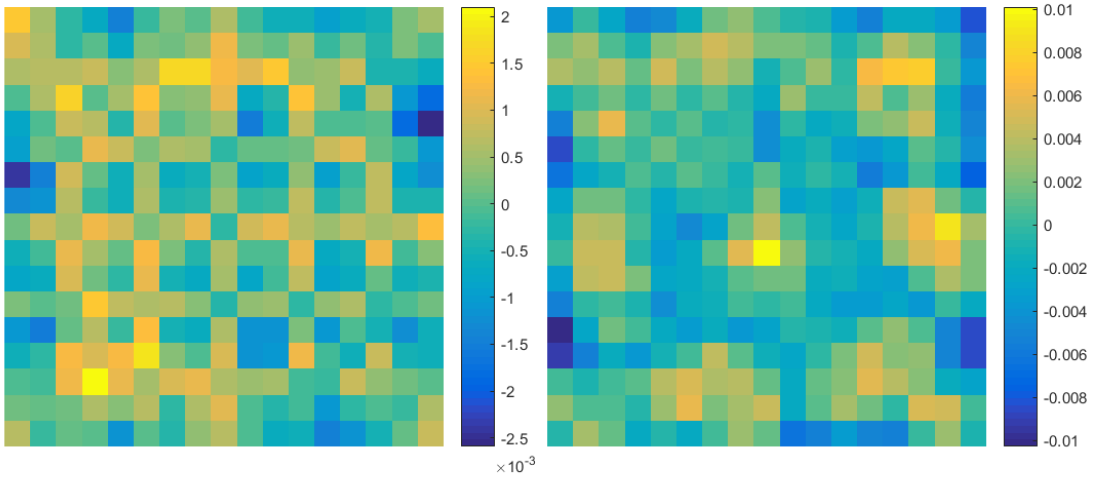

(a) Fast Group - Sample 1

(b) Thermal Group - Sample 1

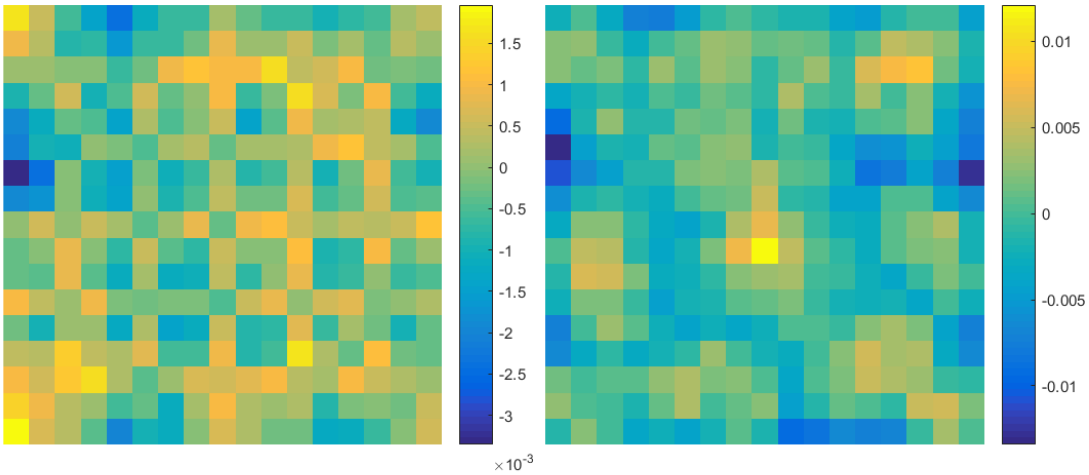

(c) Fast Group - Sample 2

(d) Thermal Group - Sample 2

Figure 4.13 Relative difference between MC solution and neutron flux reconstructed using 20 dominant modes and 100 random tallies

In the first random sample, the maximum relative error on the reconstructed neutron flux in the fast group is 0.25% while a maximum of 1% is observed in the thermal group. In the second sample, the maximum error in the fast group is around 0.3% while it is about 1.5% in the thermal group which is similar to the first sample. In order to test the reliability of random selection of tallies employed in flux mapping, 10000 samples are randomly selected and neutron flux mapping is performed. The maximum absolute error on the reconstructed neutron flux in both energy groups in each sample is recorded and histograms showing their

frequency are produced in figure 4.14.

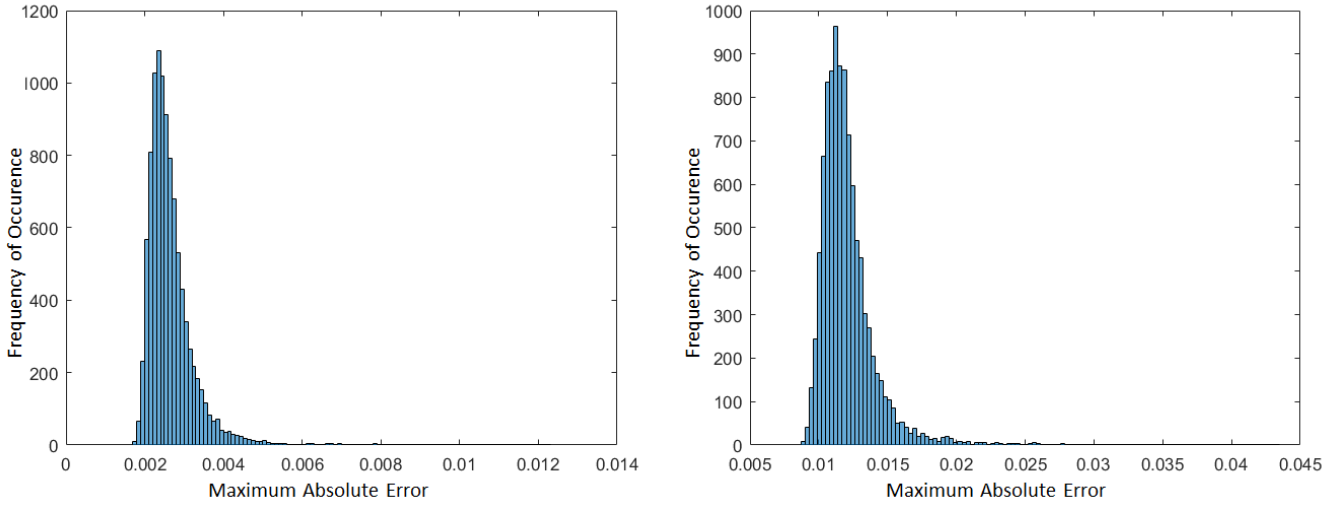

(a) Fast Group

(b) Thermal Group

Figure 4.14 Histogram of the maximum absolute relative error on the reconstructed MC flux using 20 dominant modes and 100 random tallies

In the fast energy group, the maximum absolute error on the reconstructed MC flux in most samples lies between 0.2% and 0.6%; In a very small number of samples, this maximum exceeds 1%. For the thermal group, a maximum relative error between 0.8% and 1.5% is observed in most samples. This maximum could be up to 4% in a very small number of samples. The histogram shows that the maximum relative error is centred around 1.2% in the thermal group and 0.3% in the fast group. These figures are comparable to the case where all the tallies are employed in modal expansion as shown in figure 4.10. This confirms that a MC solution can be reconstructed using the dominant modes of the transport equation and tallies in a small number of regions.

Reconstruction Using 50 Most Dominant Modes

The work described in the previous paragraph is repeated with 50 dominant modes. Results are shown in figure 4.15.

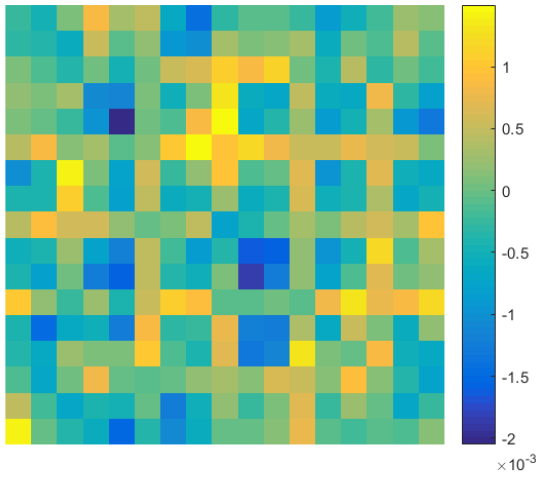

(a) Fast Group - Sample 1

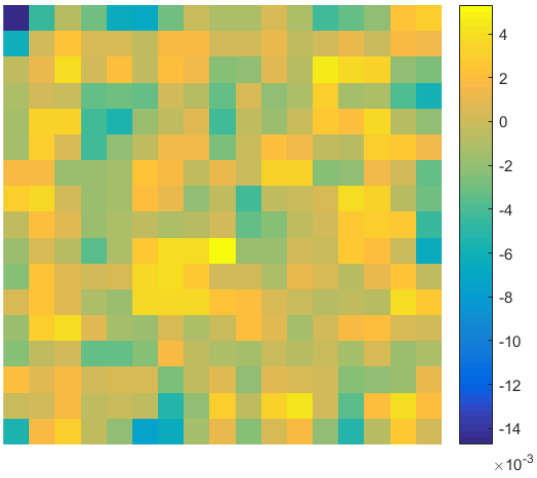

(b) Thermal Group - Sample 1

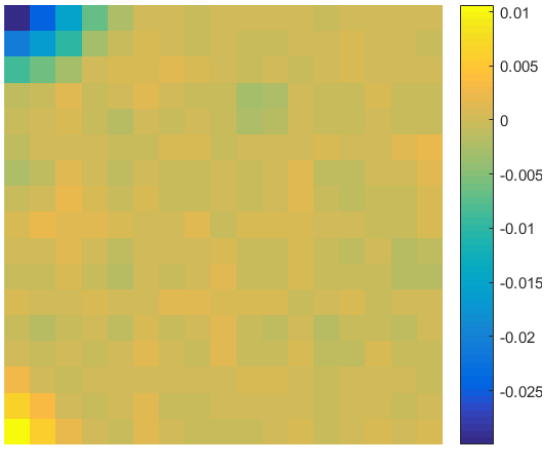

(c) Fast Group - Sample 2

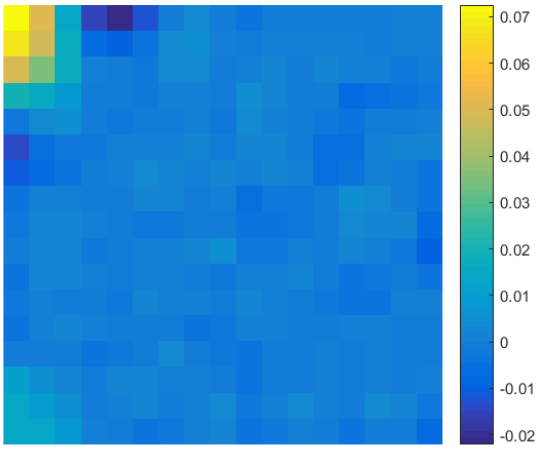

(d) Thermal Group - Sample 2

Figure 4.15 Relative difference between MC solution and neutron flux reconstructed using 50 dominant modes and 100 random tallies

In the first sample, the maximum error is about 0.2% in the fast group and 1.4% in the thermal group. In the second sample the relative error is around 0% in both energy groups; however, relatively large errors (around 3% in the fast group and 7% in the thermal group) are observed in few regions near the corners of the assembly.

To investigate the reliability of random tally selection with 50 modes, histograms of the maximum absolute error from 10000 random samples are produced and shown in 4.16.

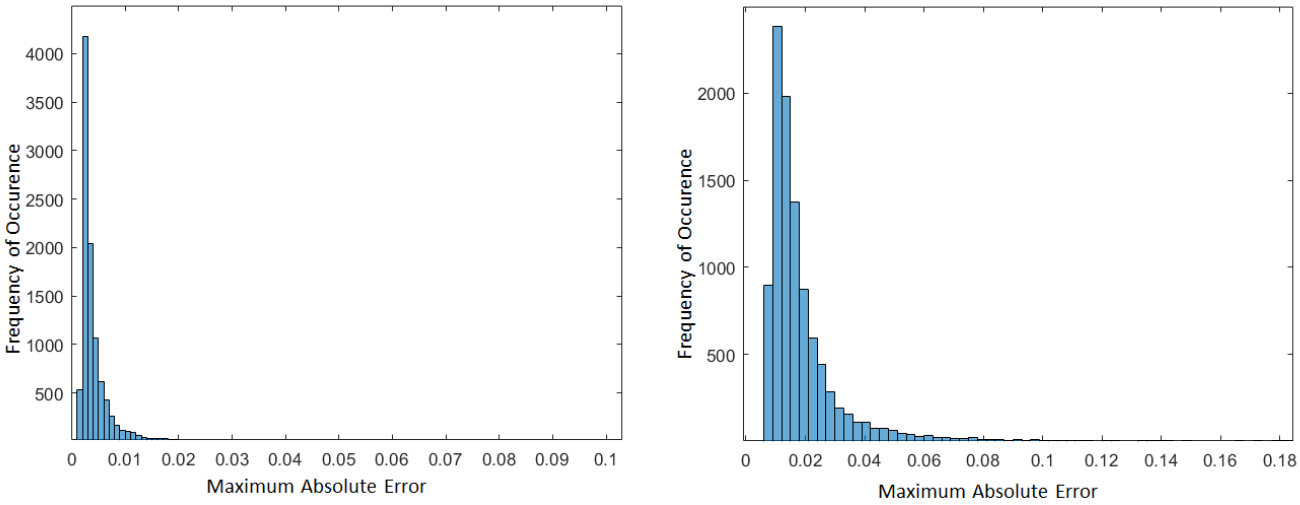

(a) Fast Group (b) Thermal Group

Figure 4.16 Histogram of the maximum absolute relative error on the reconstructed MC flux using 50 dominant modes and 100 random tallies

In most samples, the maximum relative error on the reconstructed neutron flux is below 1% in the fast group and 5% in the thermal group. Significant errors, more than 10% are observed in few samples.

In general, it can be concluded that random selection of tallies is not a reliable approach as significant errors could be observed in some samples. In addition, it is noticed that the ratio of the number of tallies to the number of modes used has some impact on the accuracy of the solution when random selection of tallies is used. Having a larger number of tallies to modes ratio produces more accurate and reliable results. This behaviour can be justified by the intrinsic properties of the least squares method. Least squares aim to obtain a solution that minimises the norm-2 of the residual for the sampled data. Hence, sampling more data points that are less represented by the modal expansion model (such as water filled cells) would lead to larger errors in other regions. In random sampling, no restriction is applied to the type of cells utilised which could lead to the relatively large differences observed in few random samples.

4.3.1 Iteratively Re-weighted Least Square

So far, the un-weighted least squares approach has been used for calculating an approximation of the modal amplitudes. In this method, it is assumed that all regions are equally represented

by the modal expansion model. However, results have shown that the model represents the flux exactly in some regions but considerable errors are observed in other regions. Employing weighted least squares for calculating the modal amplitudes could be a better approach, especially when random selection of tallies is utilised, where the contribution of different regions to the calculation of the amplitudes is weighted according to local accuracy of the modal expansion model.

In weighted least squares, the linear system of equations of eq. (3.31) is solved as:

$$a = (\Psi^{gt} W \Psi^{g})^{-1} \Psi^{gt} W \Phi^{g} \tag{4.7}$$

where W is a diagonal matrix whose elements are the weights of different regions. In this paragraph, the use of Iteratively Re-Weighted Least Squares (IRWLS) [50] approach is proposed where local weights are adjusted iteratively. IRWLS proceeds by an initial guess of the weights, such as uniform weights as in the least squares method, and calculating an initial guess of the modal amplitudes. Neutron flux map is reconstructed using modal expansion and the residual between tallied values and their corresponding reconstructed values are evaluated. The weights are then adjusted for the next iteration; weights of regions where the residual is large are decreased while they are increased in regions where the residual is small. The iteration proceeds until convergence of modal amplitudes is detected against a user specified threshold (for example 10^{-6}).

An example method for weights adjustment is the bisquare function

$$w_i = \begin{cases} \left(1 - \left(\frac{e_i}{l}\right)^2\right)^2 & if\ |e_i| < l \\ 0 & otherwise \end{cases} \tag{4.8}$$

where w_i is the weight of region i, e_i is the relative error between the MC tally and the value obtained by modal expansion as given by eq. (3.33) and l is a tuning factor chosen to be the desired maximum relative error for convenience. Equation (4.8) implies that two types of regions can be distinguished. Regions of non-zero weights are well represented by the modal expansion model and an accurate value in such regions can be obtained by flux synthesis. Regions of zero weights are poorly represented by modal expansion and an accurate value in those regions cannot be obtained by flux synthesis.

To evaluate the efficiency of using IRWLS for estimating the modal amplitudes, reconstruction of the MC flux using tallies in 100 randomly selected pincells and different number of modes is performed. The modified modal expansion model given in eq. (4.1) is employed for the calculation of the modal amplitudes with errors assumed to be related to absorption

cross sections.

IRWLS with 20 Dominant Modes

Iteratively re-weighted least squares is tested for reconstructing the neutron flux distribution obtained by MC from tallies in 100 randomly selected pincells. The modal expansion model is truncated after 20 dominant modes. The tuning factor is taken to be 0.01, i.e. the desired maximum relative error on the reconstructed flux is 1%. Results for two random samples are presented in figure 4.17.

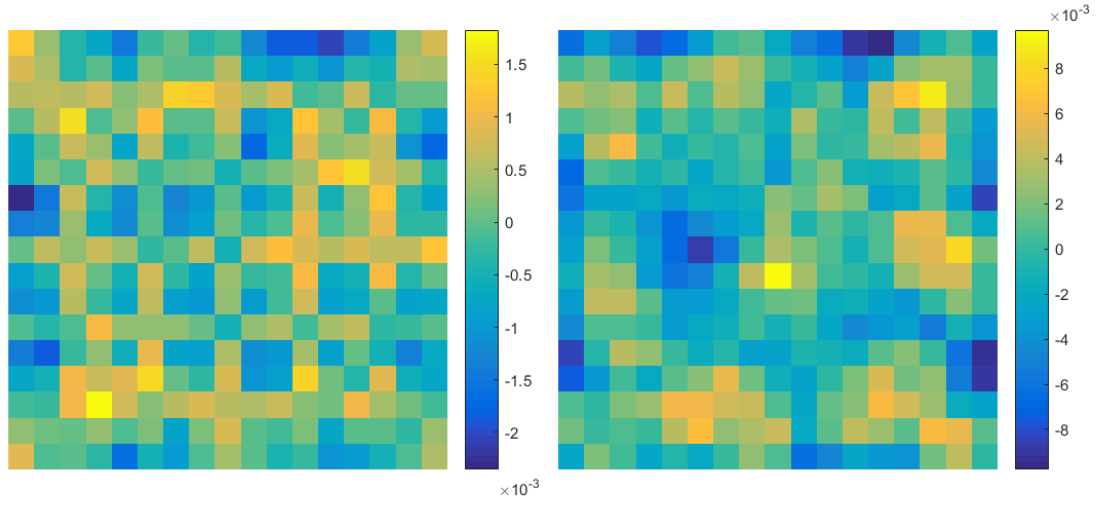

(a) Fast Group - Sample 1

(b) Thermal Group - Sample 1

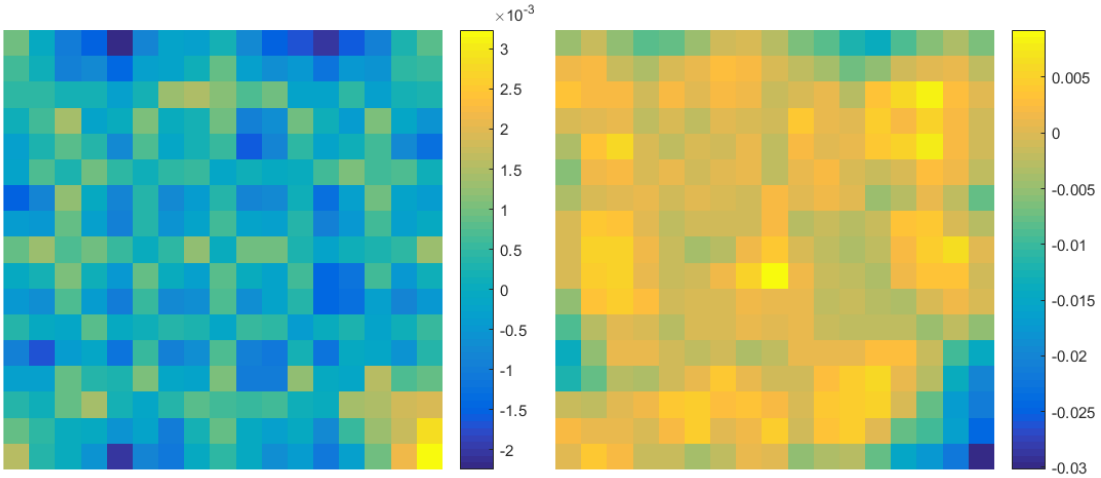

(c) Fast Group - Sample 2

(d) Thermal Group - Sample 2

Figure 4.17 Relative difference between MC solution and neutron flux reconstructed using 20 dominant modes and 100 random tallies with IRWLS

Results show that, in the first sample, IRWLS succeeds in reconstructing the neutron flux from 100 random tallies while keeping the maximum relative error below the desired value. For the first sample, the maximum relative error in the thermal group is around 0.8% while it is around 0.2% in the fast group. However, in the second sample, errors exceeding the desired maximum in the thermal group are observed in few regions.

To test the reliability of the IRWLS approach, histograms of the maximum absolute relative

error scored in 10000 random samples are produced and shown in figure 4.18.

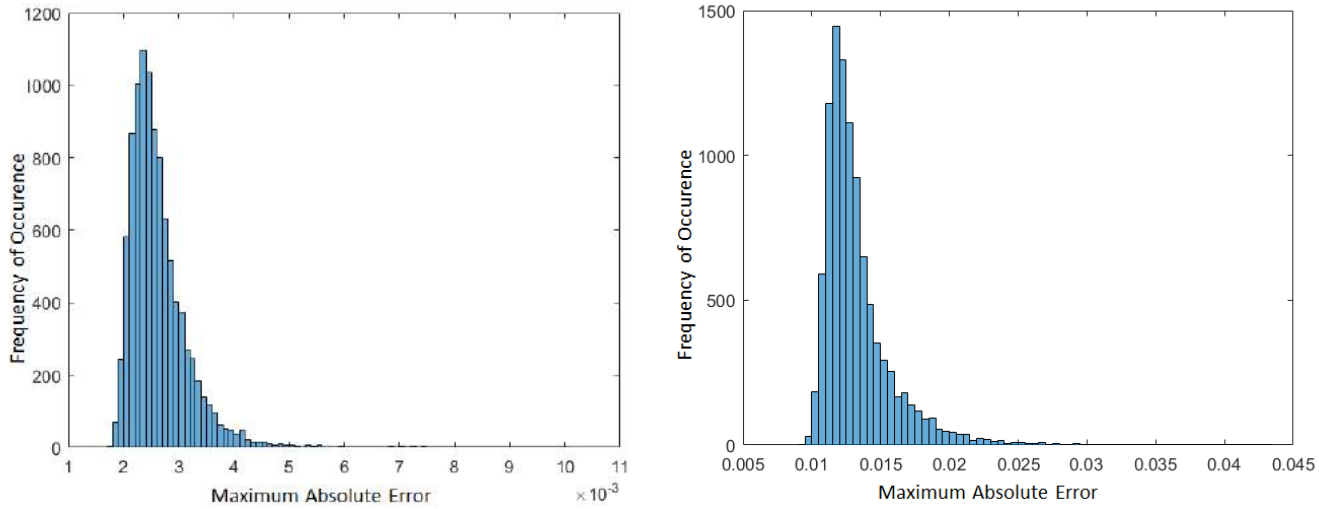

(a) Fast Group (b) Thermal Group

Figure 4.18 Histogram of the maximum absolute relative error on the reconstructed MC flux using 20 dominant modes and 100 random tallies with IRWLS

Compared to the case where least squares were used for estimating the modal amplitudes, as shown in figure 4.14, IRWLS appears to be more reliable when random tallies are used; the number of samples with a maximum relative difference of 1.2% is near 1500 sample with IRLWS compared to less than 1000 for least squares. In most cases, the maximum relative error is within 2% in the thermal group and an increase in the number of samples with a maximum error of around 1.2% is noticed. In the fast group, the vast majority of samples show a maximum error less than 0.5%.

IRWLS with 50 Dominant Modes

The work described in the previous paragraph is repeated with modal expansion truncated after 50 modes. As presented in figure 4.19, IRWLS reconstructs the neutron flux distribution from 100 random tallies with relative errors below the desired maximum. In the second sample, large errors (around 6%) in the thermal group are observed in the reconstructed thermal flux which implies that random sampling combined with IRWLS could produce unsatisfactory results.

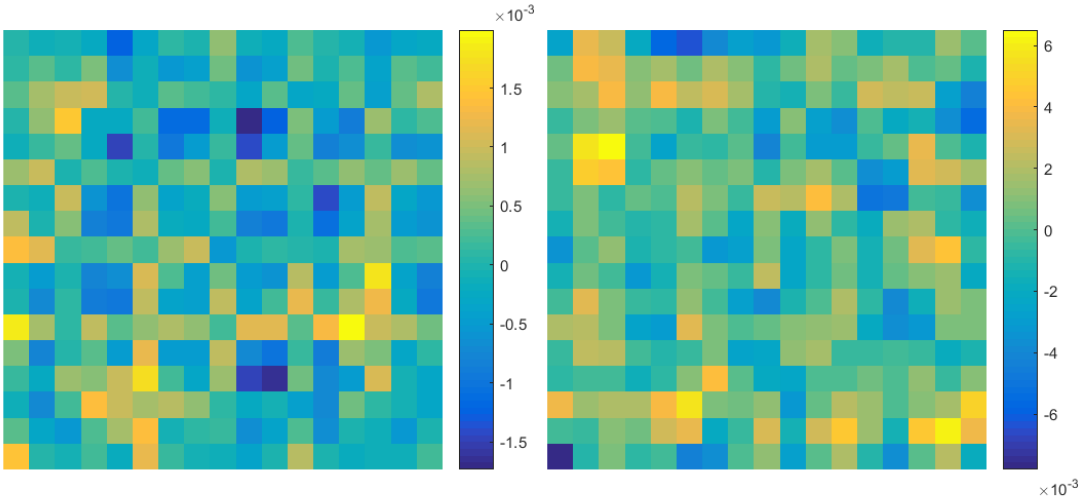

(a) Fast Group - Sample 1

(b) Thermal Group - Sample 1

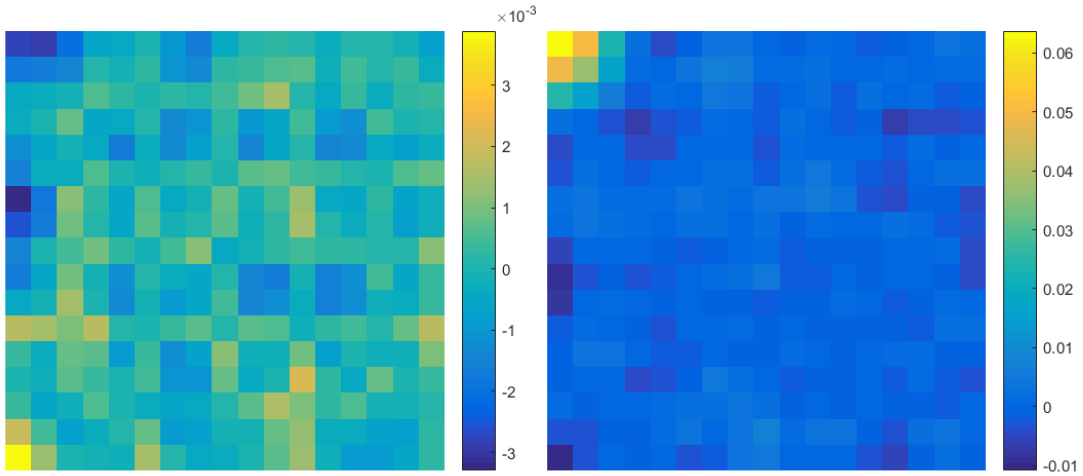

(c) Fast Group - Sample 2

(d) Thermal Group - Sample 2

Figure 4.19 Relative difference between MC solution and neutron flux reconstructed using 50 dominant modes and 100 random tallies with IRWLS

To test the reliability of the IRWLS approach for calculating the modal amplitudes, a histogram of the maximum relative error in the thermal and fast group from 10000 random samples is shown in figure 4.20. Again, it can be deduced that IRWLS is more robust compared to the least squares approach. However, random sampling cannot be trusted as in considerable number of samples, irrelevant of the number of modes, unacceptable errors are observed.

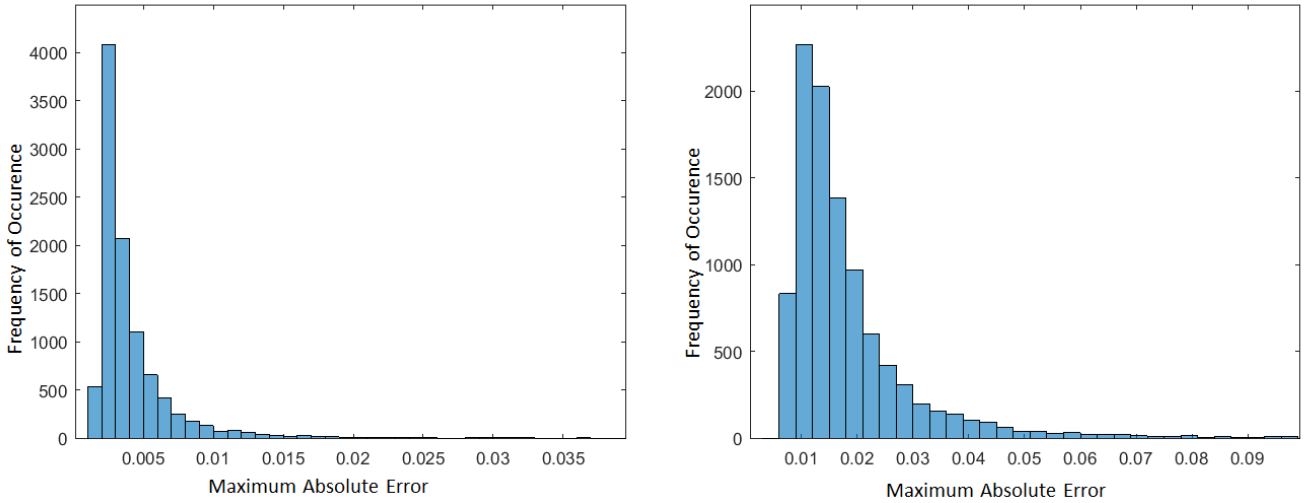

(a) Fast Group (b) Thermal Group

Figure 4.20 Histogram of the maximum absolute relative error on the reconstructed MC flux using 50 dominant modes and 100 random tallies with IRWLS

4.3.2 Tally Selection Procedure

Irrespective of the number of modes or tallies, random selection of regions to be tallied does not guarantee acceptable results. Results produced in the previous sections show that a criteria or methodology for selecting which tallies to be employed in the calculation of modal amplitudes is necessary.

The iteratively re-weighted least squares approach with the bisquare function can be utilised for defining which regions to be tallied by the MC solver. As implied in eq. (4.8), the bisquare function differentiates between two types of regions. Regions with non-zero weights are well represented by the modal expansion model and an accurate value of the neutron flux in these regions can be obtained by flux synthesis. Regions with zero weights are poorly represented by modal expansion and an accurate value cannot be obtained by flux synthesis; hence tallying of these regions by the MC solver is necessary. For the PWR example studied in this chapter, weights of different cells are evaluated using IRWLS and modified modal expansion using 20 and 50 dominant modes with a desired maximum relative error of 1%; those are shown in figure 4.21 and 4.22. In both cases, the weights of all cells in the fast group are close to unity. When 20 modes are used, weights of different cells in the thermal group range between zero and unity with most cells having weights greater than 0.6. When 50 modes are used, cells in the thermal group have a weight greater than 0.6 which means

that truncating the series expansion after 50 modes would allow reconstructing the neutron flux with 1% accuracy.

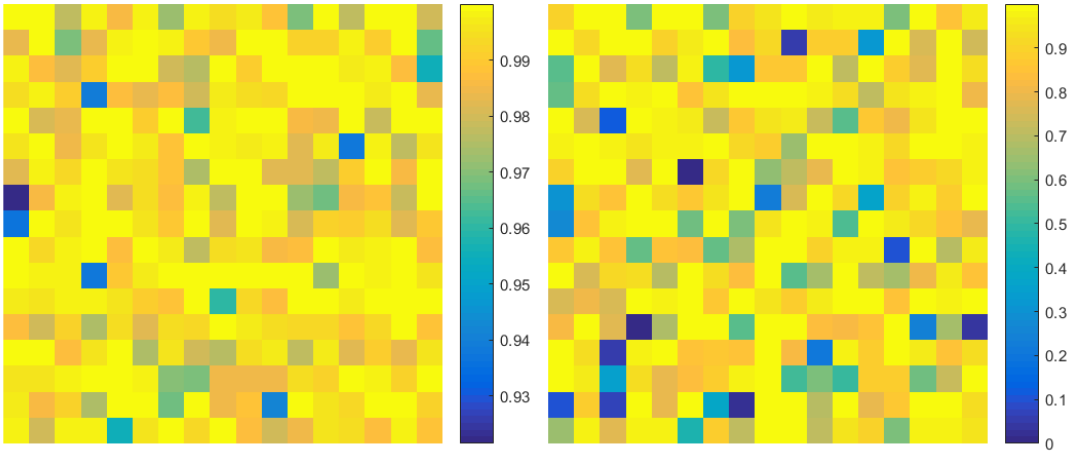

(a) Fast Group (b) Thermal Group

Figure 4.21 Weights of different cells in the calculation of modal amplitudes as determined by IRWLS using 20 dominant modes

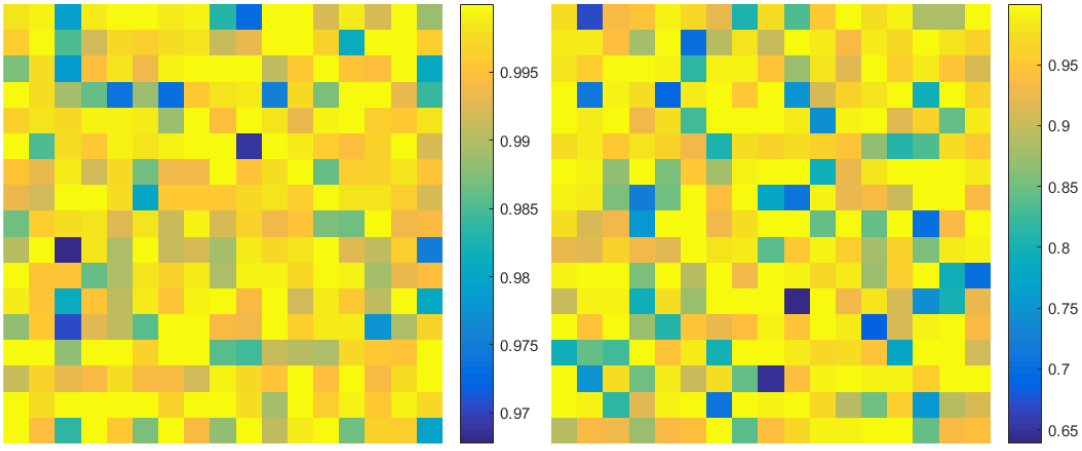

(a) Fast Group (b) Thermal Group

Figure 4.22 Weights of different cells in the calculation of modal amplitudes as determined by IRWLS using 50 dominant modes

Assuming that a rough estimate of the neutron flux distribution can be calculated by a low order approximation of the transport equation, such as diffusion, reconstruction of the low order solution using modal expansion and flux values in all regions with IRWLS would allow calculation of local weights of different regions. Based on the calculated weights, a number of regions with the highest weights are tallied and employed in the estimation of the modal amplitudes; regions with low weights are also tallied by the MC solver but not utilised in flux synthesis. For the same PWR assembly, a diffusion solution is obtained and weights of different cells are evaluated using 20 and 50 modes with the desired maximum error being 1%. Results are produced in figures 4.23 and 4.24.

Again, the weights of different regions in the fast group are close to unity in both cases. For the thermal group, a reduction in the weights of different cells is observed in both cases which is an expected result. Despite the noticeable differences in the weights between diffusion and MC, the former can still be used to decide which cells are to be scored by the stochastic solver and used in flux synthesis.

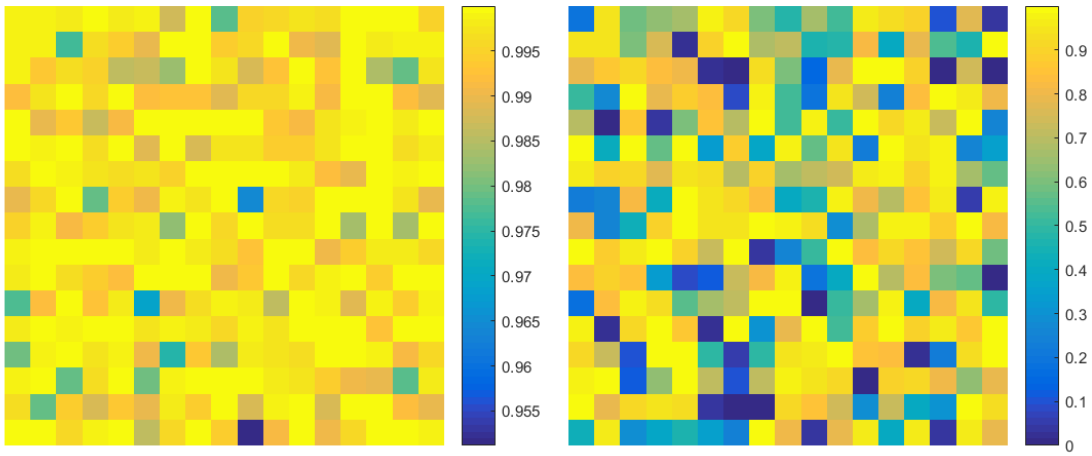

(a) Fast Group (b) Thermal Group

Figure 4.23 Weights of different cells in the calculation of modal amplitudes as determined by IRWLS using 20 dominant modes and a diffusion solution

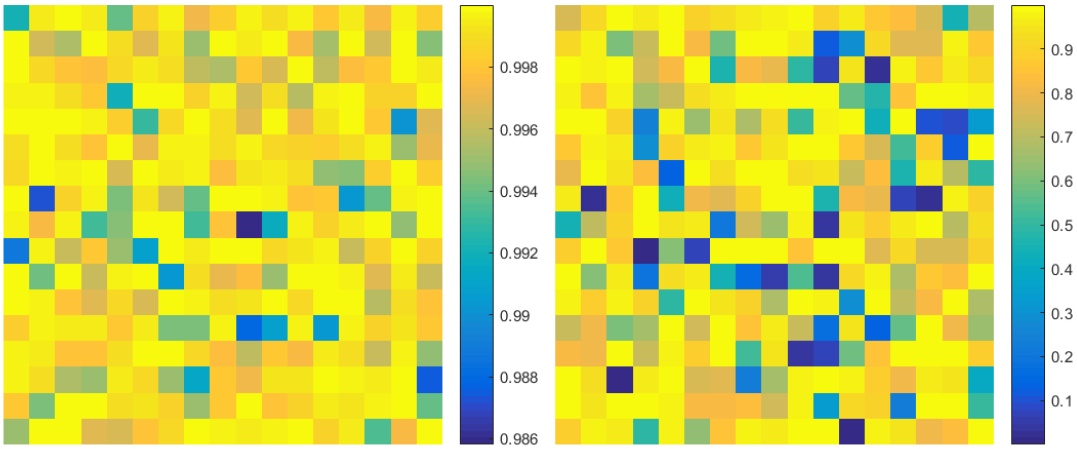

(a) Fast Group (b) Thermal Group

Figure 4.24 Weights of different cells in the calculation of modal amplitudes as determined by IRWLS using 50 dominant modes and a diffusion solution

To apply the tally selection procedure, the low order solution (diffusion) is first used to evaluate local weights of different regions. Next, a pre-determined number of regions of largest non-zero weights, determined by IRWLS with the diffusion solution, are used for solving the modal amplitudes as given in eq. (4.7). The neutron flux map is then reconstructed. Regions with zero weights (6 pincells in the studied case) are also tallied to guarantee an accurate value in these regions. To test this approach, the neutron flux distribution is reconstructed from 20 and 50 dominant modes using tallies in 100 pincells of the largest weights. Results are produced in figure 4.25 and 4.26 respectively.

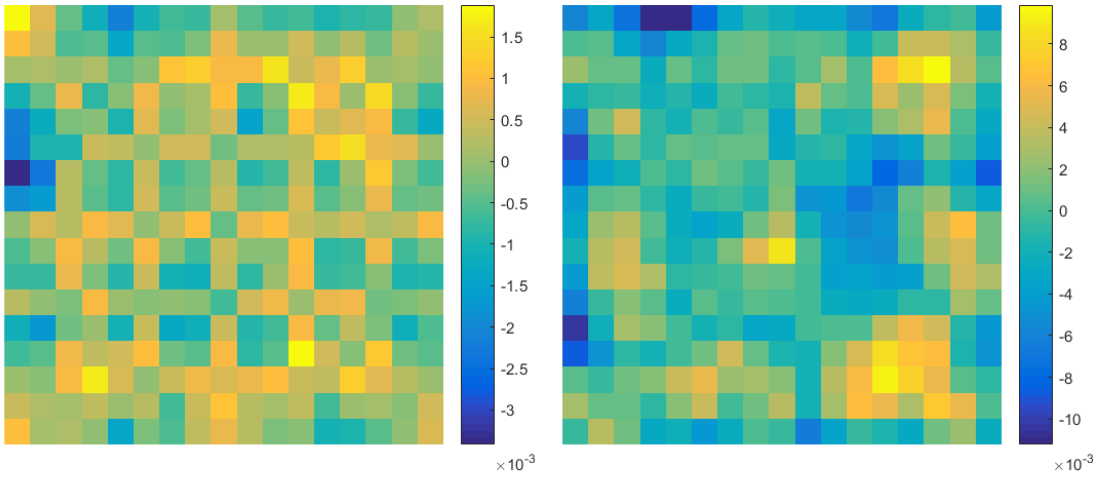

(a) Fast Group (b) Thermal Group

Figure 4.25 Relative error on the reconstructed neutron flux from tallies in 100 cells of largest weights and 20 modes

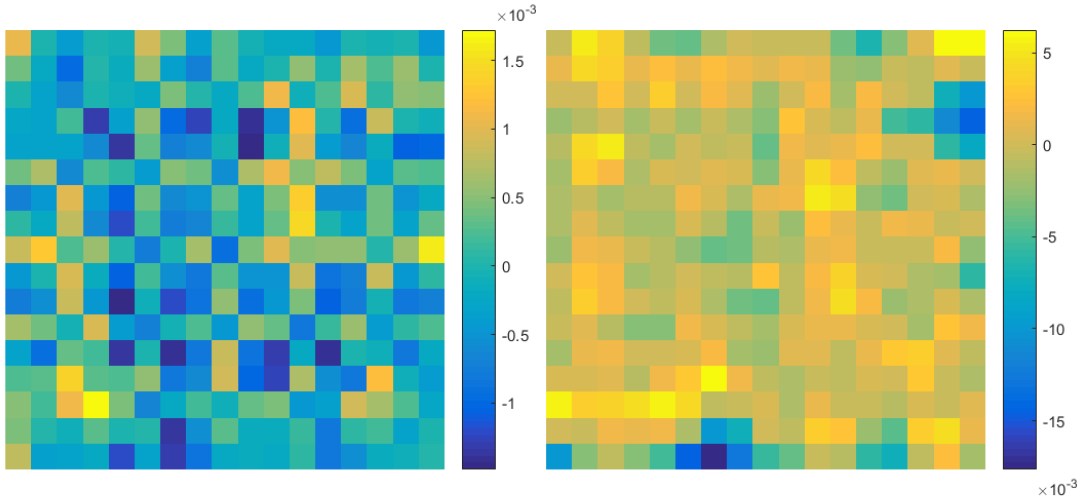

(a) Fast Group (b) Thermal Group

Figure 4.26 Relative error on the reconstructed neutron flux from tallies in 100 cells of largest weights and 50 modes

Results confirm that the tally selection procedure is efficient for deciding which tallies to be used in flux synthesis. For the case of 20 modes, the maximum error in the thermal group is

roughly 1% while it is below 0.4% in the fast group. For the case of 50 modes, the maximum error in the thermal group is around 1.6% and less than 0.2% in the fast group. These results again signify the importance of having a relatively large number of modes to number of tallies ratio in the calculation of modal amplitudes.

4.4 Summary

In this chapter, the feasibility of reconstructing the neutron flux distribution on a unit cell level by combining neutron flux tallies in few regions with the dominant modes of the transport equation is investigated. Expansion of the neutron flux distribution in terms of the dominant modes is a feasible approach for obtaining a solution that is comparable in accuracy to a stochastic solution. Results presented in this chapter prove that a MC solution can be reconstructed to an acceptable accuracy from tallies in a small number of regions by using flux synthesis. Effects of truncating the number of modes in flux synthesis are evaluated; results show that considerable errors are observed when some of the eigenvectors with non-zero eigenvalues are ignored. However, truncation errors as well as errors caused by other factors can be accounted for by modifying the modal expansion model. Reconstruction of the neutron flux from tallies selected randomly cannot be reliable irrespective to the number of modes used. A tally selection criteria based on IRWLS for the calculation of modal amplitudes is presented. Results confirm that the proposed hybrid method is capable of achieving 65% reductions in the number of tallies in the studied example while maintaining 1% accuracy compared to MC.

CHAPTER 5 PRACTICAL IMPLEMENTATION AND APPLICATION

In the previous chapters, the calculation of the dominant modes of the transport equation and their application in neutron flux synthesis are described. The concept of a hybrid method based on combining MC with deterministic flux synthesis for reducing the computation costs of full core MC calculations, through minimising the number of tallies scored, is introduced. Alternatively, the concept of combining coarse mesh MC tallies with the dominant modes for reconstructing a fine mesh solution can be employed for minimising the number of neutron histories to be tracked and the number of tallies scored. Hence, significant reductions in the computational costs in full core calculations can be achieved. In this chapter, the hybrid method is optimised to allow significant reductions in the computational costs. The method is applied to study a number of 2D and 3D example problems. The accuracy of the approach and its performance are evaluated.

5.1 Improved Hybrid Method

When accounting for burnup or multiphysics feedback, the neutron flux must be known on a very fine mesh. In this case, full core MC calculations become extremely computationally expensive where both the number of neutron histories for acceptable statistics and the number of tallies scored become very large. To address the computational burden in such cases, the hybrid method is developed to reconstruct a fine mesh neutron flux distribution from a coarse mesh solution.

As presented in section 3.4, a fine mesh solution can be reconstructed from a coarse mesh solution using the dominant modes of the transport equation. The basic concept of the presented hybrid method is to perform a full core MC simulation with detailed geometry definition and score the tallies on a coarse mesh covering the full spatial domain with low statistical error and reconstruct a fine mesh solution, required for burnup and optimisation studies, using the modes of the transport equation. The simulation would proceed with the MC simulation. A number of inactive cycles are executed to converge the fission source; acceleration techniques described previously may be used to reduce the number of inactive cycles. Then, the active cycles are started and sufficient number neutron histories for low statistical error are tracked. The output of the active cycles would be the neutron flux scored on a coarse mesh over the full core and macroscopic neutron cross sections required for solving the transport equation and obtaining the high order modes in a single unit cell or assembly. Once the modes are obtained, the coarse mesh MC solution and the fine mesh transport

modes are combined together to estimate the modal amplitudes and reconstruct a fine mesh solution. By following this approach, a full core neutron flux distribution is obtained on a fine mesh with an accuracy which is comparable to the MC method while keeping the computational expenses reasonably low. The approach is summarised in the flow chart of figure 5.1.

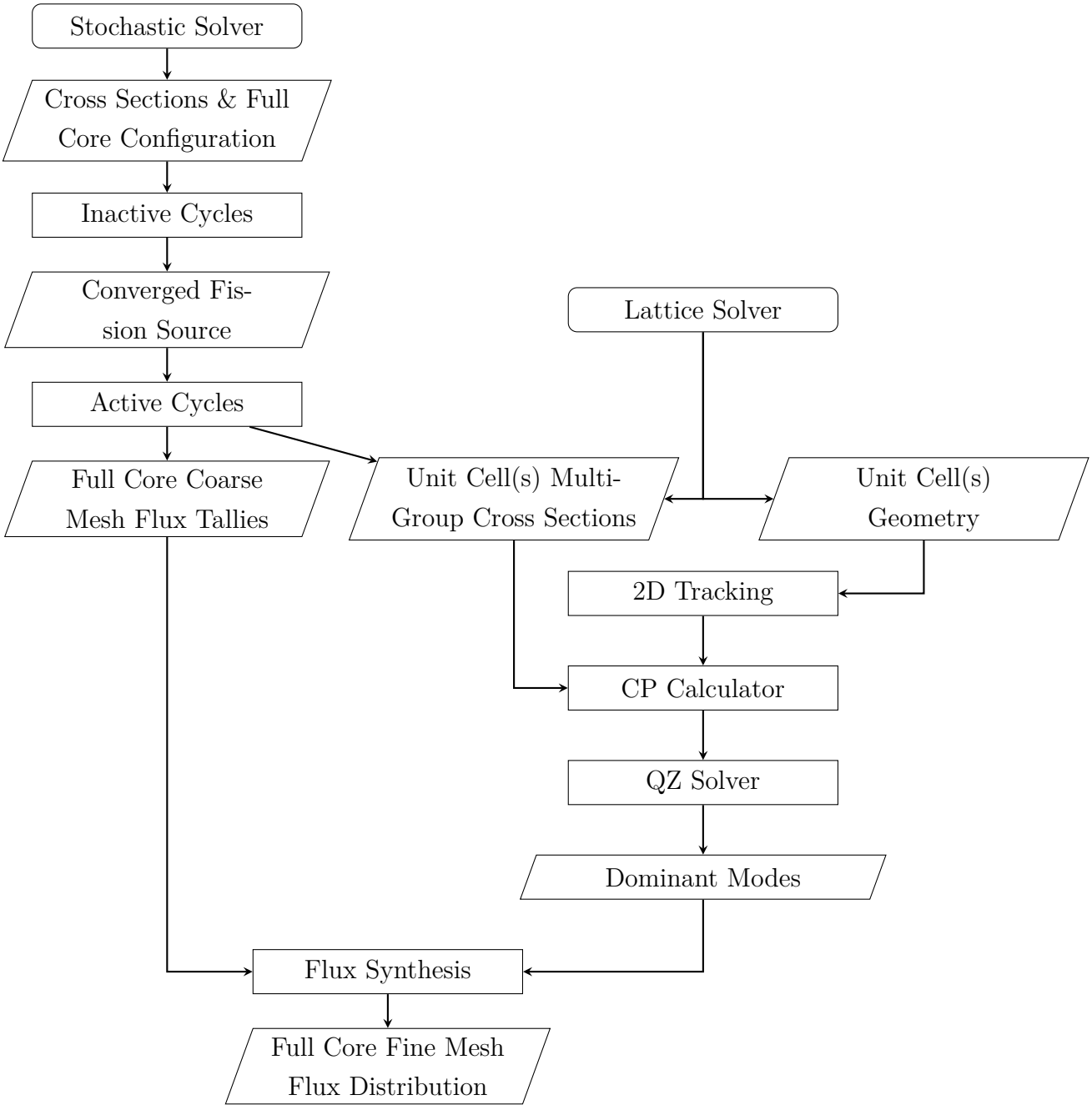

Figure 5.1 Flow chart of the hybrid method

5.2 Application to Single Fuel Assembly

The above described approach is applied for studying the neutron flux distribution in the 2D PWR 17×17 fuel assembly described in section 4.2. In this section, it is desired to obtain the neutron flux distribution on a very fine spatial mesh. Hence, in each fuel cell, the fuel pellet is split radially into 10 burnup zones, the cladding and the coolant channel are each treated as single region; water filled guide tubes are split into 3 radial regions. The MC code *Serpent* [24] is used to simulate the exact problem with reflective boundary conditions and obtain a reference neutron flux distribution in two energy groups. The neutron flux distribution in the two energy groups is shown in figure 5.2; the flux is normalised such that the euclidean norm of the vector Φ is unity. The standard deviation on the shown solution is below 0.5% and 1% in the fast and thermal groups respectively.

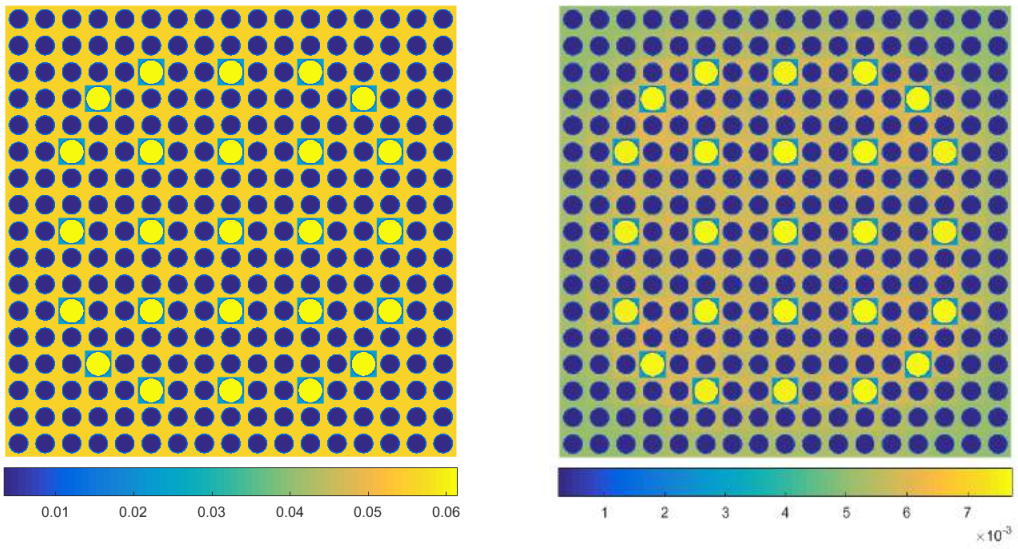

(a) Fast Group (b) Thermal Group

Figure 5.2 Reference fine mesh MC solution for the neutron flux in a PWR assembly

In the next paragraphs, attempts are made to obtain the fine mesh solution presented in figure 5.2 starting with a fine mesh solution and the dominant modes of the transport equation.

5.2.1 Cross Sections Generation and Modes Calculation

As described in the flowchart of figure 5.1, an output of the MC solver is multigroup neutron cross sections homogenised over the spatial mesh. Typically, a number of cells of similar

properties are spatially homogenised together for the calculation of cross sections.

In order to determine which cells are homogenised together, the MC solver is employed to tally one energy group neutron flux distribution and the fission interaction rates; the ratio between the two distributions is the one group fission cross section. Considering the values of the fission cross sections in different regions, those with similar values can be homogenised together. In figure 5.3a, one group neutron macroscopic total cross section are plotted where 5 groups of cells can be identified as shown in figure 5.3b.

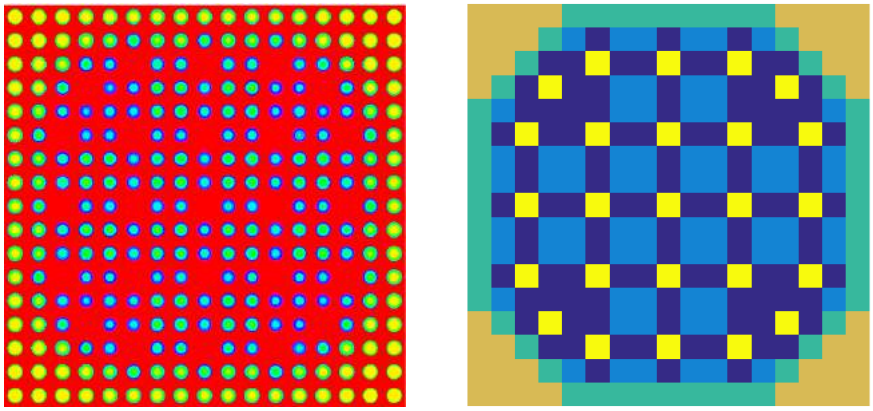

(a) One Group Fission Cross Sections

(b) Cell Grouping

Figure 5.3 Calculation of the macroscopic cross sections in the MC solver

5.2.2 Fine Mesh Flux Reconstruction

The hybrid method is applied to reconstruct the neutron flux distribution shown in figure 5.2 starting from the flux distribution in homogenised fuel cells as given in figure 4.1. Since the modal amplitudes in the expansion model of eq. (3.30) are assumed independent of the spatial mesh, they can be calculated using coarse mesh flux tallies and dominant modes then employed in flux reconstruction on a fine mesh.

Using the cell grouping shown in figure 5.3, the total, scattering, and fission production cross sections are homogenised per mesh element for two energy groups. These are fed to the deterministic solver where geometry tracking and collision probabilities are evaluated to calculate the assembly dominant modes of the transport equation on a fine mesh of 10 radial zones per fuel pellet. The modes are combined with the neutron flux distribution estimated by *Serpent* in homogenised pincells, shown in figure 4.1, in order to estimate the modal amplitudes using eq. (3.32). Once the modal amplitudes are obtained, a fine mesh neutron flux distribution is reconstructed and compared to the reference solution presented in figure

5.2.

The approach is applied to reconstruct the neutron flux using 20, 50, 89 and 200 dominant modes. The relative errors between the flux reconstructed using modal expansion and the reference MC solution are evaluated and plotted in figures 5.4 through 5.7. In the case where 20 dominant modes are used, the fine mesh solution is reconstructed with an accuracy of 1.2% in the fast group and 3% in the thermal group. When 50 modes are used, very similar results are observed in the fast group and slight improvements are noticed in the thermal group where the maximum relative error is 2.5%. Using a larger number of modes in the modal expansion series does not bring much changes. Given that the standard deviation on the reference solution is around 1%, the results produced by flux synthesis can be considered to be satisfactory.

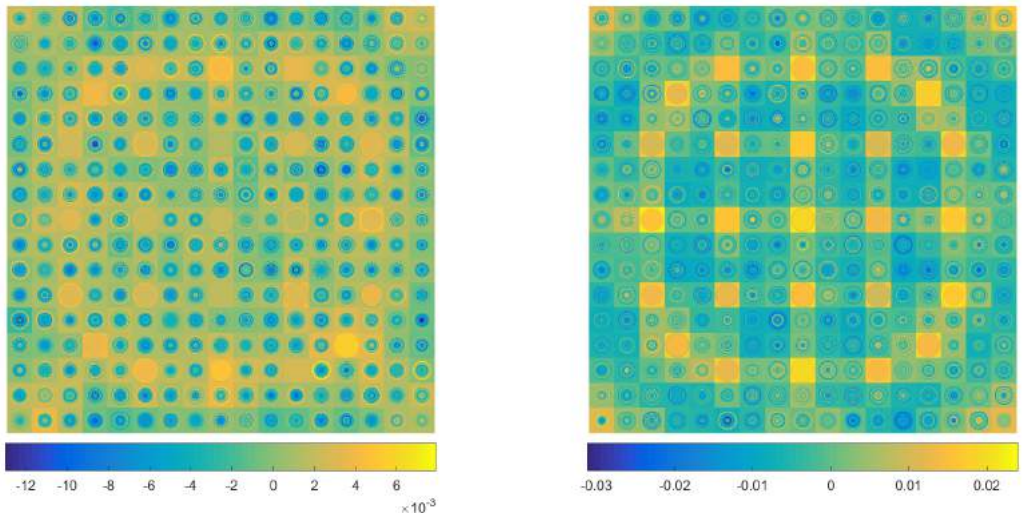

(a) Fast Group (b) Thermal Group

Figure 5.4 Relative errors between reference fine mesh MC solution and the flux reconstructed from 20 dominant modes

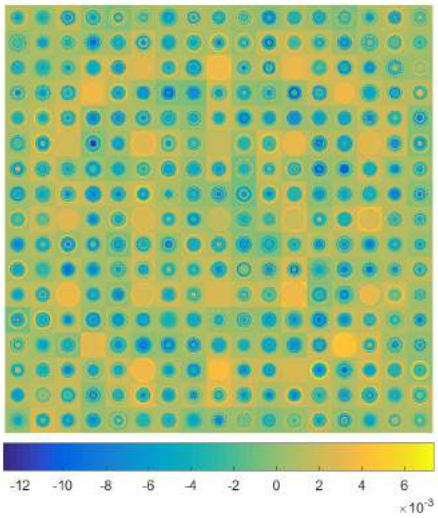

(a) Fast Group

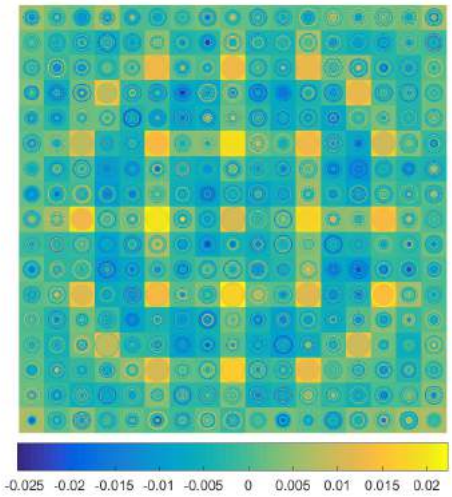

(b) Thermal Group

Figure 5.5 Relative errors between reference fine mesh MC solution and the flux reconstructed from 50 dominant modes

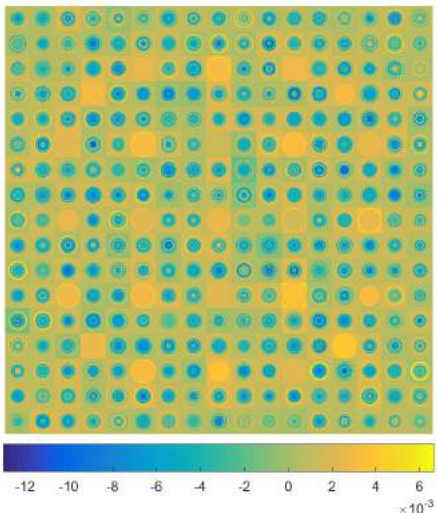

(a) Fast Group

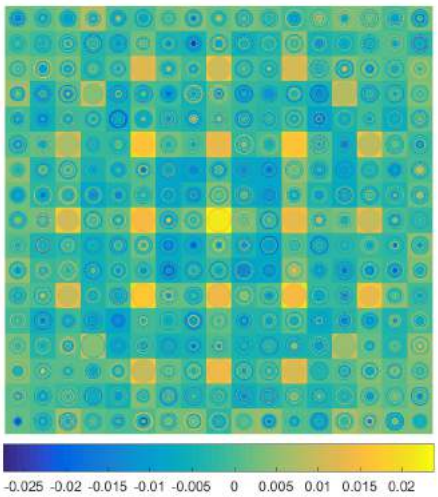

(b) Thermal Group

Figure 5.6 Relative errors between reference fine mesh MC solution and the flux reconstructed from 89 dominant modes

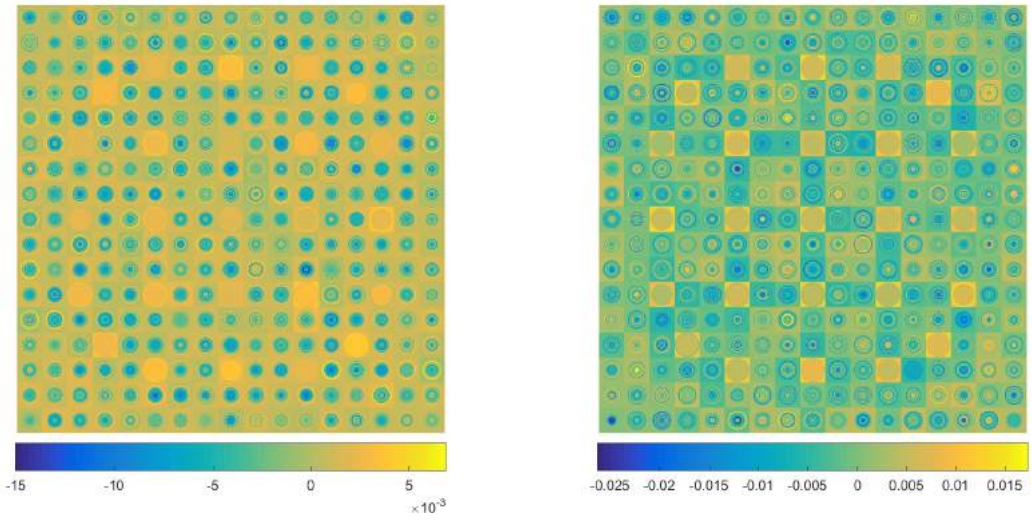

(a) Fast Group (b) Thermal Group

Figure 5.7 Relative errors between reference fine mesh MC solution and the flux reconstructed from 200 dominant modes

In fine mesh calculations where burnup or multiphysics feedback are considered, the reaction rates are of more interest compared to the neutron flux. In the presented hybrid method, the cross sections generated in MC and the reconstructed flux are used to calculate any reaction rates of interest according to:

$$R^g_{xi}(\vec{r}) = \Sigma^g_{xi}(\vec{r}) \times \phi^g_{xi}(\vec{r}) \tag{5.1}$$

where R^g_{xi} is the reaction rate of type x in energy group g in region i, Σ_{xi} is the multigroup macroscopic cross section and ϕ^g_{xi} is the total neutron flux density in region i. For example, the fission rate determines both energy deposition and consumption of fissile material. The reference MC solution of the local fission rate is shown in figure 5.8. The reconstructed fission rate in the case of 50 dominant modes is compared to the reference MC estimate; the relative errors are produced in figure 5.9. The relative errors on the fission rate are below 2% in most regions for both energy groups with errors up to 3.5% observed in some regions for the thermal group. Again, these results can be assumed to be satisfactory given that the standard deviation on the reference solution is 1%.

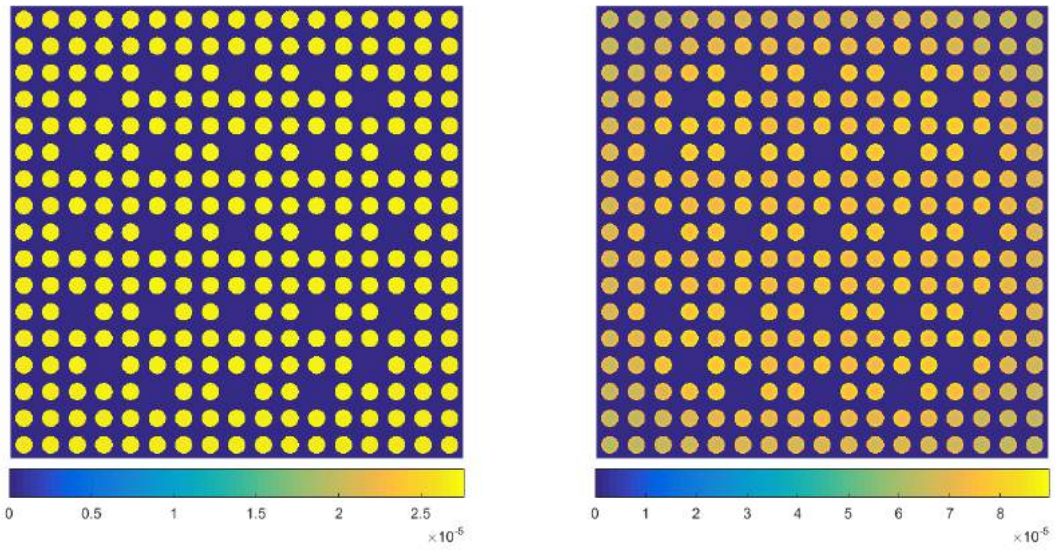

(a) Fast Group (b) Thermal Group

Figure 5.8 Reference fine mesh MC solution for the fission rate in a PWR assembly

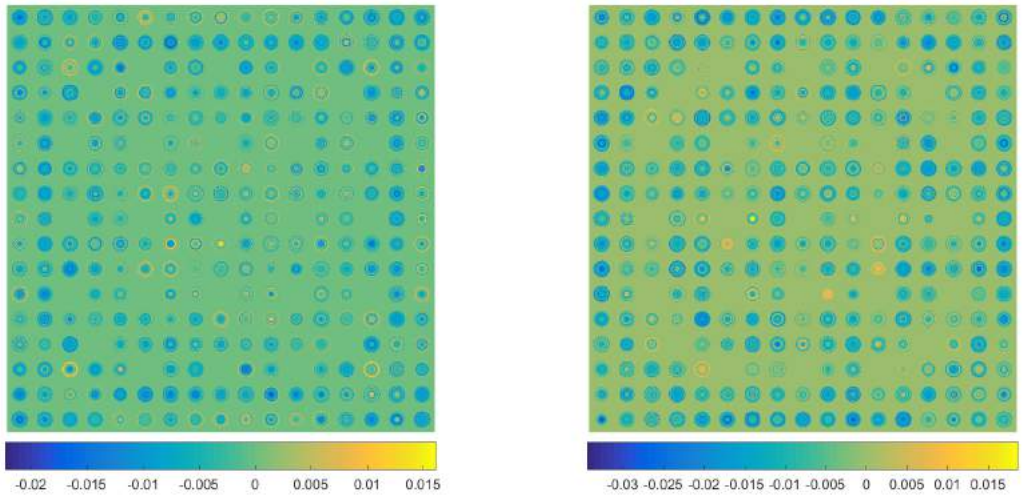

(a) Fast Group (b) Thermal Group

Figure 5.9 Relative errors between reference MC solution and the fission rate distribution reconstructed from 50 dominant modes

5.2.3 Error Estimation

In order to improve neutron flux reconstruction, an attempt to estimate the mapping error is performed:

$$\boldsymbol{\epsilon} = \boldsymbol{\Phi}_g - \boldsymbol{\Psi}_g a \tag{5.2}$$

This equation can be used to calculate the error between the coarse mesh MC tally and that estimated by modal expansion. Assuming that a coarse mesh element i comprises J sub-mesh elements, the total error on the reconstructed neutron flux in region i is:

$$\epsilon_i = \sum_{j=1}^{J} \epsilon_{ij} \tag{5.3}$$

Assuming that the average error is constant, the mapping error in the sub-mesh element j is then:

$$\epsilon_{ij} = \frac{\epsilon_i V_{ij}}{V_i} \tag{5.4}$$

Error estimation is applied for the cases of 20, 50, 89 and 200 dominant modes; the relative errors between the reference MC and the reconstructed flux map plus estimated error for each case are produced in figures 5.10 through 5.13. Results show that the maximum relative error in the case of 20 modes is reduced by about 1% in the thermal group; slight reductions are noticed when a larger number of modes is utilised. The main advantage of the error estimation approach is that the relative error becomes apparently less sensitive to the number of modes used.

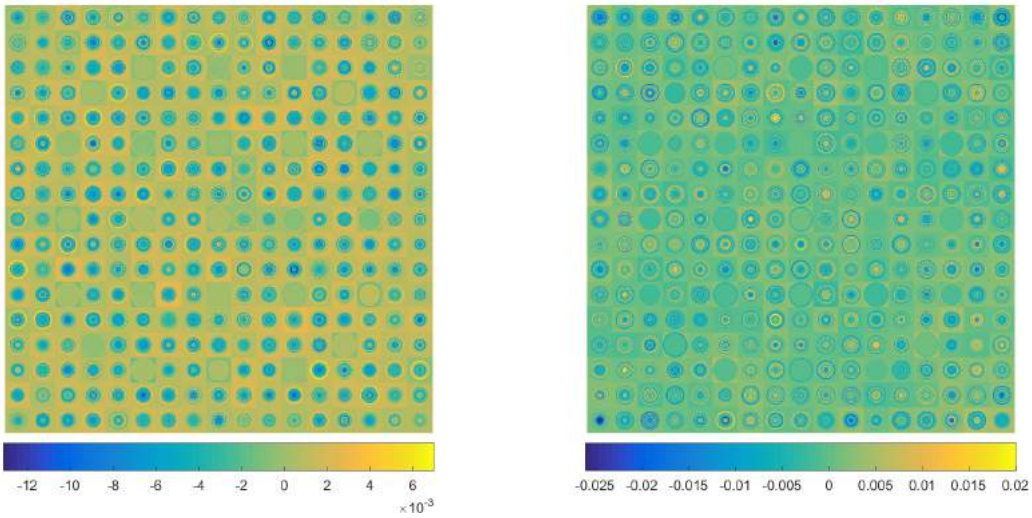

(a) Fast Group (b) Thermal Group

Figure 5.10 Relative errors between reference fine mesh MC solution and the flux reconstructed from 20 dominant modes plus estimated error

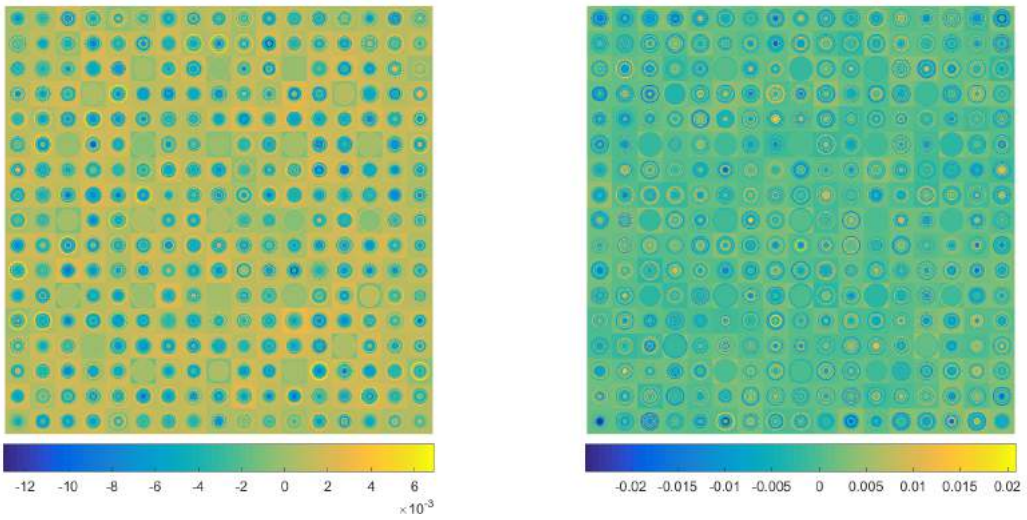

(a) Fast Group (b) Thermal Group

Figure 5.11 Relative errors between reference fine mesh MC solution and the flux reconstructed from 50 dominant modes plus estimated error

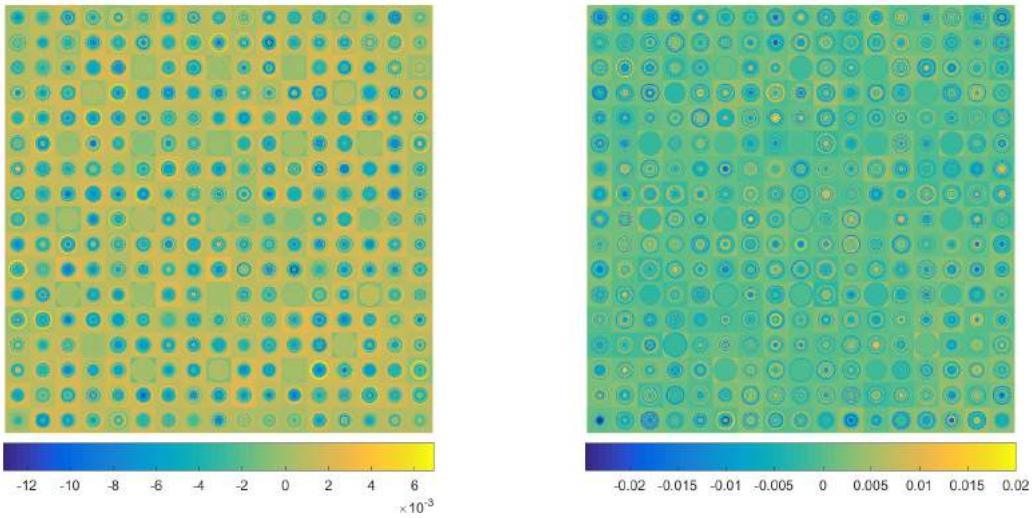

(a) Fast Group (b) Thermal Group

Figure 5.12 Relative errors between reference fine mesh MC solution and the flux reconstructed from 89 dominant modes plus estimated error

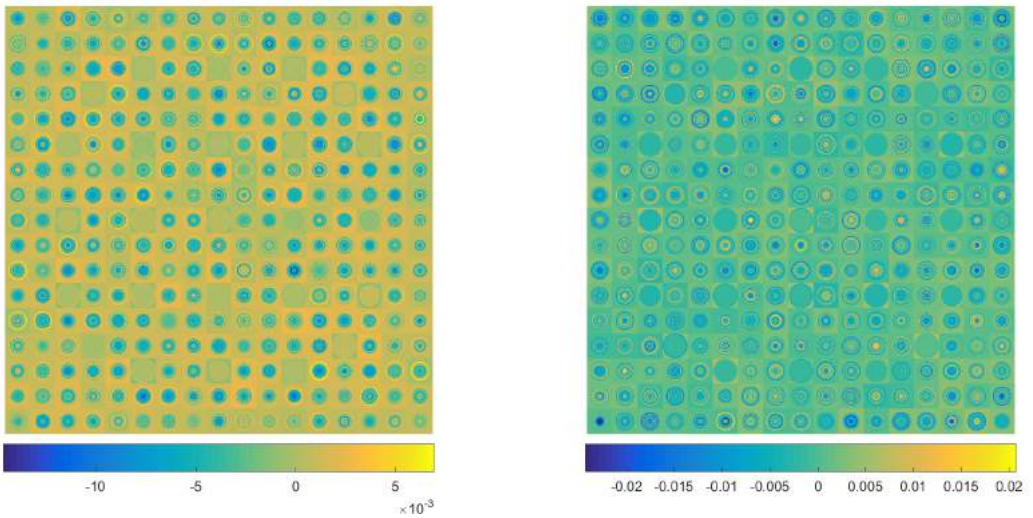

(a) Fast Group (b) Thermal Group

Figure 5.13 Relative errors between reference fine mesh MC solution and the flux reconstructed from 200 dominant modes plus estimated error

5.3 Application to 2D Supercell

In the previous sections, the hybrid method has been applied to study the neutron flux in single fuel assembly with reflection boundary conditions. However, real reactors are built from a number of assemblies arranged next to each other and different types of assemblies might be used. Since the hybrid method uses dominant modes of the transport equation calculated for single assemblies in flux reconstruction, it is important to evaluate its accuracy when perturbations such as the presence of different types of assemblies at the boundaries are included. For this purpose, a 2D 3×3 PWR supercell is studied; the geometry of the supercell is shown in figure 3.7. In the studied supercell, peripheral assemblies contain uranium dioxide at mid-burnup stage identical to the one described in table 4.1 while the central assembly is fresh uranium dioxide at 3.25% enrichment. Reflective boundary conditions are imposed on the external surfaces of the configuration.

A reference solution on a fine mesh featuring 10 burnup zones per fuel pellet is produced by the code *Serpent* is shown in figure 5.14; the reference solution is normalised such that the euclidean norm of the flux vector Φ is unity. The fission rate on a fine mesh is also tallied and results are produced in figure 5.15. The standard deviation on the shown reference solution is below 1% for both energy groups.

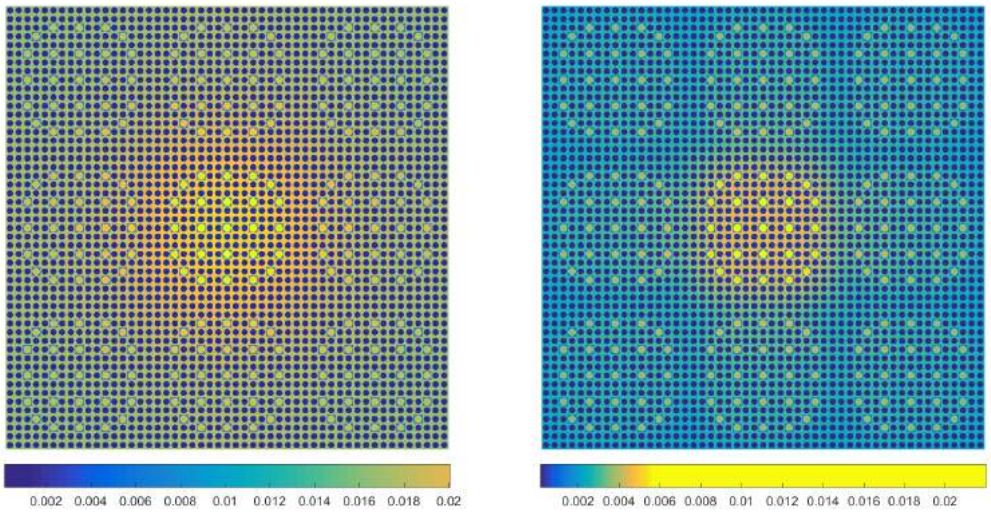

(a) Fast Group (b) Thermal Group

Figure 5.14 Reference fine mesh MC solution for the flux distribution a PWR 3×3 supercell

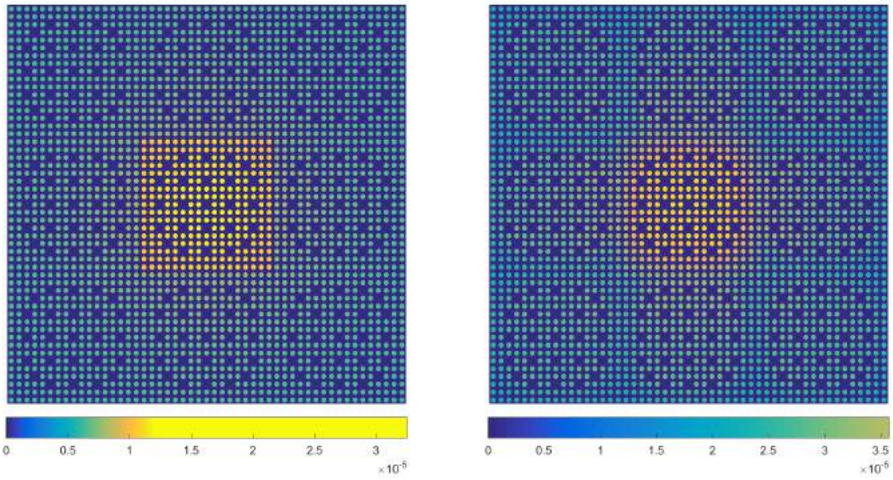

(a) Fast Group (b) Thermal Group

Figure 5.15 Reference fine mesh MC solution for the fission rate in a PWR 3×3 supercell

For the hybrid calculation, the MC code *Serpent* is utilised for calculating 2 energy groups cross sections homogenised on fine mesh as described in figure 5.3b for each of the two types of fuel assemblies. In addition, the neutron flux distribution in homogenised pincells are tallied across the whole supercell. The cross sections are fed to the lattice code *Dragon* where an independent lattice calculation for each type of assemblies is performed to calculate the dominant modes of the transport equation using the collision probability method. Once the modes are available, an independent modal amplitude calculation using least squares (eq. (3.32)) is performed for each assembly in the supercell to obtain local amplitudes and reconstruct a fine mesh flux distribution. In order to examine the effects of boundary conditions when calculating the modes on the accuracy of flux mapping, two cases are considered. Reflection boundary conditions are defined when the modes are calculated in the first case while albedo boundary conditions are defined in the second case. In the following paragraphs, modal expansion is truncated after 50 dominant modes.

5.3.1 Case 1: Reflection Boundary Conditions

The dominant modes for each type of fuel assemblies are calculated assuming reflective boundary conditions using the collision probability method and QZ decomposition as discussed in section 3.3.1. These are then combined with MC tallies of neutron flux in homogenised pincells to estimate modal amplitudes and reconstruct a fine mesh solution. The reconstructed flux map is compared to the MC reference of figure 5.14 and the relative errors are shown in

figure 5.16. The fission rate is calculated from the reconstructed flux map and compared to the reference solution; the relative errors on the fission rate are shown in figure 5.15.

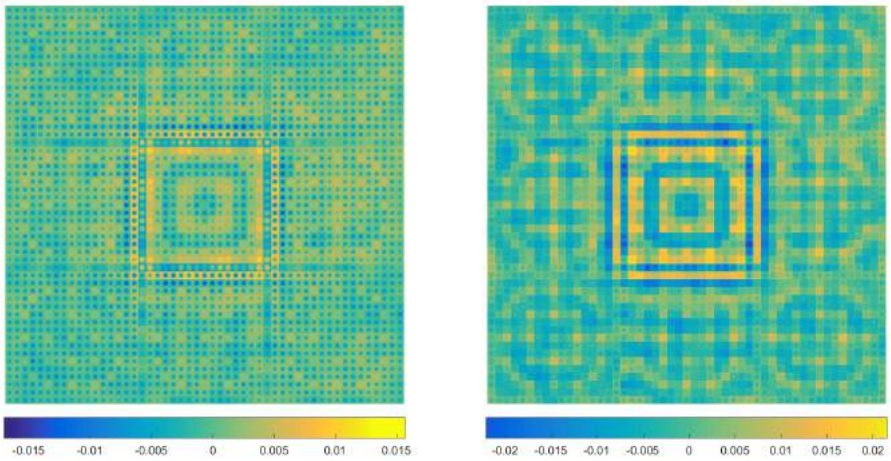

(a) Fast Group (b) Thermal Group

Figure 5.16 Relative errors between reference fine mesh MC solution for a PWR 3×3 supercell and reconstructed flux using modal expansion - case 1

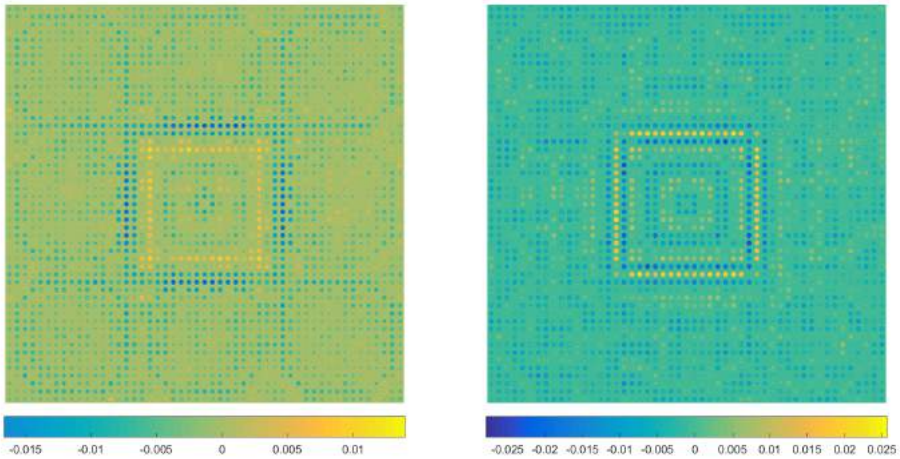

(a) Fast Group (b) Thermal Group

Figure 5.17 Relative errors between reference fine mesh MC solution for a PWR 3×3 supercell and reconstructed fission rate using modal expansion - case 1

The relative errors on the reconstructed neutron flux in the fast group are below 1.5% while

they are below 2.2% in the thermal group; similar values are observed for the fission rate. It is clear from the results that the largest errors are observed near the interfaces between peripheral assemblies and the central one. Despite the differences, the results can be considered satisfactory given that the standard deviation on the reference solution is around 1%.

5.3.2 Case 2: Albedo Boundary Conditions

In this case, the calculation of the dominant modes for each type of fuel assemblies is performed using albedo boundary conditions. Using a trial and error approach, uniform constant albedos are defined on each of the four bounding surfaces of each assembly such that the eigenvalue of the fundamental mode in each assembly is identical to the effective multiplication factor of the supercell as determined by *Serpent*. For the central assembly with higher enrichment, an albedo which is less than one is defined while an albedo greater than one is defined for the assembly containing burned fuel. The relative errors on the reconstructed neutron flux and fission rate are produced in figures 5.18 and 5.19

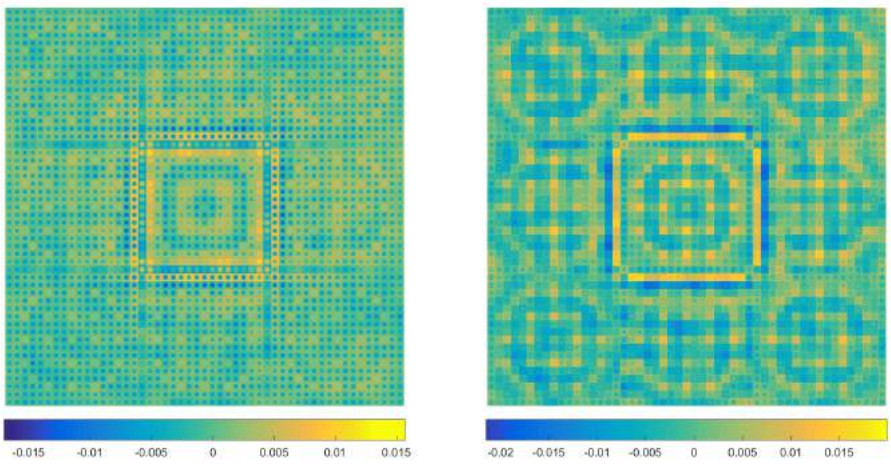

(a) Fast Group (b) Thermal Group

Figure 5.18 Relative errorss between reference fine mesh MC solution for a PWR 3×3 supercell and reconstructed flux using modal expansion - case 2

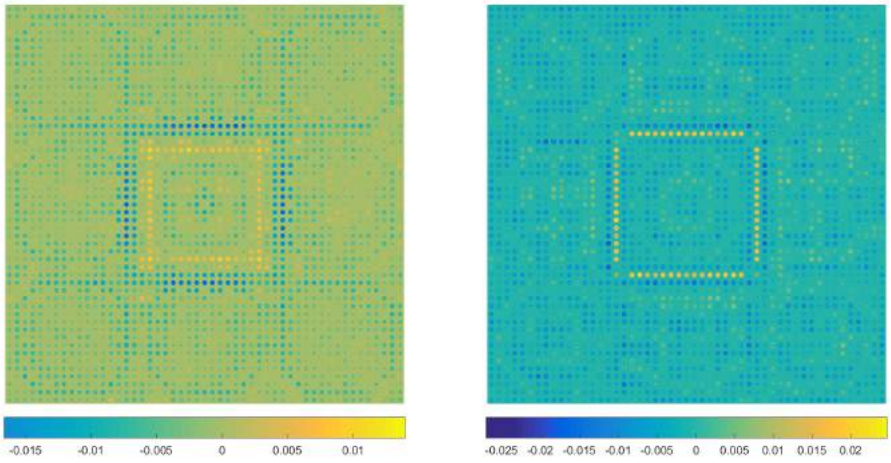

(a) Fast Group (b) Thermal Group

Figure 5.19 Relative errors between reference fine mesh MC solution for a PWR 3×3 supercell and reconstructed fission rate using modal expansion - case 2

Results in this case are comparable to the ones shown in figures 5.16 and 5.17 where the maximum error is less than 1.5% and 2.2% for the fast and thermal energy groups respectively. However, reduction in the reconstruction errors near the interfaces is observed. The relative errors near the interfaces for the thermal group are about 1.5% in this case compared to 2.2% for the previous case where reflection boundary conditions were considered.

5.4 Application to 3D Supercell & Performance Evaluation

Nuclear reactors extend in 3 dimensions and, in practical applications, it is of great interest to understand the neutron flux and power distribution along the axis of the reactor core. Similar to 2D cases described above, the hybrid method can be applied in 3D calculations. However, calculation of deterministic 3D transport modes would demand large computer resources and might counter any benefits of the hybrid approach.

The approach is applied to study the 3D neutron flux distribution in the PWR supercell described in section 5.3. The supercell extends 366 cm along the axial direction with reflection boundary conditions defined in the radial direction and void boundary conditions imposed on the axial direction. The MC code *Serpent* is utilised for calculating a reference fine mesh solution where neutron tallies in 10 burnup zones per fuel pellet and 10 axial planes are recorded. The reference solution for the neutron flux distribution in planes 1 (bottom plane) up to 5 (midplane) are shown in figures 5.20 through 5.25; results of the remaining planes are

not shown as they are identical by symmetry to the ones presented. The flux distribution is normalised such that the euclidean norm of the vector Φ is unity and the standard deviation in all planes is below 1%.

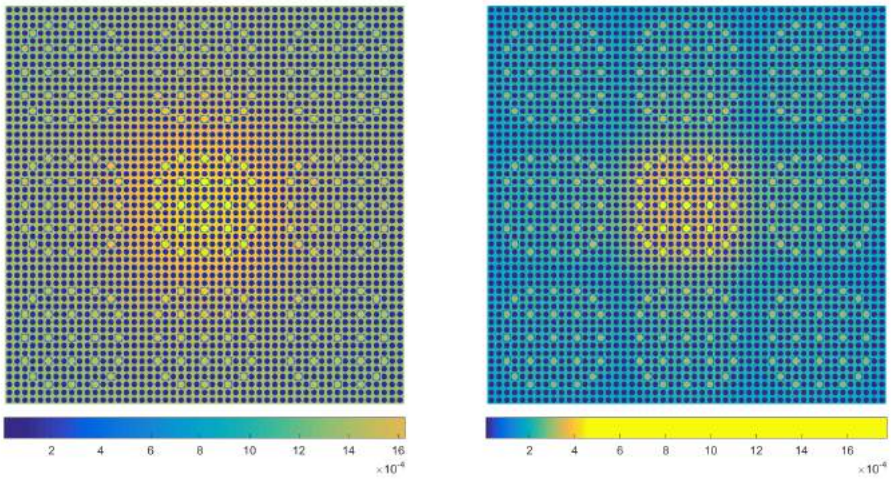

(a) Fast Group (b) Thermal Group

Figure 5.20 Reference fine mesh MC solution for the flux distribution a PWR 3×3 supercell in axial plane 1

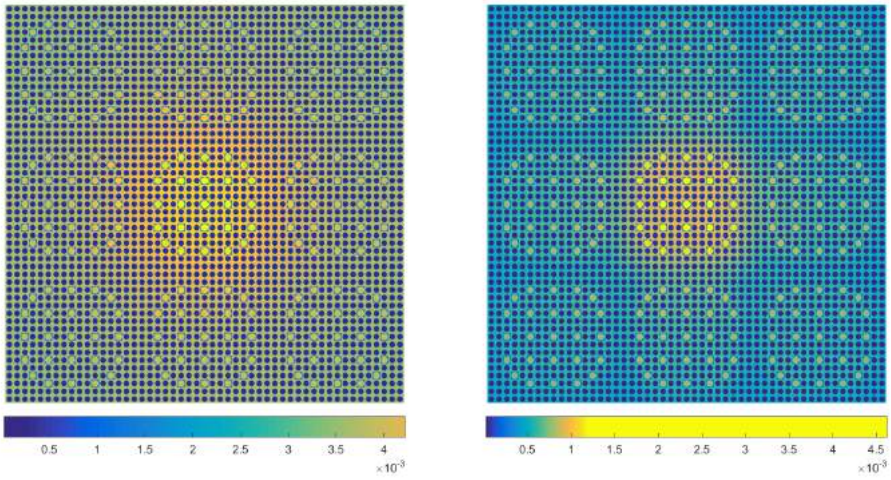

(a) Fast Group (b) Thermal Group

Figure 5.21 Reference fine mesh MC solution for the flux distribution a PWR 3×3 supercell in axial plane 2

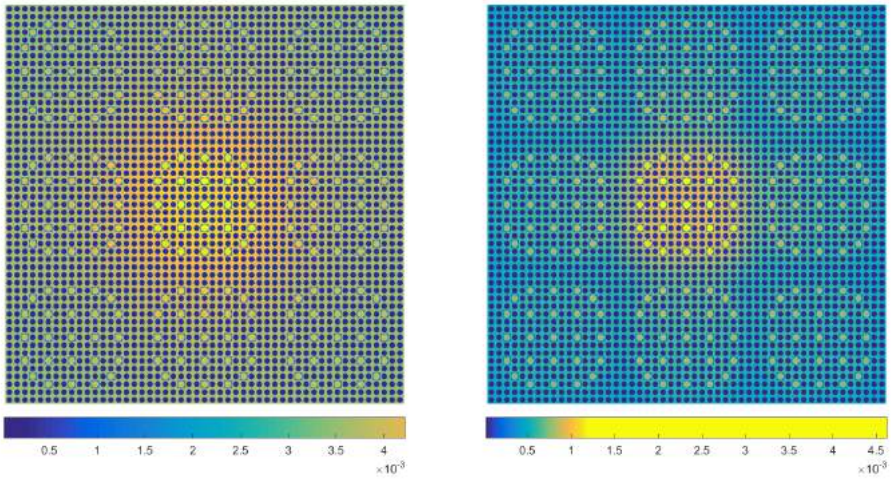

(a) Fast Group (b) Thermal Group

Figure 5.22 Reference fine mesh MC solution for the flux distribution a PWR 3×3 supercell in axial plane 2

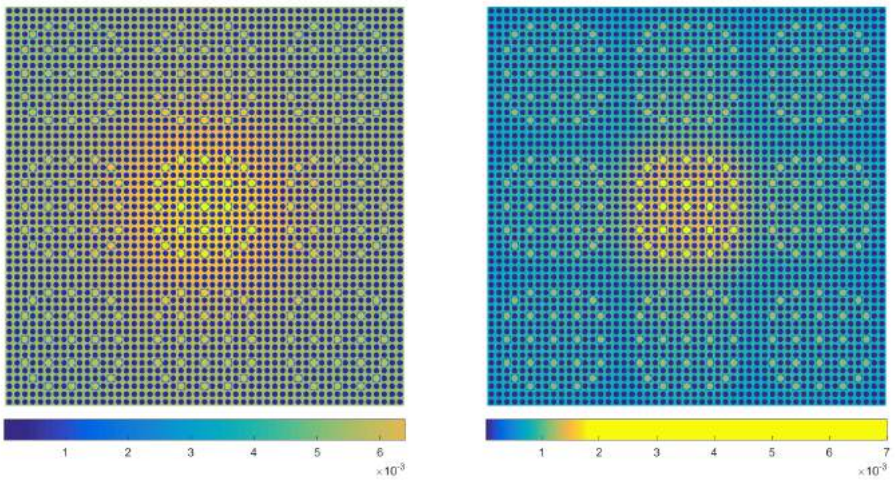

(a) Fast Group (b) Thermal Group

Figure 5.23 Reference fine mesh MC solution for the flux distribution a PWR 3×3 supercell in axial plane 3

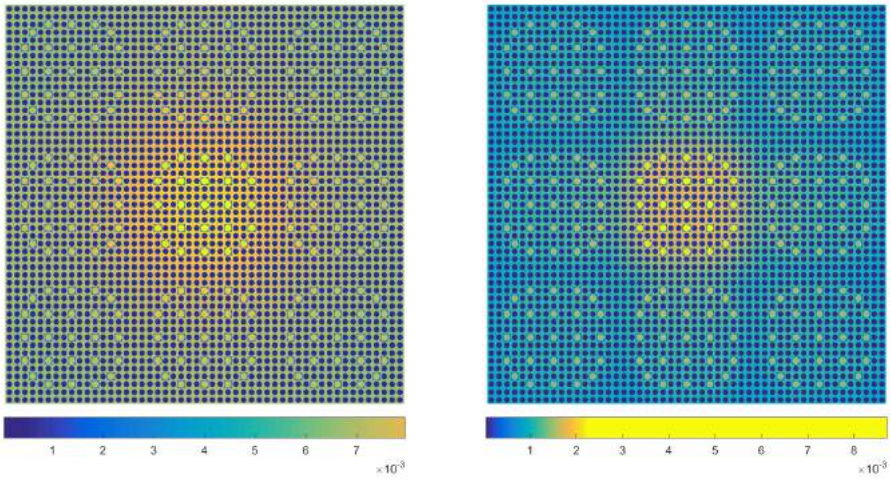

(a) Fast Group (b) Thermal Group

Figure 5.24 Reference fine mesh MC solution for the flux distribution a PWR 3×3 supercell in axial plane 4

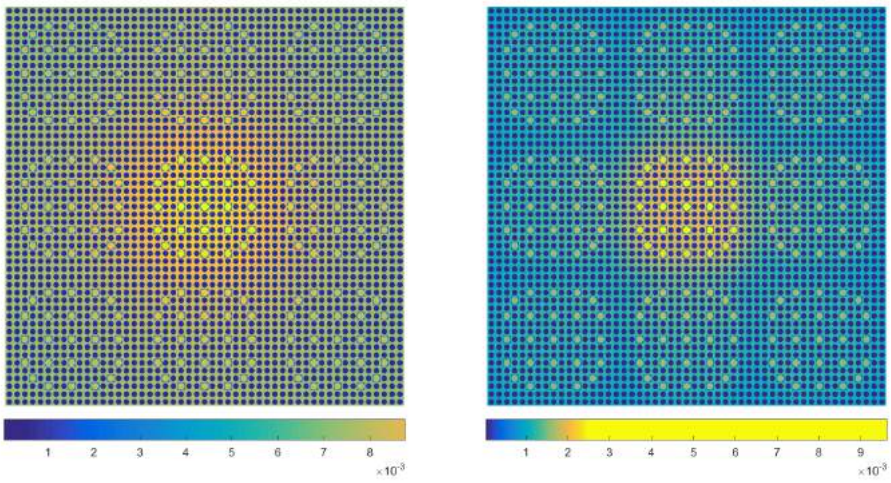

(a) Fast Group (b) Thermal Group

Figure 5.25 Reference fine mesh MC solution for the flux distribution a PWR 3×3 supercell in axial plane 5

5.4.1 3D Flux Reconstruction

The MC solver is employed to obtain the neutron flux distribution in homogenised pincells in 10 axial planes of equal thickness. In addition, neutron cross sections necessary for calcu-

lating 2D dominant modes of the transport equation assuming albedo boundary conditions as described in section 5.3.2 are evaluated.

In order to reconstruct 3D fine mesh flux distribution, an independent modal amplitudes evaluation is performed for each axial plane; i.e. it is assumed that the modal amplitudes vary along the axial direction. 50 dominant modes are employed in flux reconstruction and no correction for mapping errors is performed. The relative errors between the reference solution and the one obtained by the hybrid method for planes 1 up to 5 are shown in figures 5.26 through 5.30.

In plane 1, figure 5.26, the relative errorw between the reconstructed neutron flux and the reference solution in the fast group are below 2% in most regions with errors up to 4% observed in a limited number of regions. In the thermal group, the relative errors are within 3% in most regions and errors up to 5% are observed in some regions. In plane 2, figure 5.27, smaller maximum relative errors are observed compared to plane 1 where the largest error is about 3% and 3.5% in the fast and thermal energy groups respectively. In planes 3, 4 and 5, figures 5.28 through 5.30, the maximum relative errors are less than 2% in the fast group and 2.5% in the thermal group. Taking into consideration that the standard deviation on the reference solution is 1%, it can be assumed that the results produced by the hybrid method can be assumed satisfactory.

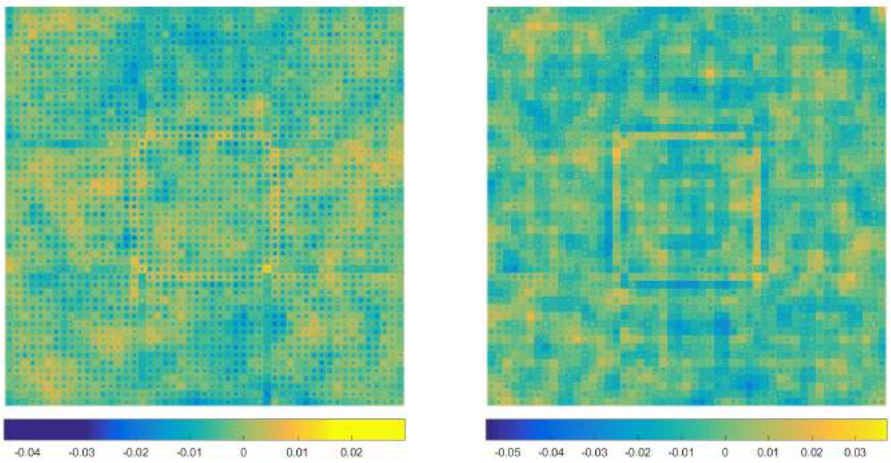

(a) Fast Group (b) Thermal Group

Figure 5.26 Relative errors between MC reference solution and reconstructed flux map in axial plane 1

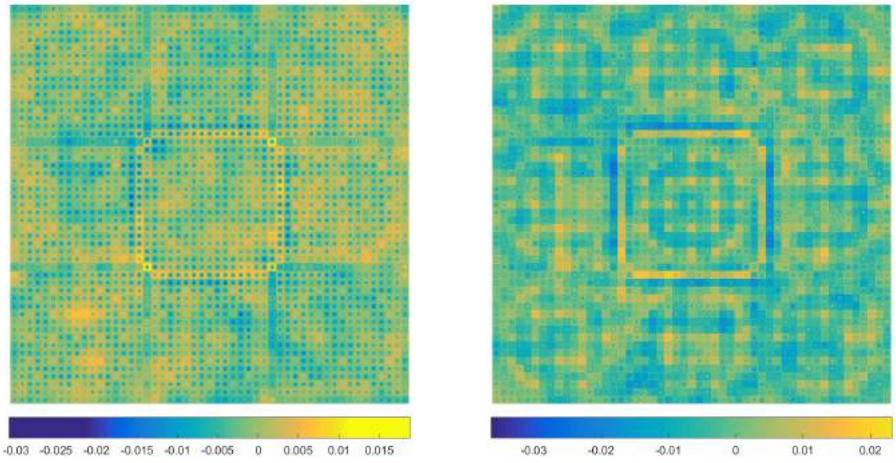

(a) Fast Group (b) Thermal Group

Figure 5.27 Relative errors between MC reference solution and reconstructed flux map in axial plane 2

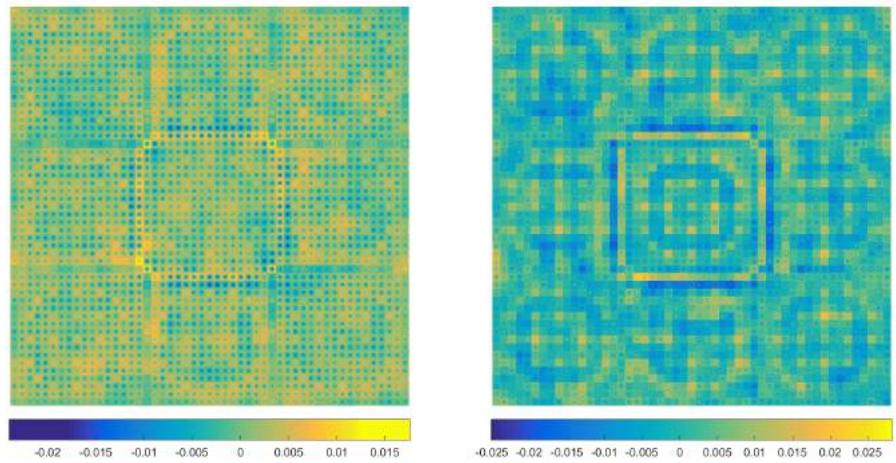

(a) Fast Group (b) Thermal Group

Figure 5.28 Relative errors between MC reference solution and reconstructed flux map in axial plane 3

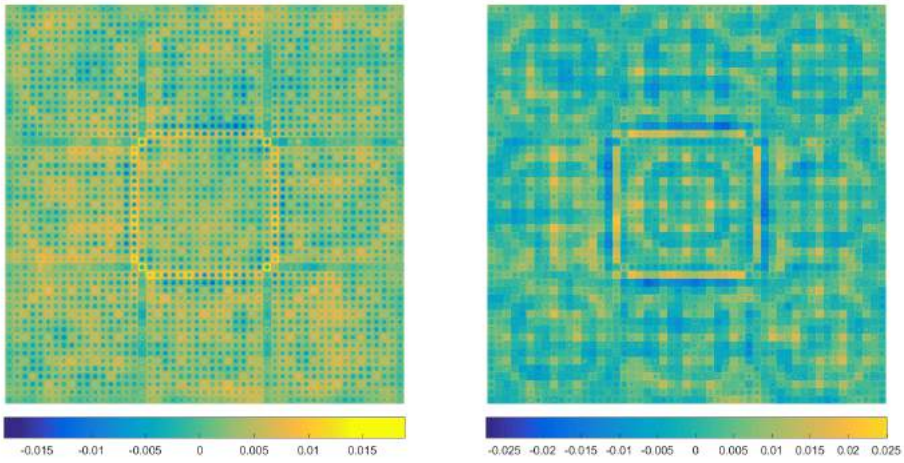

(a) Fast Group (b) Thermal Group

Figure 5.29 Relative errors between MC reference solution and reconstructed flux map in axial plane 4

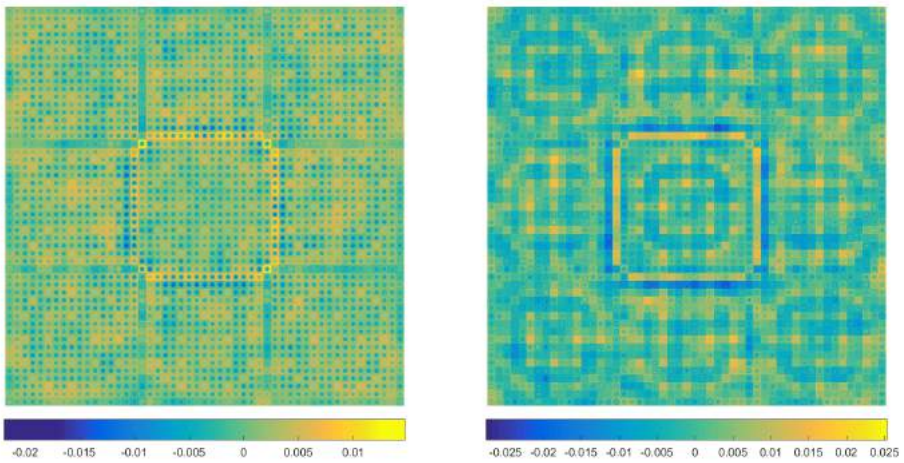

(a) Fast Group (b) Thermal Group

Figure 5.30 Relative errors between MC reference solution and reconstructed flux map in axial plane 5

The fission rate distribution estimated by the hybrid method is compared to the reference solution in planes 1 and 5. Results are produced in figures 5.31 and 5.32. In the first axial plane, the relative error on the fission rate is within 3% in both energy groups with a

maximum error of about 5% observed in a limited number of regions. In the mid plane, the relative error between the reference solution and the hybrid estimate is within 2.5% in both energy groups.

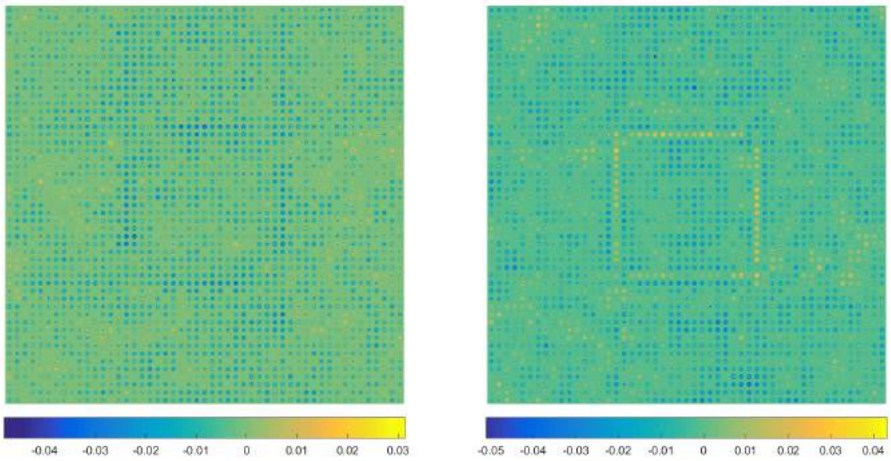

(a) Fast Group (b) Thermal Group

Figure 5.31 Relative errors between MC reference solution and reconstructed fission rate map in axial plane 1

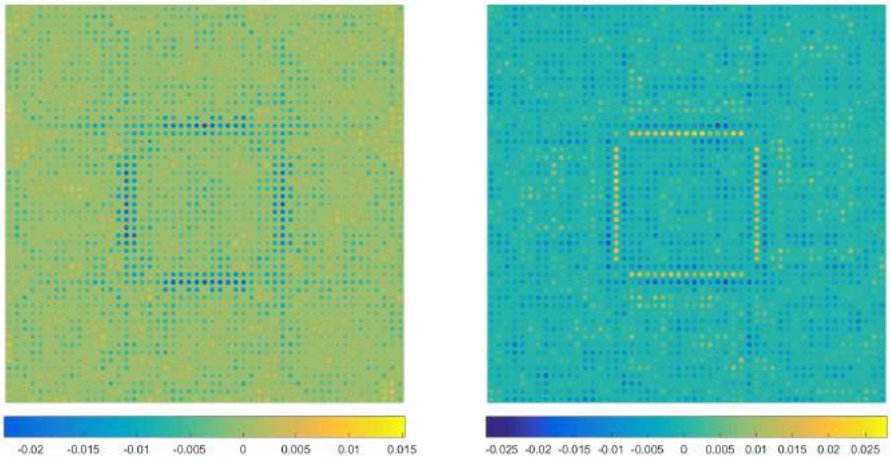

(a) Fast Group (b) Thermal Group

Figure 5.32 Relative errors between MC reference solution and reconstructed fission rate map in axial plane 5

5.4.2 Computational Costs and Performance

For the 3D supercell considered, the reference solution is obtained using a MC simulation composed of 20 inactive and 50000 active cycles each of 200000 neutron histories. The standard deviation on the neutron flux distribution in all planes is below 1%. The simulation is performed on a workstation with core i7-4470 CPU using parallel processing on 8 threads. The total run time to obtain a reference solution is 3061 minutes.

The computational time of the hybrid calculation is composed of three components:

- The computation time of the stochastic calculation to obtain the neutron flux distribution on a coarse mesh and the neutron cross sections on a fine mesh
- The compuatation time for calculating the dominant modes of the transport equation on a unit cells (assembly)
- The computation time for flux mapping.

For the stochastic part of the simulation, 20 inactive and 5000 active cycles are used each of 200000 neutron histories. Neutron flux tallies in homogenised pincells in 10 axial planes are recorded in addition to the neutron cross sections in 10 burnup zones per fuel pellet. The standard deviation on the neutron flux is below 1% in all axial planes while the standard deviation on the neutron macroscopic cross sections is below 0.1%. The calculation is performed on the same workstation and the run time for the MC part is 293 minutes. Two independent deterministic calculations are performed in parallel, one for each type of unit cells on a single CPU thread, to calculate the dominant modes of the transport equation. The total run time for the deterministic calculation is 58 minutes on the same workstation. Finally, the calculation of the modal amplitudes and fine mesh flux reconstruction in each assembly and axial plane is performed in series on a single CPU thread; the computation time for this component is 4 minutes. Hence, the total running time for the hybrid method is 355 minutes. Compared to conventional MC, the hybrid method can be up to 88% faster.

5.5 Application with Burnup Studies

MC simulations become excessively computationally expensive when fuel burnup is included in the simulation. This is due to the necessity of performing the simulation on a fine tally mesh and tracking the accumulation and depletion of a large number of isotopes. In the proposed hybrid method, the stochastic simulation is performed with a small number of neutron histories and tallies scored on a coarse mesh as illustrated in the previous sections.

For burnup studies, the hybrid method reconstructs a fine mesh solution for the neutron flux using modal synthesis and the results can be employed for calculating different reaction rates and solving the Bateman equations to update the isotopic composition of the fuel. The updated composition is then utilised for the next stochastic calculation. Since the composition of the fuel varies during burnup, neutron cross sections change between burnup cycles hence variations in the dominant modes are expected.

As discussed in section 5.4.2, the hybrid method can achieve up to 88% acceleration compared to the MC method in static calculations. It is also noticed that the calculation of the dominant modes takes considerable time of the calculation cycle. If recalculation of the dominant modes is not required at each burnup step, further reductions in computation time can be achieved. To investigate the accuracy of the hybrid method with burnup studies, two cases are evaluated for a single fuel assembly of 3.25% enriched uranium dioxide. In the first case, the dominant modes are evaluated only at 0MWd/t burnup and these are employed at each burnup step for fine mesh flux reconstruction. In the second case, the dominant modes are re-evaluated at the end of the stochastic calculation of each burnup step. In both cases, fuel burnup up to 10MWd/Kg with burnup steps of 1MWd/Kg at a power density of $38.6 KW/g$ is studied; 50 dominant modes are employed in flux synthesis.

5.5.1 Case -1 Reconstruction with Modes of 0 Burnup

The fine mesh neutron flux distribution reconstructed using coarse mesh MC solution and modes calculated at 0MWd/Kg for each burnup step is compared to a MC fine mesh reference solution. The relative errors between the reconstructed flux and the reference in the fast and thermal energy groups are produced in figures 5.33 through 5.43. At the initial fuel composition (0MWd/Kg), flux synthesis reconstructs fine mesh solution at an accuracy of 1.5% in the fast group and 3% in the thermal group as shown in figure 5.33. Similar results are observed in the fast energy group for all burnup steps. For the therml flux at higher burnup, reconstruction with zero burnup modes is less accurate. Relative errors up to 3.5% are observed at 1MWd/Kg and 2MWd/Kg, as shown in figures 5.34 and 5.35, while errors up to 4.5% are observed at 3MWd/Kg and 4MWd/Kg as illustrated in figure 5.36 and 5.37. At 5MWd/Kg and 6MWd/Kg, errors around 5% are observed on the reconstructed thermal neutron flux distribution; results are presented in figures 5.38 and 5.39. At higher burnup rates, the maximum relative error on the thermal flux is around 6% as shown in figures 5.40 through 5.43.

Results shown in this section show that flux synthesis without modes recalculation when burnup is considered produces less accurate flux distribution compared to static studies.

These results suggest that the recalculation of the modes at the end of each burnup step is required.

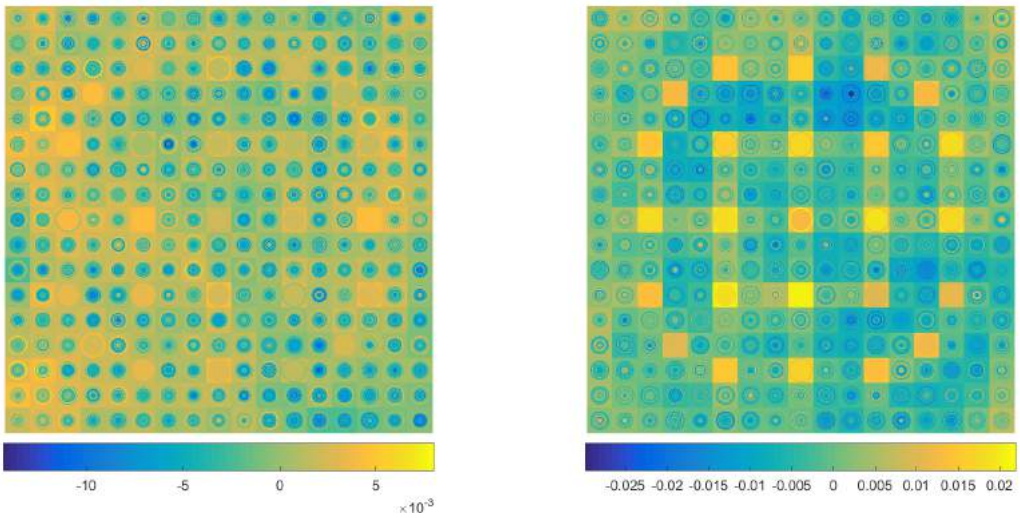

(a) Fast Group (b) Thermal Group

Figure 5.33 Relative errors between reference fine mesh MC solution and the flux reconstructed at 0MWd/Kg burnup - case 1

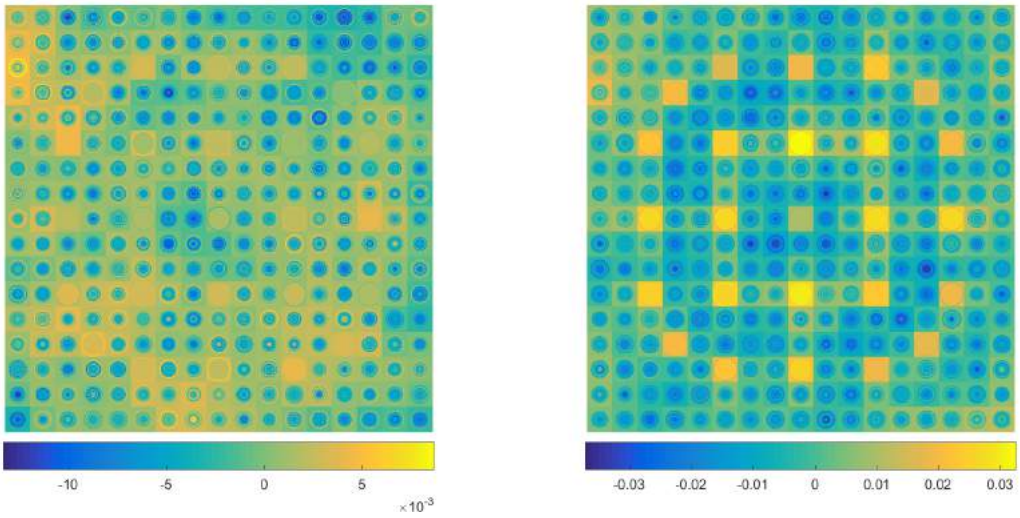

(a) Fast Group (b) Thermal Group

Figure 5.34 Relative errors between reference fine mesh MC solution and the flux reconstructed at 1MWd/Kg burnup - case 1

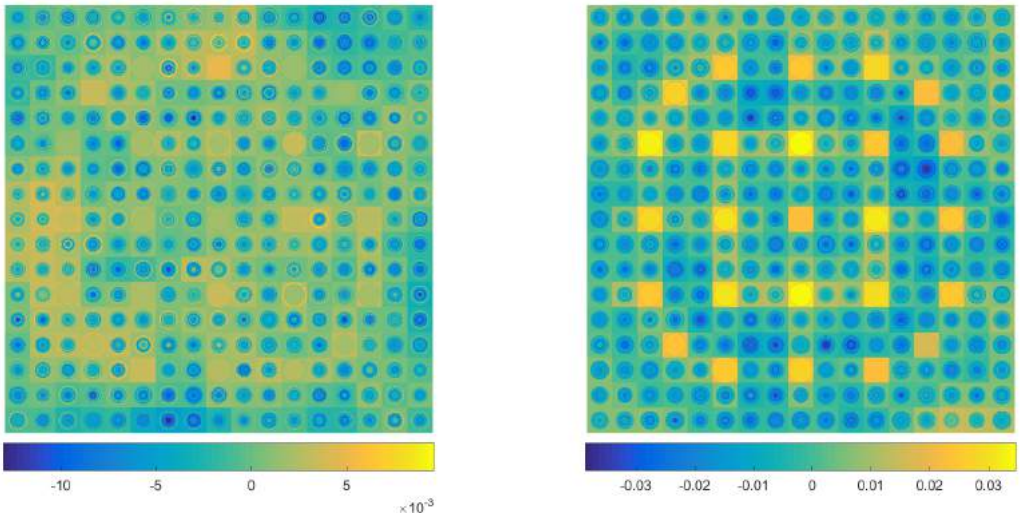

(a) Fast Group (b) Thermal Group

Figure 5.35 Relative errors between reference fine mesh MC solution and the flux reconstructed at 2MWd/Kg burnup - case 1

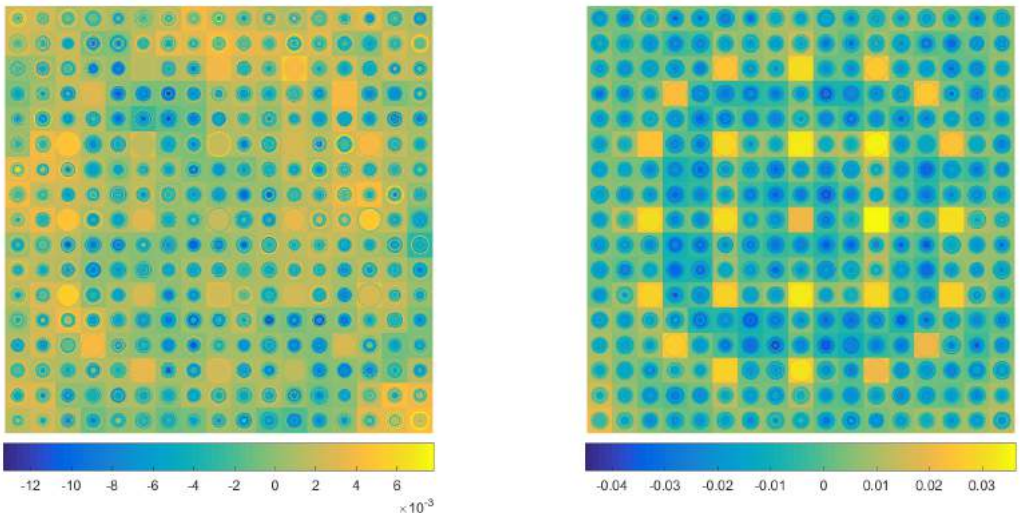

(a) Fast Group (b) Thermal Group

Figure 5.36 Relative errors between reference fine mesh MC solution and the flux reconstructed at 3MWd/Kg burnup - case 1

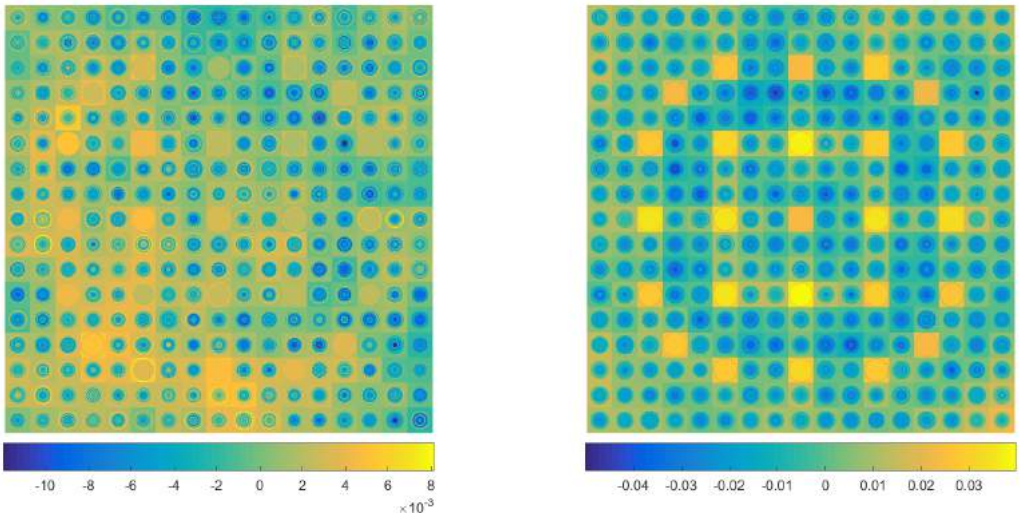

(a) Fast Group (b) Thermal Group

Figure 5.37 Relative errors between reference fine mesh MC solution and the flux reconstructed at 4MWd/Kg burnup - case 1

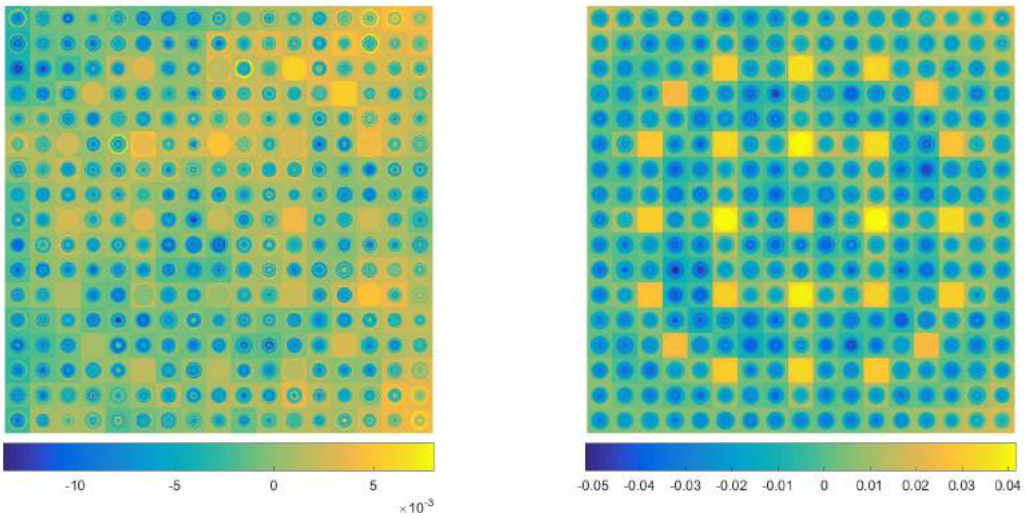

(a) Fast Group (b) Thermal Group

Figure 5.38 Relative errors between reference fine mesh MC solution and the flux reconstructed at 5MWd/Kg burnup - case 1

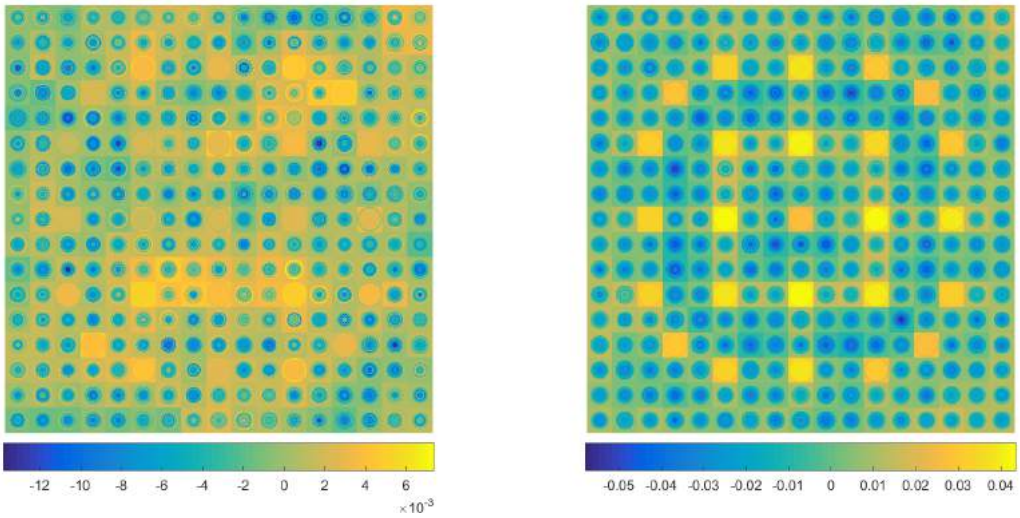

(a) Fast Group (b) Thermal Group

Figure 5.39 Relative errors between reference fine mesh MC solution and the flux reconstructed at 6MWd/Kg burnup - case 1

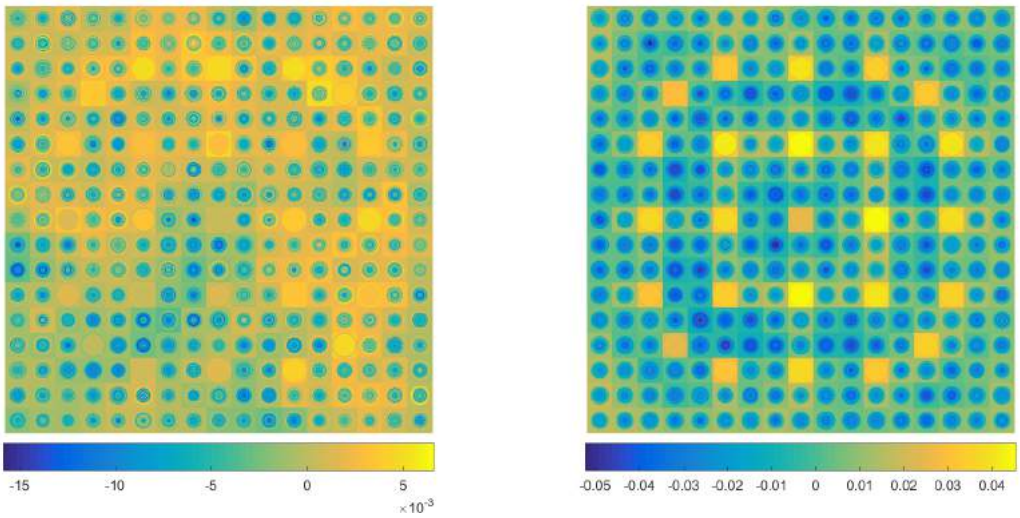

(a) Fast Group (b) Thermal Group

Figure 5.40 Relative errors between reference fine mesh MC solution and the flux reconstructed at 7MWd/Kg burnup - case 1

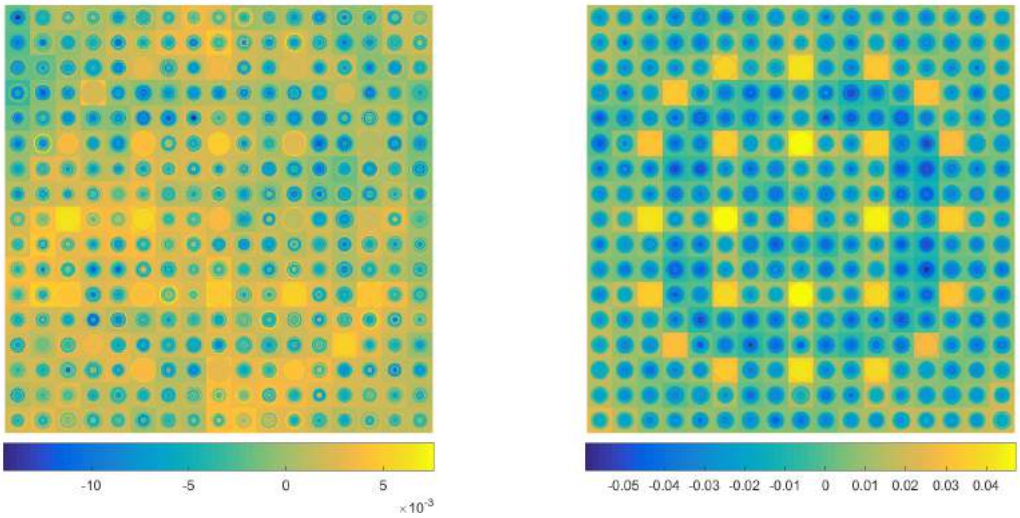

(a) Fast Group (b) Thermal Group

Figure 5.41 Relative errors between reference fine mesh MC solution and the flux reconstructed at 8MWd/Kg burnup - case 1

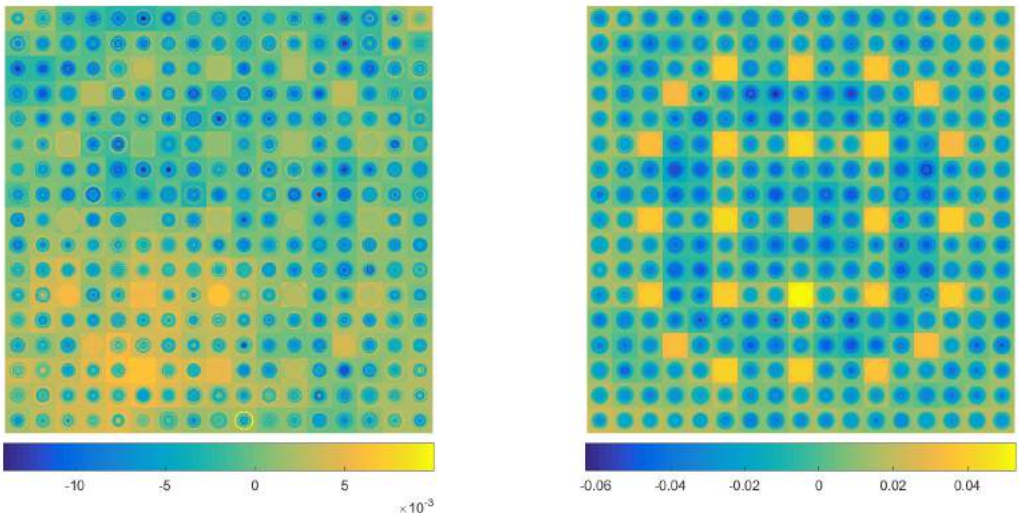

(a) Fast Group (b) Thermal Group

Figure 5.42 Relative errors between reference fine mesh MC solution and the flux reconstructed at 9MWd/Kg burnup - case 1

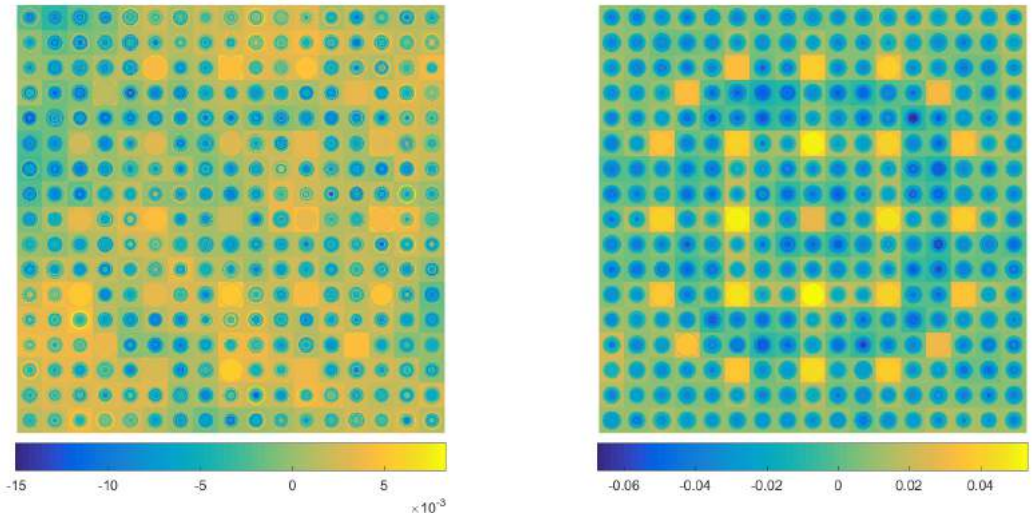

(a) Fast Group (b) Thermal Group

Figure 5.43 Relative errors between reference fine mesh MC solution and the flux reconstructed at 10MWd/Kg burnup - case 1

5.5.2 Case -2 Reconstruction with Modes Recalculated at Each Burnup Step

In the following, the stochastic solver is employed to tally the neutron flux in homogenised picells and neutron cross sections at the end of each burnup step. Then, the deterministic solver is utilised to calculate the dominant modes for the assembly configuration. Flux mapping is then employed to construct a fine mesh solution to be used for the next burnup calculation. Results produced in figures 5.44 through 5.54 show that, in all cases, the relative errors between the reconstructed fast flux and the MC reference are below 1.5% while it is below 3% in the thermal group.

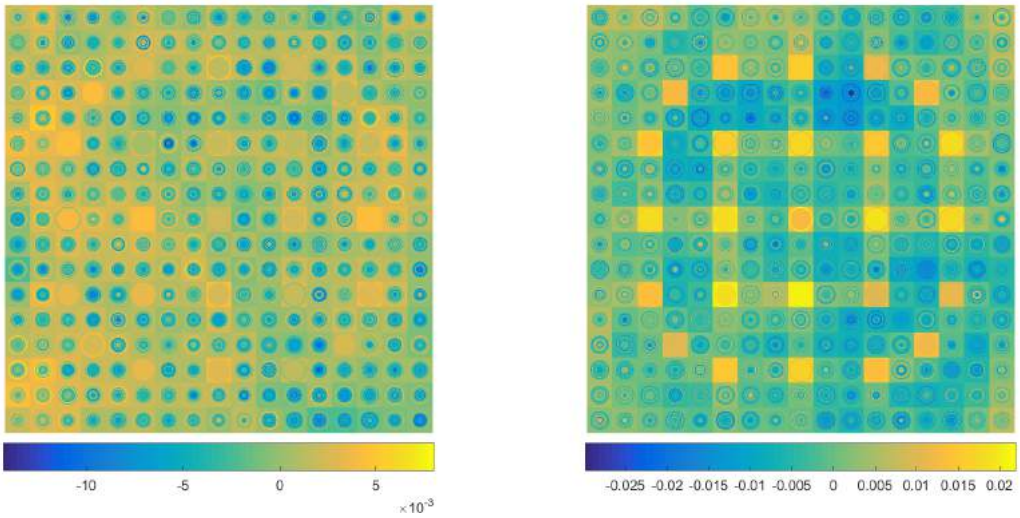

(a) Fast Group (b) Thermal Group

Figure 5.44 Relative errors between reference fine mesh MC solution and the flux reconstructed at 0MWd/Kg burnup - case 2

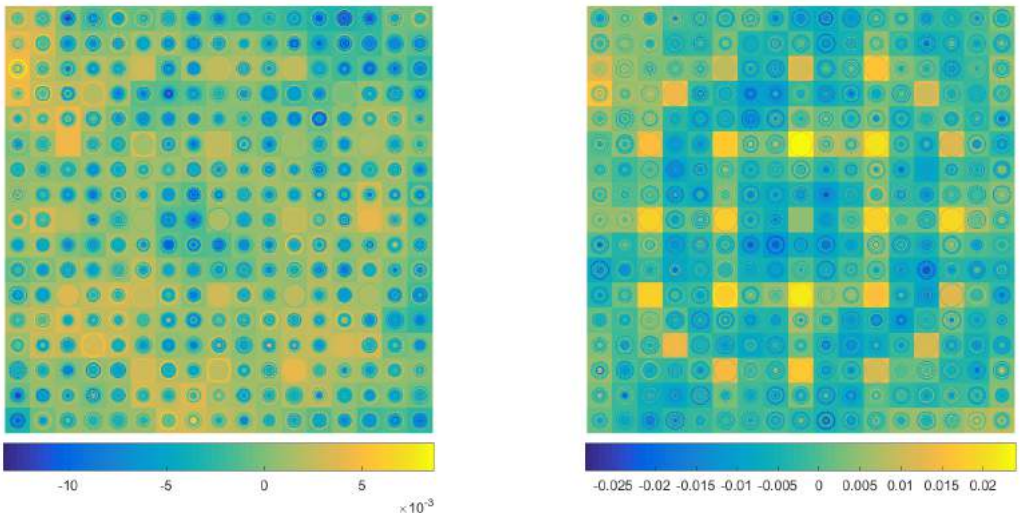

(a) Fast Group (b) Thermal Group

Figure 5.45 Relative errors between reference fine mesh MC solution and the flux reconstructed at 1MWd/Kg burnup - case 2

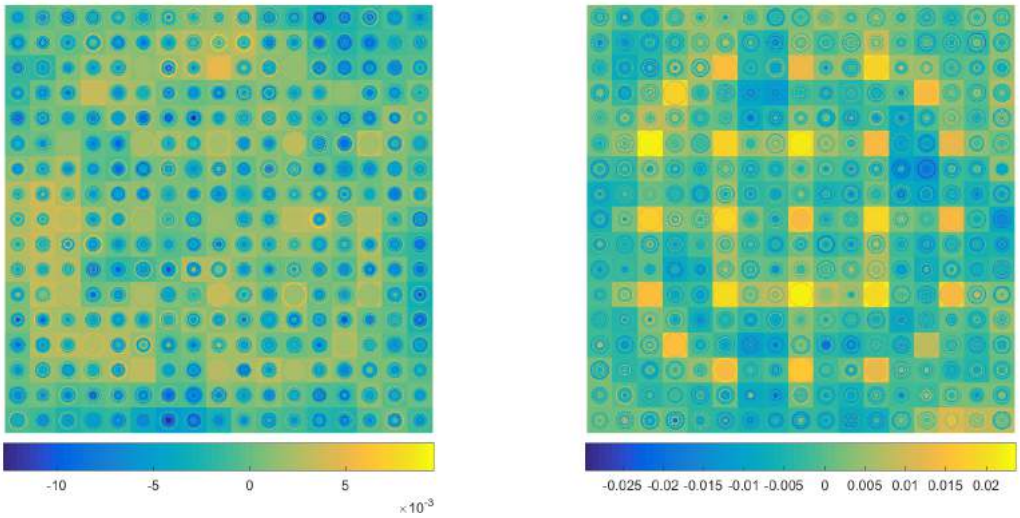

(a) Fast Group (b) Thermal Group

Figure 5.46 Relative errors between reference fine mesh MC solution and the flux reconstructed at 2MWd/Kg burnup - case 2

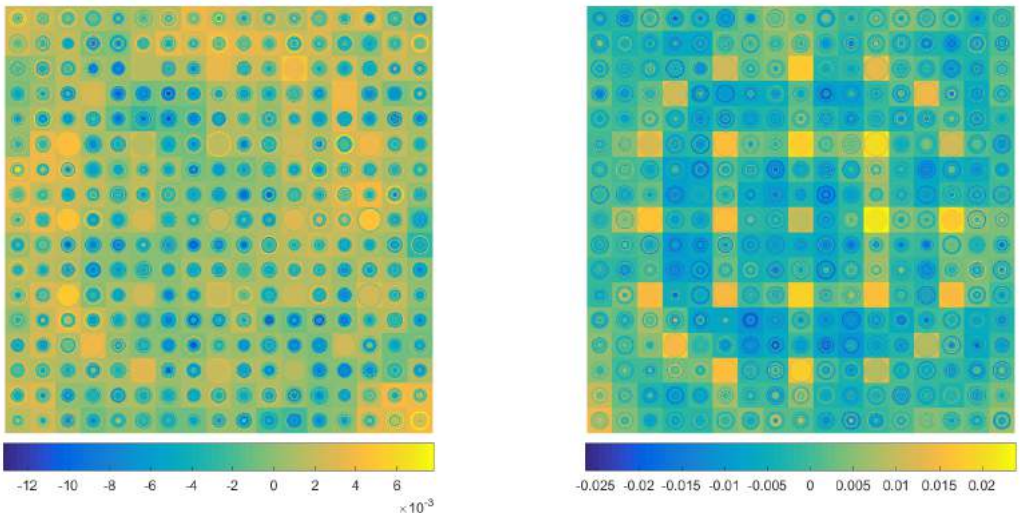

(a) Fast Group (b) Thermal Group

Figure 5.47 Relative errors between reference fine mesh MC solution and the flux reconstructed at 3MWd/Kg burnup - case 2

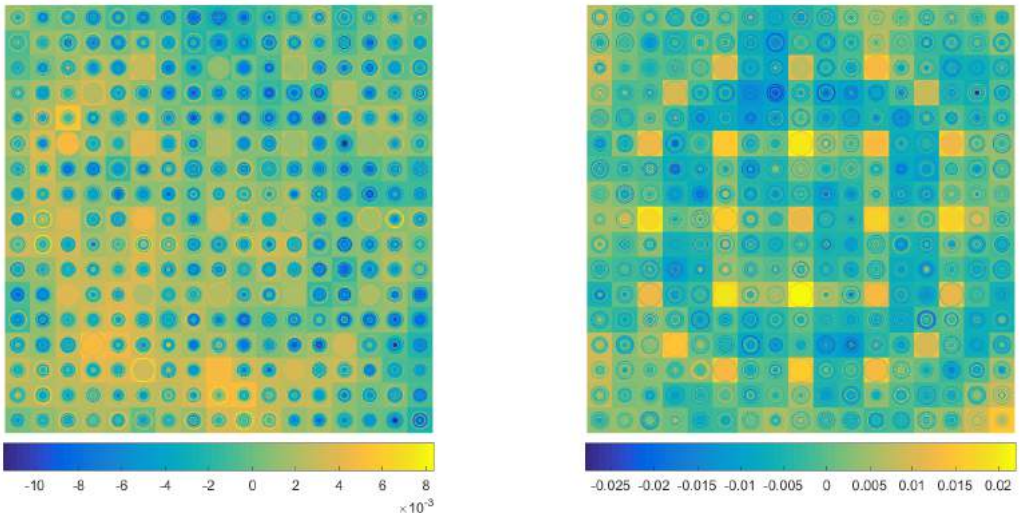

(a) Fast Group (b) Thermal Group

Figure 5.48 Relative errors between reference fine mesh MC solution and the flux reconstructed at 4MWd/Kg burnup - case 2

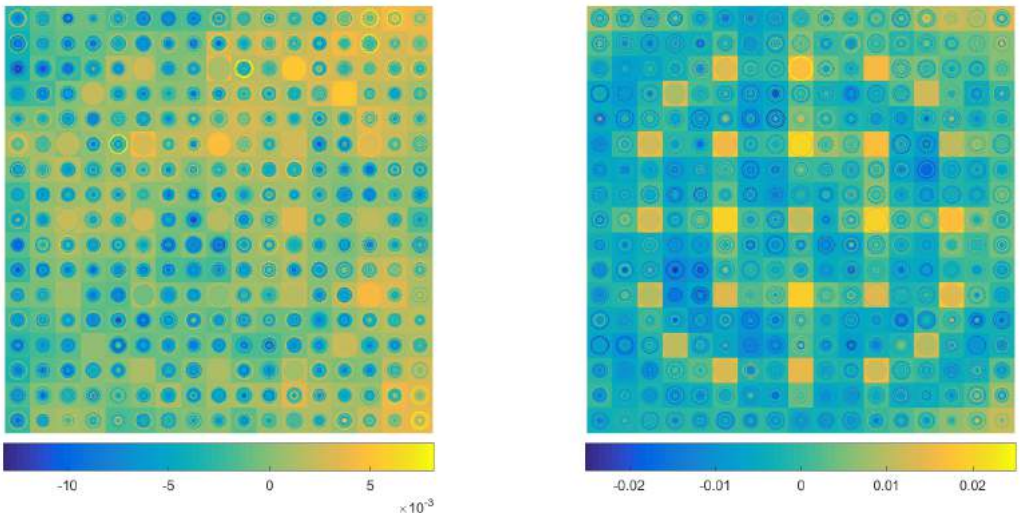

(a) Fast Group (b) Thermal Group

Figure 5.49 Relative errors between reference fine mesh MC solution and the flux reconstructed at 5MWd/Kg burnup - case 2

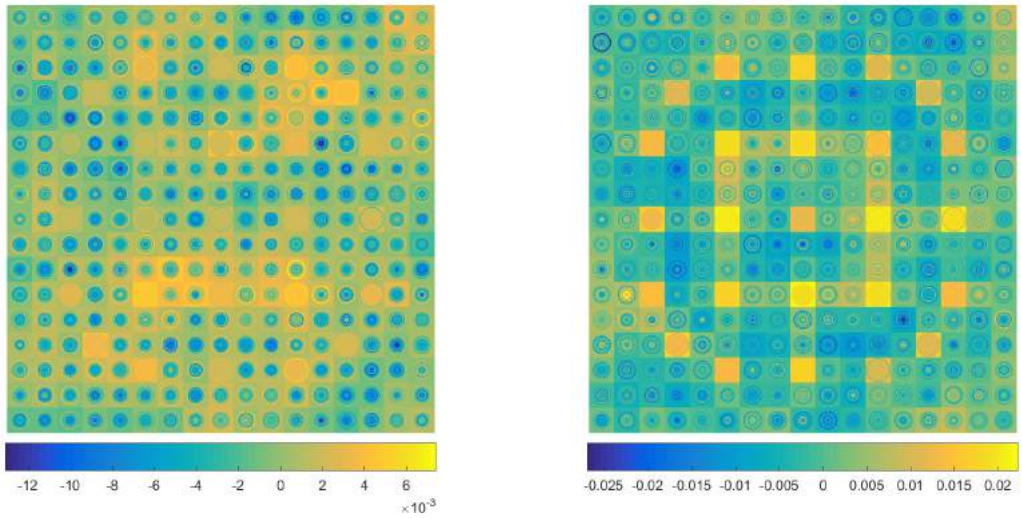

(a) Fast Group (b) Thermal Group

Figure 5.50 Relative errors between reference fine mesh MC solution and the flux reconstructed at 6MWd/Kg burnup - case 2

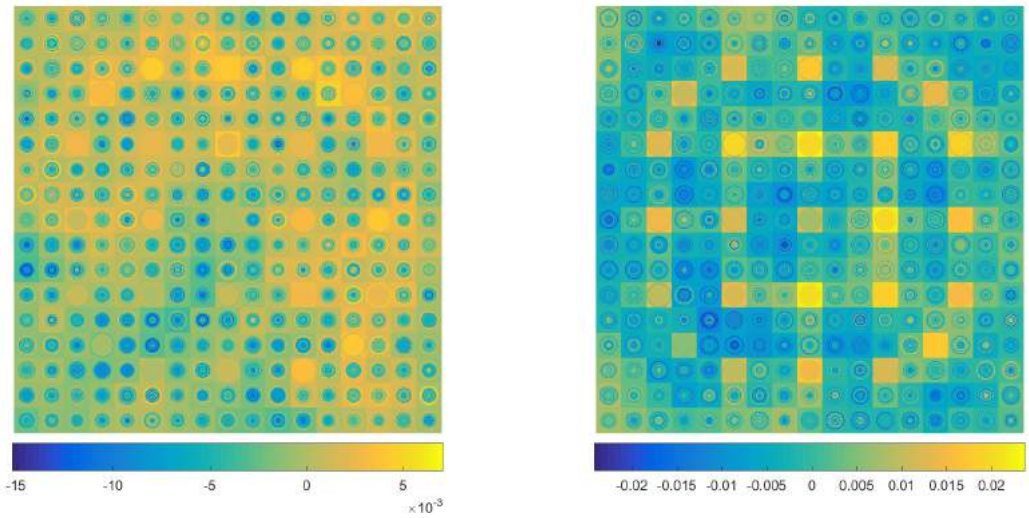

(a) Fast Group (b) Thermal Group

Figure 5.51 Relative errors between reference fine mesh MC solution and the flux reconstructed at 7MWd/Kg burnup - case 2

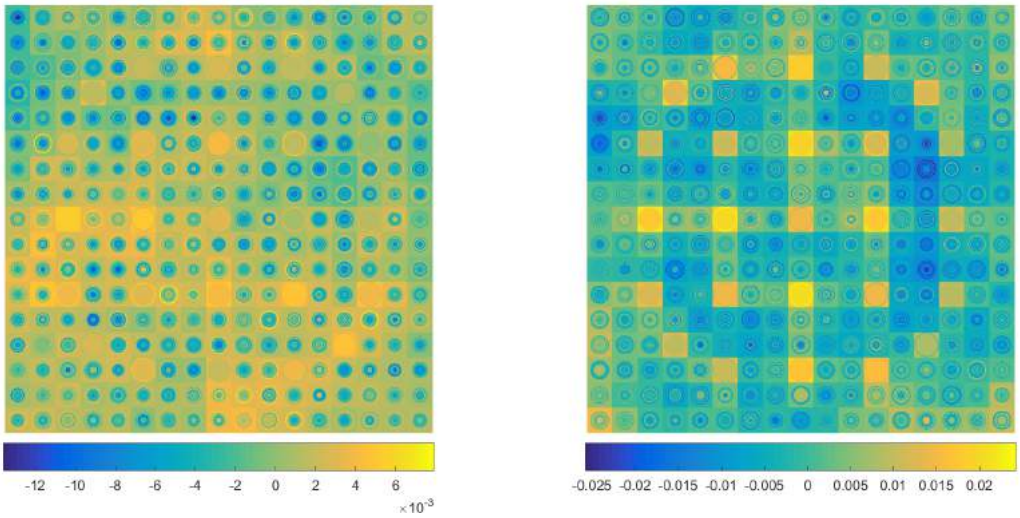

(a) Fast Group (b) Thermal Group

Figure 5.52 Relative errors between reference fine mesh MC solution and the flux reconstructed at 8MWd/Kg burnup - case 2

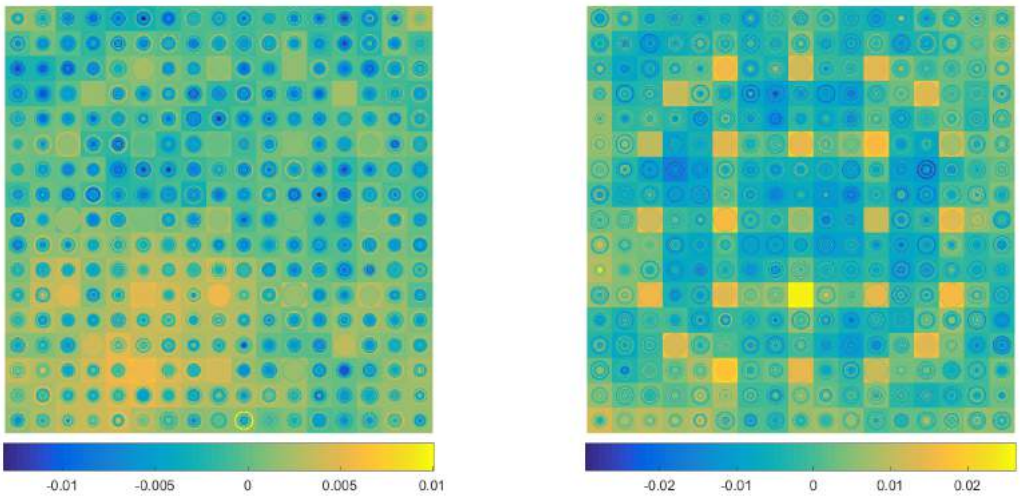

(a) Fast Group (b) Thermal Group

Figure 5.53 Relative errors between reference fine mesh MC solution and the flux reconstructed at 9MWd/Kg burnup - case 2

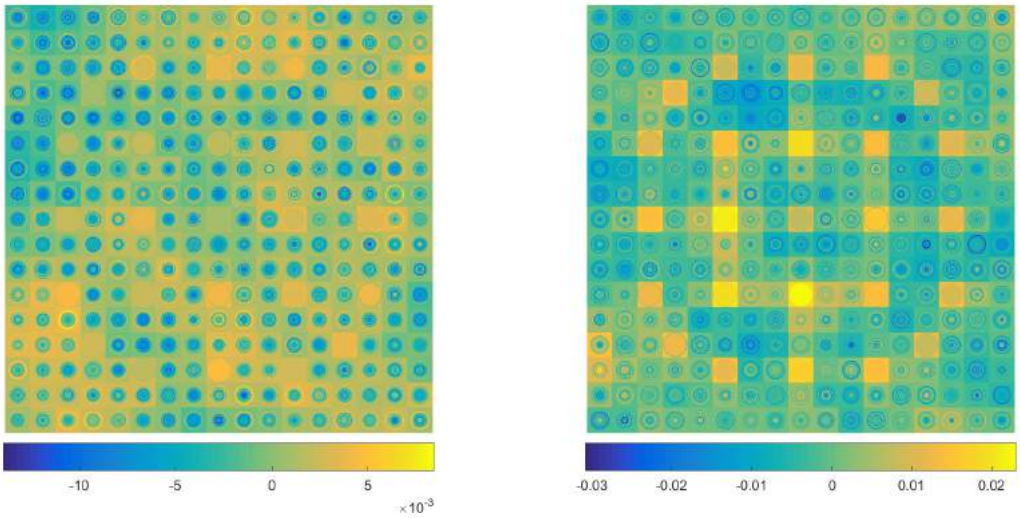

(a) Fast Group (b) Thermal Group

Figure 5.54 Relative errors between reference fine mesh MC solution and the flux reconstructed at 10MWd/Kg burnup - case 2

5.6 Summary

In this chapter, the hybrid method is modified and developed to allow the reconstruction of fine mesh flux and reaction rate distributions in full cores starting from coarse mesh MC estimated flux distributions and the dominant modes of the transport equation. The approach is applied to a 2D single fuel assembly and 3D supercell to illustrate its accuracy and computational performance. For the 2D examples, the hybrid method is capable of reconstructing a MC reference solution with an accuracy that is better the 3%. In 3D problems, the hybrid method produces the same accuracy in middle axial planes. However, in planes near the axial boundaries, where leakage is more significant, the accuracy of method is slightly reduced. This suggests that methods for accounting for axial leakage need to be developed. In terms of computational performance, the hybrid method can achieve at least 88% reduction in the computation time compared to conventional MC for a partial reactor core which is an encouraging result. Finally, effects of fuel burnup are evaluated where it is concluded that dominant modes recalculation at the end of each burnup step is recommended to achieve a better performance with the modal expansion method.

CHAPTER 6 CONCLUSION

A novel hybrid method for full core neutronics based on coupling stochastic reactor physics simulators to deterministic flux mapping is presented. In the previous chapters, challenges for full core MC simulations are summarised. The transport equation and its high order solutions are described. The hybrid method and its application to a number of example problems are illustrated. In this chapter, a summary of the work presented is provided. The of limitations of the hybrid method and unanswered questions are highlighted. The work is concluded by recommendations for future development.

6.1 Summary

Current neutronic methods for simulating full reactor cores either suffer from relatively low accuracy or require extreme computational resources and time. The advancement in nuclear reactor designs demand for novel methods that are both accurate and practical in production applications for simulating and studying neutronics.

In this work, a review of the MC method and its challenges is included. The MC method relies on statistically tracking neutrons based on physical probability distributions which makes it very close to a virtual reactor. The solution it provides is widely accepted as an accurate estimate of the neutron flux distribution with the expense of extreme computational expenses. In full core MC studies, a large number of physical parameters are recorded and the size of the statistical sample must be very large to obtain a solution with high confidence. The extreme computational expense of full core simulations based on MC renders it impractical in production calculations and the method has been limited for benchmarking and validation. Other challenges for full core MC studies is the slow convergence of the fission source, the difficulty in coupling to multiphysics feedback solvers, and the estimation of the true variance.

Deterministic methods in reactor physics are based on discretising the transport equation in the phase space and obtaining an approximate solution using numerical methods. A review of the transport equation and the collision probability approximation is presented. In addition to the fundamental mode solution which describes the asymptotic neutron flux distribution, the transport equation assumes a large number of solutions that can be very useful in perturbation studies and neutron flux mapping and synthesis. Methods for calculating the high order solutions of the transport equation such as deflation and QZ decomposition are reviewed. These are applied to a number of example problems and a comparison is made

between them. Deflation suffers from poor convergence and long running time while QZ guarantees convergence of the solutions to the high order modes in reasonable time. Application of the dominant modes of the transport equation in flux mapping is described where the reconstruction of a fine mesh transport-like solution from homogeneous diffusion solution is presented.

The hybrid method is then introduced. The approach commences by a stochastic simulation to produce neutron flux tallies in few regions or coarse mesh tallies in addition to neutron cross sections. The cross sections are employed in a deterministic lattice calculation to obtain the dominant modes of the transport equation. Once the dominant modes are calculated, they are combined with the tallies scored by the MC solver in order to estimate the amplitudes of the modes and perform flux synthesis and obtain a complete flux distribution. A feasibility study is included to evaluate the accuracy of reconstructing a MC solution using the dominant modes of the transport equation and flux mapping. In the feasibility study, the possibility of reconstructing the neutron flux distribution from tallies in few regions is evaluated. Based on the results produced, the study confirms that the hybrid approach is capable of reconstructing a MC flux distribution from flux tallies in few region. Hence, a considerable reduction in the computational expense is achievable. For better performance, the hybrid method is developed to reconstruct a fine mesh solution starting with a coarse mesh MC solution using the dominant modes of the transport equation. The method is applied to a number of 2D and 3D problems and the accuracy and computational performance are evaluated. Results confirm that in a full core simulation, the hybrid approach could be up to 90% faster than conventional MC while maintaining a comparable accuracy. Solutions produced by the hybrid method for the studied examples are compared to MC reference. In most cases, the relative error between the hybrid solution and the reference is below 2% while errors up to 5% are observed in few cases. Finally, the effects of fuel burnup where evaluated and it is concluded that the method can cope well with dynamic simulations provided the dominant modes are recalculated at the end of each burnup step.

6.2 Limitations

In the presented work, the hybrid method is applied to study the neutron flux in two energy groups in all studied examples. As discussed in section 5.4.2, the computational time to obtain the dominant modes of the transport equation in two energy groups on a fine spatial mesh constitutes about 16% of the computational time of the hybrid method for the examples considered. This time is expected to increase significantly if the number of energy groups is increased. In addition, the memory demand for the calculation of the dominant modes

will be relatively large when a more detailed energy group structure or a finer spatial mesh is used. The increased computational time and memory demand for the calculation of the dominant modes might counter any savings achieved in the computational expenses. Hence, it might be inferred that the hybrid method is limited to problems where the neutron flux distribution is required in few energy groups.

6.3 Future Development

The presented study investigates the effects of several factors such as the number of dominant modes used in modal expansion, the effects of boundary conditions, and error estimation.

In the studied examples, different number of modes are employed in flux mapping. A comparison between the results shows that the accuracy of the reconstructed solution is slightly sensitive to the number of modes employed in the modal expansion model. It appears that increasing the number of modes does not guarantee a better solution compared to cases where few modes where utilised. A strategy for selecting the number of modes in flux synthesis is not decided in this work. Hence, the development of a criteria for truncating the modal expansion model is required. Such a criteria could be the use of modes with non-zero eigenvalues or those with eigenvalues greater than a predetermined threshold.

When effects of boundary conditions are included, relatively large errors are observed near the boundaries or interfaces. Results confirm that the boundary conditions used in the calculation of the dominant modes has a significant influence on the accuracy of the solution. The use of a trial and error approach to define albedo boundary conditions confirms that including interface effects in the deterministic solver improves the accuracy of the solution near the boundaries. However, a trial and error approach is impractical. A method for determining the optimum boundary conditions in the calculation of the dominant modes needs to be developed. A possibly useful approach is to define albedo boundary conditions by using flux currents on the interfaces tallied by the stochastic solver. In 3D problems with void boundary conditions in the axial direction, the accuracy of flux reconstruction with 2D modes is less accurate in planes near the boundaries. This highlights the effects of axial leakage and the necessity of accounting for these in the calculation of the modes and flux mapping.

An attempt to estimate the mapping error is included. The method appears to be useful in eliminating or reducing the sensitivity of the hybrid approach to the number of dominant modes. However, the error estimation method is not successful in estimating or reducing mapping errors. Hence, a better approach for evaluating mapping errors is necessary. In

problems with homogenised fuel pincells, it is deduced that the mapping error is related to neutron absorption; perhaps, a similar approach can be developed for problems with fine mesh heterogeneous problems.

Finally, the hybrid method described in this work uses QZ decomposition method with the isotropic collision probability approximation to calculate the dominant modes of the transport equation. The QZ approach could be computationally demanding when more details are required. Hence, alternative numerical methods for solving eigenvalue problems need to be investigated. Calculating the dominant modes of the transport equation from alternative models such as discrete ordinates or method characteristics should be considered.

REFERENCES

[1] James J. Duderstadt. *Nuclear Reactor Analysis*. John Wiley Sons, 1976.

[2] William L. Dunn. *Exploring Monte Carlo Methods*. Academic Press, 2012.

[3] William R. Martin. Challenges and prospects for whole-core Monte Carlo analysis. *Nuclear Engineering and Technology*, 44(2):151–160, 2012.

[4] Alain Hébert. *Applied Reactor Physics*. Presse Internationale Polytechnique, 2009.

[5] Alex F. Bielajew. *Fundamentals of the Monte Carlo Method for Neutral and Charged Particle Transport*. University of Michigan http://www-personal.umich.edu/ bielajew/MCBook/book.pdf, 2001.

[6] David P. Griesheimer, William R. Martin, and James Paul Holloway. Estimation of flux distributions with Monte Carlo functional expansion tallies. *Radiation Protection Dosimetry*, 115(1-4):428–432, 2005.

[7] Kaushik Banerjee and William R. Martin. Kernel density estimation method for Monte Carlo global flux tallies. *Nuclear Science and Engineering*, 170(3):234–250, 2012.

[8] Gokhan Yesilyurt, William R. Martin, and Forrest B. Brown. On-the-fly Doppler broadening for Monte Carlo codes. *Nuclear Science and Engineering*, 171(3):239–257, 2012.

[9] Kord Smith. Monte Carlo for practical LWR analysis: what's needed to get to the goal? In *M&C Division Computational Roundtable, American Nuclear Society Summer Meeting, Hollywood, FL*, 2011.

[10] Kord Smith. Reactor core methods. In *Invited lecture at the M&C 2003 International Conference*, 2003.

[11] Hj Matzke. On the rim effect in high burnup UO2 LWR fuels. *Journal of Nuclear Materials*, 189(1):141–148, 1992.

[12] Takanori Kitada and Toshikazu Takeda. Effective convergence of fission source distribution in Monte Carlo simulation. *Journal of Nuclear Science and Technology*, 38(5):324–329, 2001.

[13] John C. Wagner, Douglas E. Peplow, Scott W. Mosher, and Thomas M. Evans. Review of hybrid (deterministic/Monte Carlo) radiation transport methods, codes, and applications at Oak Ridge National Laboratory. *Progress in Nuclear Science and Technology*, pages 808–814, 2010.

[14] Min-Jae Lee, Han Gyu Joo, Deokjung Lee, and Kord Smith. Multigroup Monte Carlo reactor calculation with coarse mesh finite difference formulation for real variance reduction. Technical report, Oak Ridge National Laboratory (ORNL), 2010.

[15] Min Jae Lee, Han Gyu Joo, Deokjung Lee, and Kord Smith. Coarse mesh finite difference formulation for accelerated Monte Carlo eigenvalue calculation. *Annals of Nuclear Energy*, 65:101–113, 2014.

[16] Edward W. Larsen and Yang Jinan. A functional Monte Carlo method for k-eigenvalue problems. *Nuclear Science and Engineering*, 159(2):107–126, 2008.

[17] Taro Ueki. Intergenerational correlation in Monte Carlo k-eigenvalue calculation. *Nuclear Science and Engineering*, 141(2):101–110, 2002.

[18] Taro Ueki, Takamasa Mori, and Masayuki Nakagawa. Error estimations and their biases in Monte Carlo eigenvalue calculations. *Nuclear science and engineering*, 125(1):1–11, 1997.

[19] Forrest B. Brown. A review of Monte Carlo criticality calculations: convergence, bias, statistics. *Proceedings M&C*, pages 3–7, 2009.

[20] E.M. Gelbard and R. Prael. Computation of standard deviations in eigenvalue calculations. *Progress in Nuclear Energy*, 24(1):237–241, 1990.

[21] E.M. Gelbard and R.E. Prael. Monte Carlo work at Argonne National Laboratory. 1974.

[22] Jin Shim Hyung, Yonghee Kim, and Chang Hyo Kim. History-based batch method for a real variance estimation in Monte Carlo eigenvalue calculations. *Transactions of the American Nuclear Society*, 100:300–301, 2009.

[23] William L. Dunn and J. Kenneth Shultis. *Exploring Monte Carlo Methods*. Elsevier, 2011.

[24] Jaakko Leppänen. *Development of a New Monte Carlo Reactor Physics Code*. VTT Technical Research Centre of Finland, 2007.

[25] T.M. Sutton, T.J. Donovan, T.H. Trumbull, P.S. Dobreff, E. Caro, D.P. Griesheimer, L.J. Tyburski, D.C. Carpenter, and H. Joo. The MC21 Monte Carlo transport code. In *Joint Int. Conf. on Math. & Comp. and Supercomputing in Nuclear Applications, Monterey, Calif*, 2007.

[26] DP Griesheimer, DF Gill, BR Nease, TM Sutton, MH Stedry, PS Dobreff, DC Carpenter, TH Trumbull, E Caro, H Joo, and D.L. Millman. MC21 v. 6.0–a continuous-energy Monte Carlo particle transport code with integrated reactor feedback capabilities. In *Proc. Joint International Conference on Supercomputing in Nuclear Applications and Monte Carlo (SNA+ MC)*, 2013.

[27] J.L. Hunter and T.M. Sutton. A method for reducing the largest relative errors in Monte Carlo iterated-fission-source calculations. In *Proceedings of the 2013 International Conference on Mathematics and Computational Methods Applied to Nuclear Science and Engineering-M and C 2013*, 2013.

[28] Daniel J. Kelly, Brian N. Aviles, and Bryan R. Herman. MC21 analysis of the MIT PWR benchmark: Hot zero power results. In *Proceedings of the 2013 International Conference on Mathematics and Computational Methods Applied to Nuclear Science and Engineering-M and C 2013*, 2013.

[29] J. Eduard Hoogenboom, William R. Martin, and Bojan Petrovic. The Monte Carlo performance benchmark test-aims, specifications and first results. In *International Conference on Mathematics and Computational Methods Applied to Nuclear Science and Engineering*, volume 2, page 15, 2011.

[30] N. Horelik, B. Herman, B. Forget, and K. Smith. Benchmark for evaluation and validation of reactor simulations (BEAVRS), v1. 0.1. In *Proc. Int. Conf. Mathematics and Computational Methods Applied to Nuc. Sci. & Eng*, 2013.

[31] Daniel J. Kelly, T.H. M. Sutton, T.H. Trumbull, and Peter S. Dobreff. MC21 Monte Carlo analysis of the Hoogenboom-Martin full-core PWR benchmark problem-301. 2010.

[32] Hyung Jin Shim, Beom Seok Han, Jong Sung Jung, Ho Jin Park, and Chang Hyo Kim. McCARD: Monte Carlo code for advanced reactor design and analysis. *Nuclear Engineering and Technology*, 44(2):161–176, 2012.

[33] Serpent, a Continuous-energy Monte Carlo Reactor Physics Burnup Calculation Code. http://montecarlo.vtt.fi/. Accessed: March 2015.

[34] Jaakko Leppänen. Two practical methods for unionized energy grid construction in continuous-energy Monte Carlo neutron transport calculation. *Annals of Nuclear Energy*, 36(7):878–885, 2009.

[35] S.M. Girard. MNCP–A General Monte Carlo N-Particle Transport Code, Version 5 Volume I: Overview and Theory. *www-rsicc. ornl. gov/. LA-UR-03-1987 (Los Alamos National Laboratory)*, 2003.

[36] Jaakko Leppäenen. Use of the Serpent Monte Carlo Reactor Physics Code for Full-core Calculations. In *Proceedings of SNA + MC2010*, 2010.

[37] Paul K. Romano and Benoit Forget. The OpenMC Monte Carlo particle transport code. *Annals of Nuclear Energy*, 51:274–281, 2013.

[38] OpenMC theory and methodology. http://mit-crpg.github.io/openmc/methods/index.html. Accessed: November 2014.

[39] Elmer Lewis. *Computational Methods in Neutron Transport*. American Nuclear Society, 1984.

[40] Guy Marleau. Dragon Theory Manual, Part 1: Collision Probability Calculations. Technical Report IGE-236, Institute de Génie Nucléaire, 2001.

[41] Cleve B. Moler and Gilbert W. Stewart. An algoritm for generalised matrix eigenvalue problems. *SIAM Journal on Numerical Analysis*, 10(2):241–256, 1973.

[42] Biswa Nath Datta. *Numerical Linear Algebra and Applications*. Siam, 2010.

[43] Guy Marleau, Alain Hébert, and Robert Roy. A user's guide for DRAGON version-5. Technical Report IGE-335, Institute de Génie Nucléaire, 2016.

[44] Seyed Rida Housseiny Milany and Guy Marleau. Implementation of a Dominant Modes Solver in DRAGON. *Proceedings of the 36th Annual CNS Meeting*, June 2016.

[45] James H. Wilkinson. Inverse iteration in theory and in practice. In *Symposia Mathematica Volume X*, pages 361–379, 1972.

[46] Youcef Saad. *Numerical Methods for Large Eigenvalue Problems*, volume 158. SIAM, 1992.

[47] D. Gucci. *Handbook of Nuclear Engineering*. Springer, 2010.

[48] M.E.w Pomerantz, CR Calabrese, and C Grant. Nuclear reactor power and flux distribution fitting from a diffusion theory model and experimental data. *Annals of Nuclear Energy*, 29(9):1073–1083, 2002.

[49] Seyed Rida Housseiny Milany and Guy Marleau. Application of the dominant modes of the tansport equation in flux mapping. *Proceedings of the 40th Student CNS Meeting*, June 2016.

[50] Paul W Holland and Roy E Welsch. Robust regression using iteratively reweighted least-squares. *Communications in Statistics-Theory and Methods*, 6(9):813–827, 1977.